Bringing Light to a Dark Matter Search

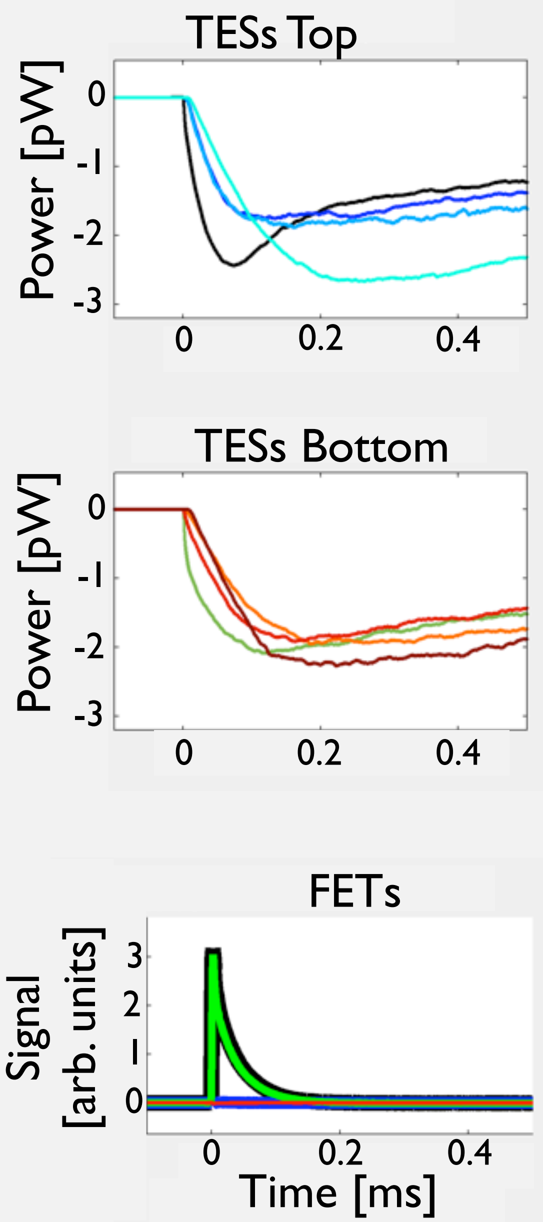

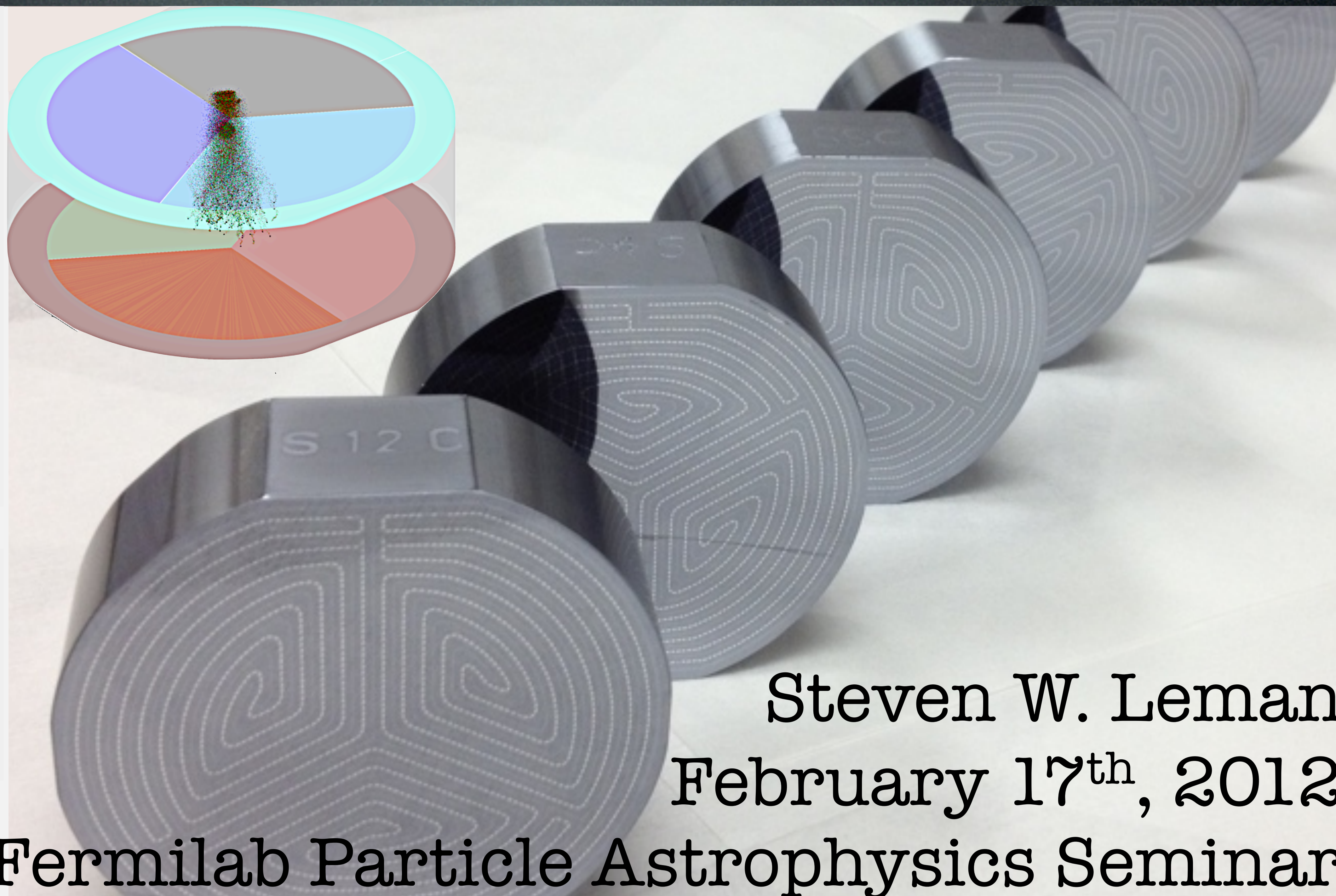

Steven W. Leman

February 17th, 2012

Fermilab Particle Astrophysics Seminar

Dark Matter


Galaxy Clusters

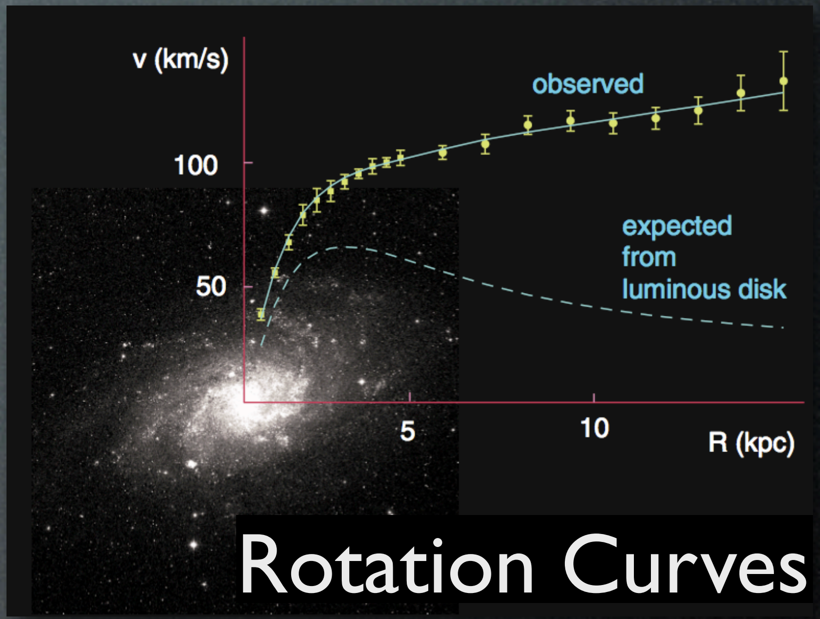
v (km/s)
observed
100
50
expected
from
luminous disk
5
10
R (kpc)
Rotation Curves

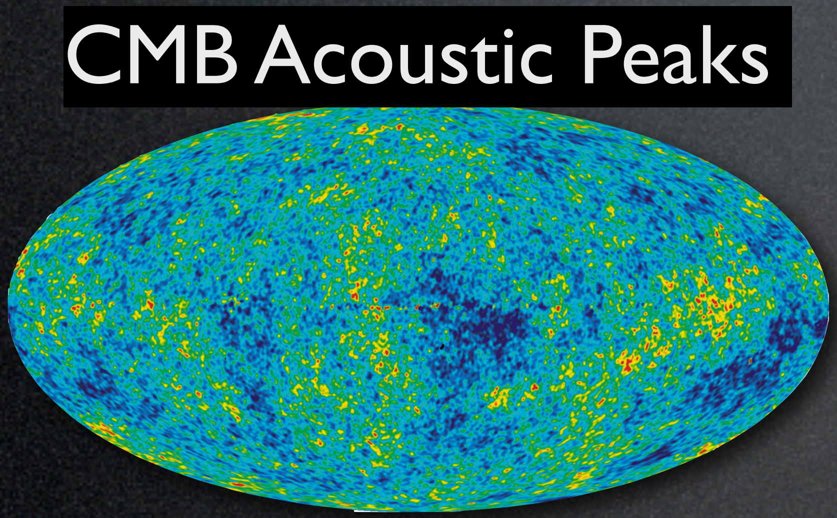
CMB Acoustic Peaks


Gravitational Lensing

ΛCDM Model

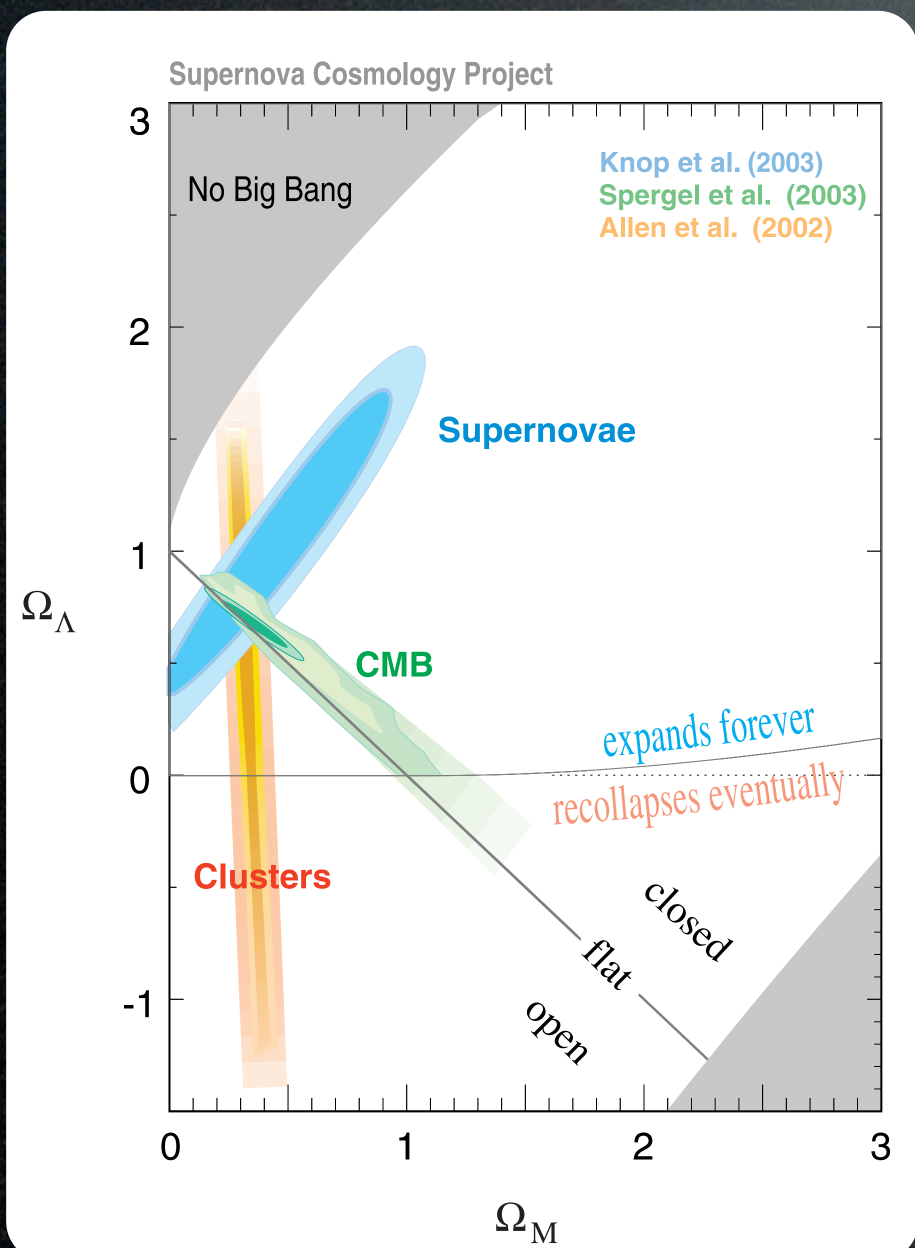

Supernova Cosmology Project
No Big Bang
Knop et al. (2003)
Spergel et al. (2003)
Allen et al. (2002)
Supernovae
CMB
Clusters
expands forever
recollapses eventually
closed
flat
open
Ω_Λ
Ω_M
3
2
1
0
-1
0
1
2
3

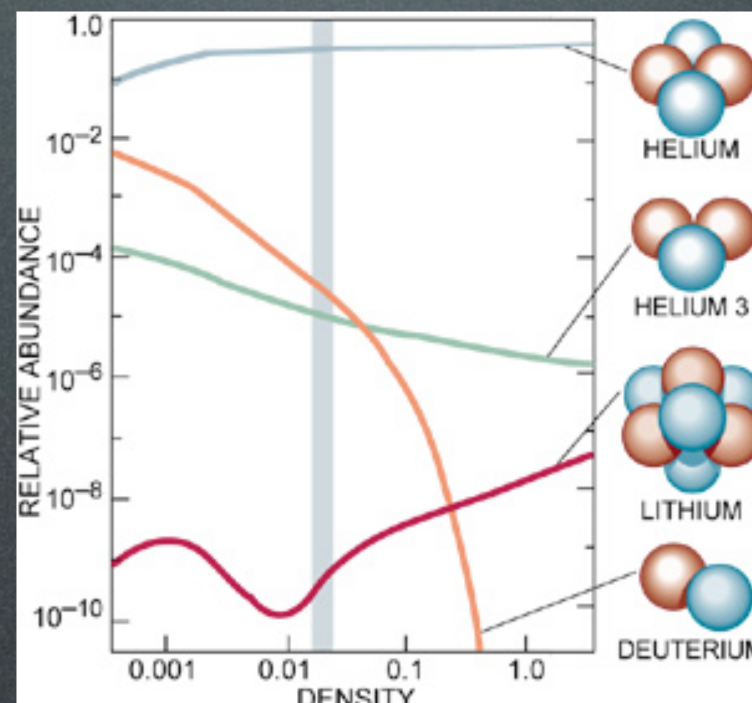

RELATIVE ABUNDANCE
DENSITY
1.0
10^{-2}
10^{-4}
10^{-6}
10^{-8}
10^{-10}
0.001
0.01
0.1
1.0
HELIUM
HELIUM 3
LITHIUM
DEUTERIUM

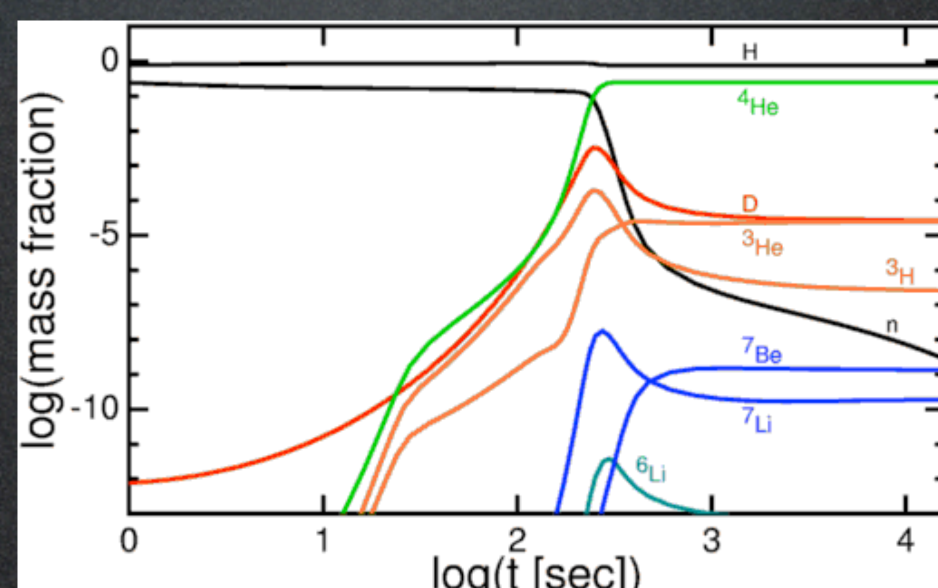

log(mass fraction)
log(t [sec])
0
-5
-10
0
1
2
3
4
H
^{4}He
D
^{3}He
^{3}H
n
^{7}Be
^{7}Li
^{6}Li

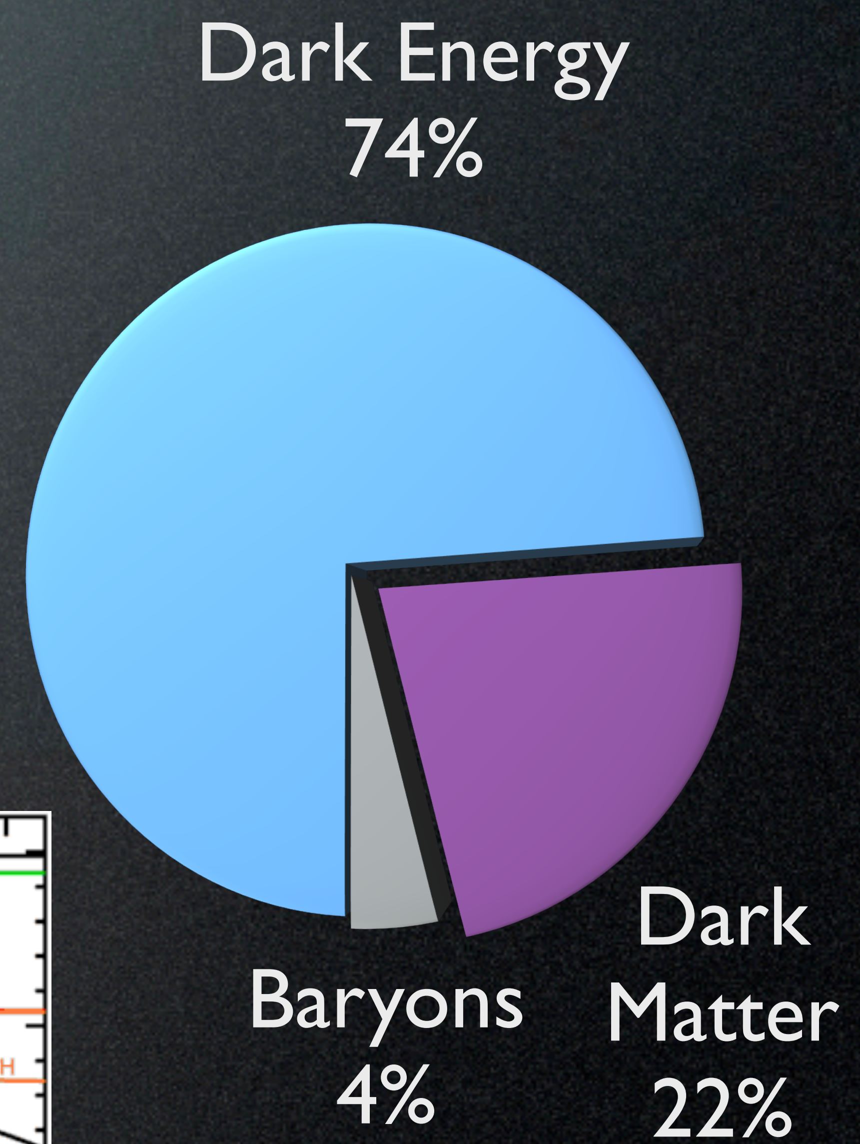

Dark Energy
74%
Baryons
4%
Dark
Matter
22%

Readout Methods

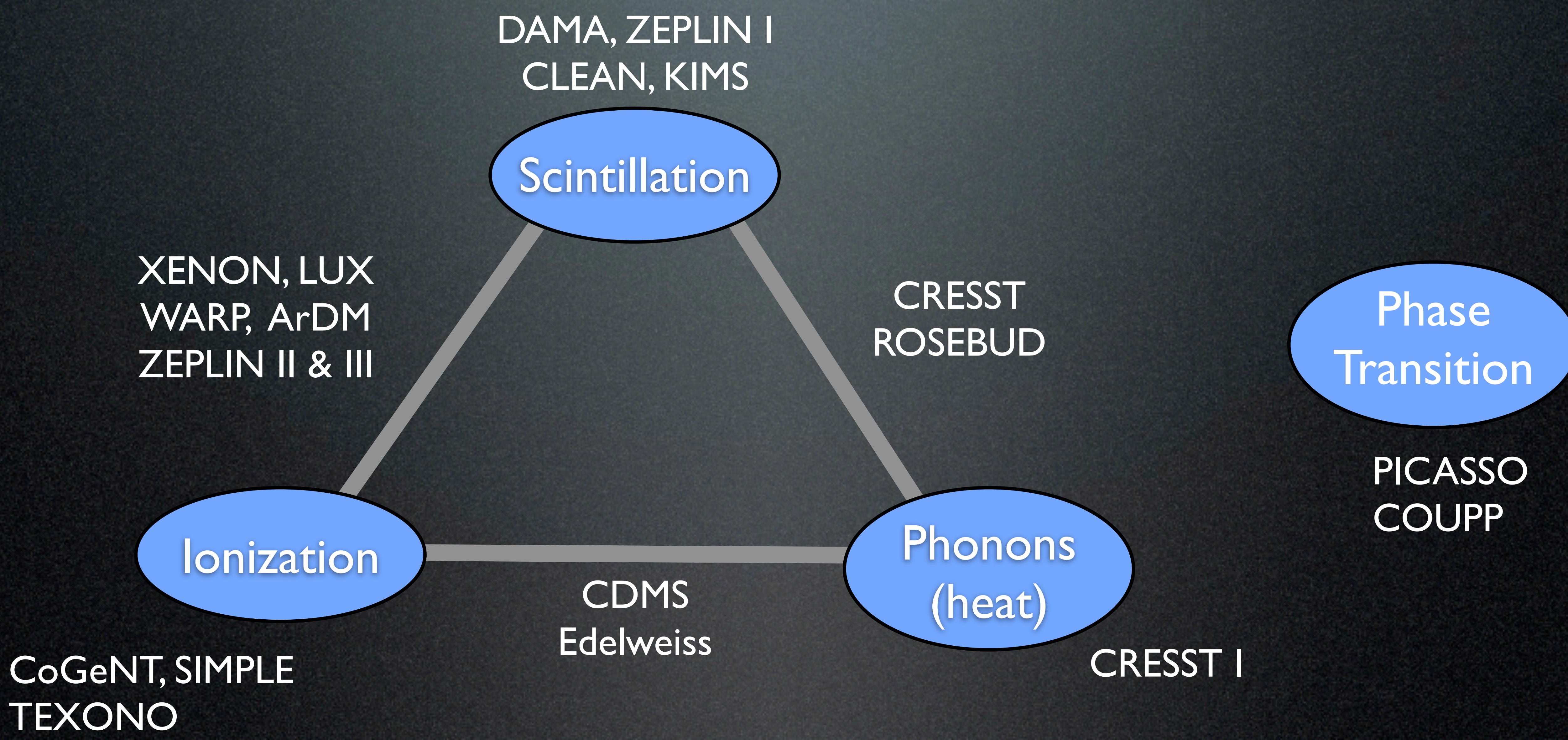

Phonon Readout

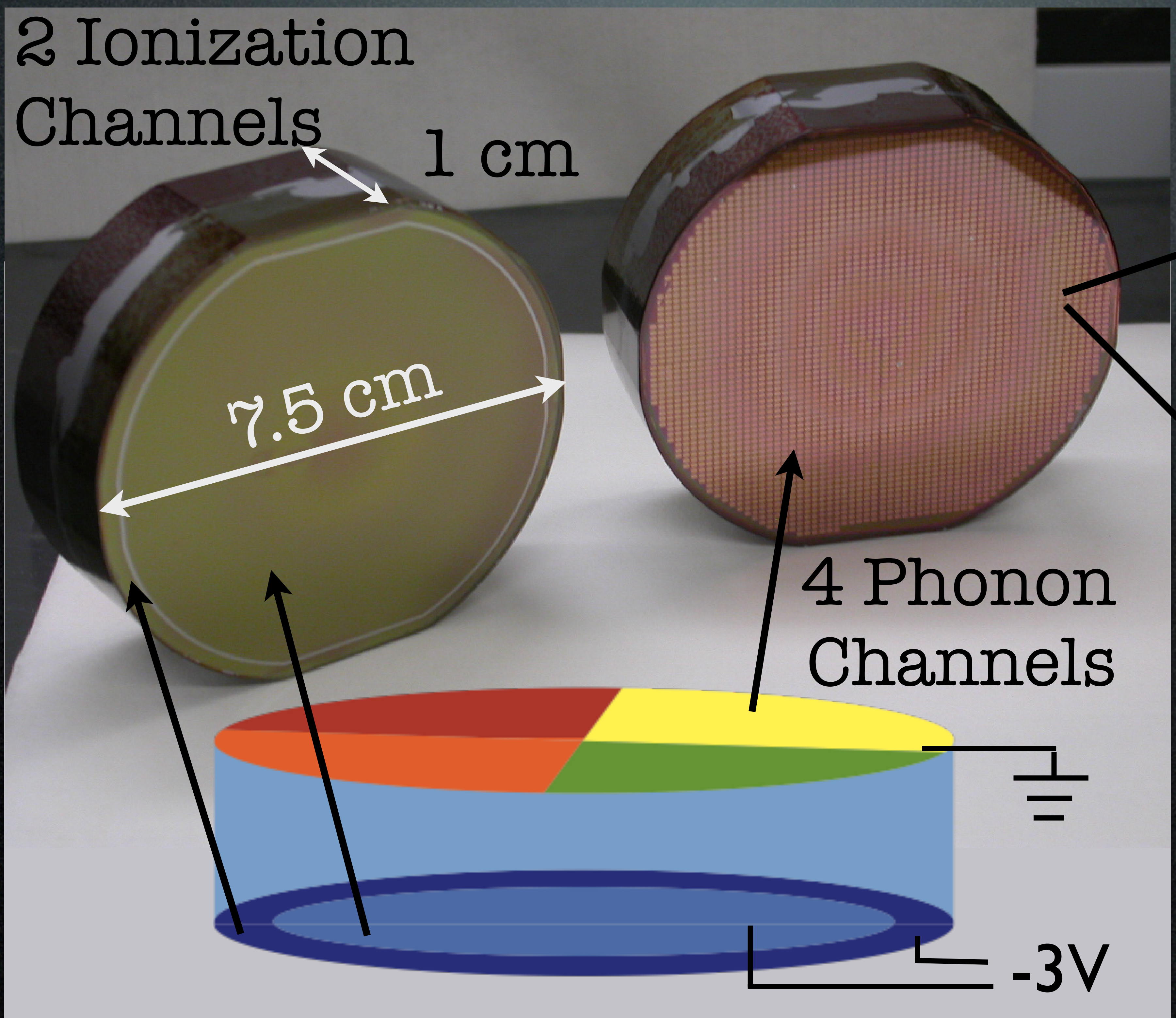

Al fins absorb phonons

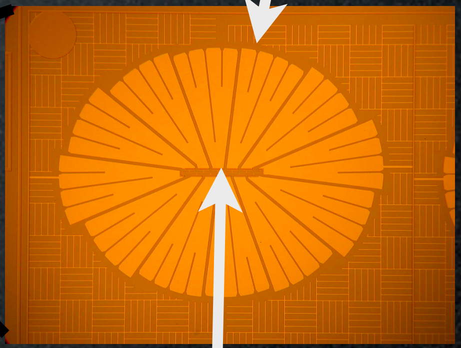

Transition Edge Sensors readout phonon energy

Carrier Transient

- Carriers initially high energy and can transport into the wrong electrode

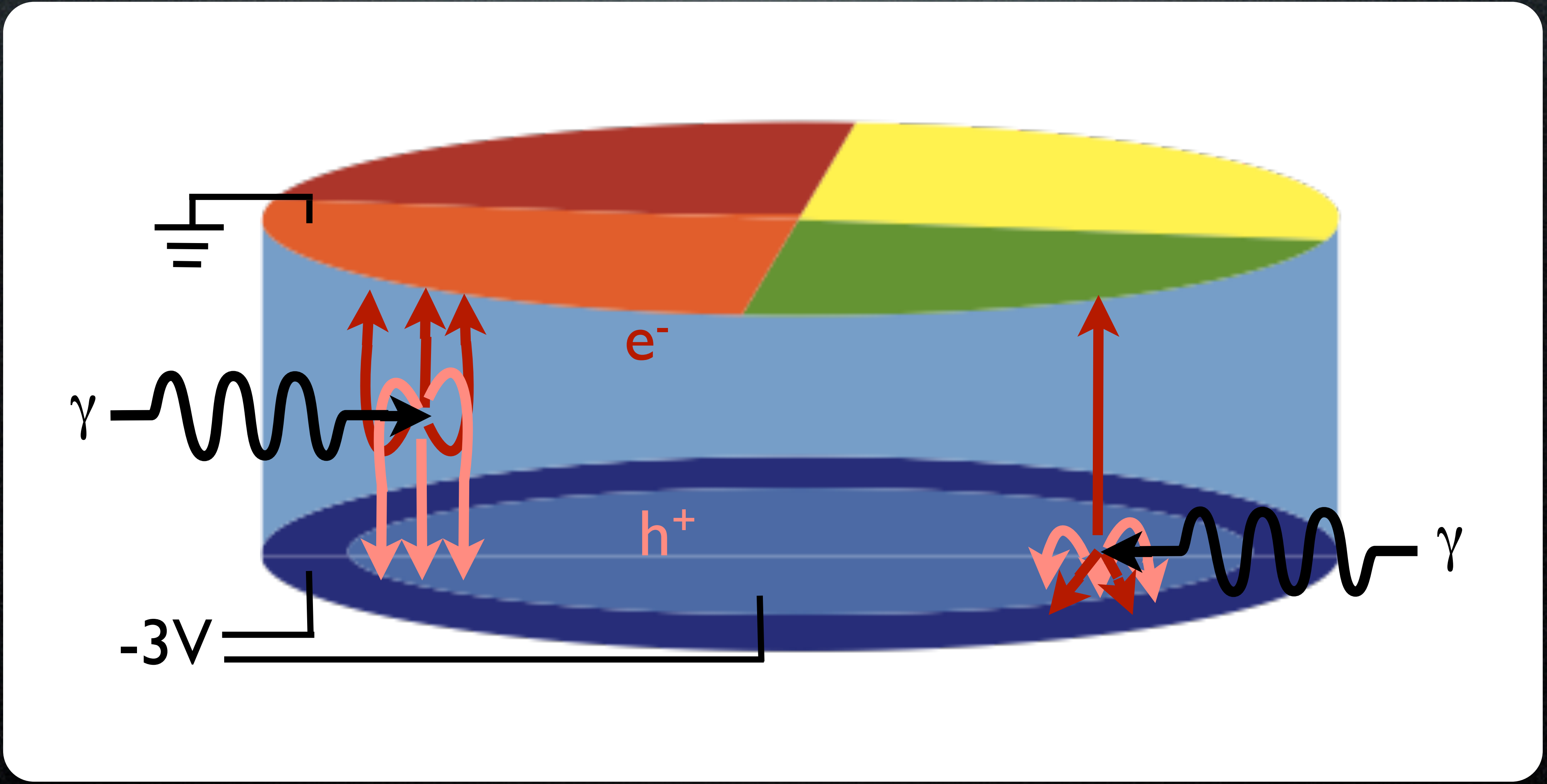

CDMS-II Data

- 612 kg days Ge
- 2 events pass timing and NR cuts

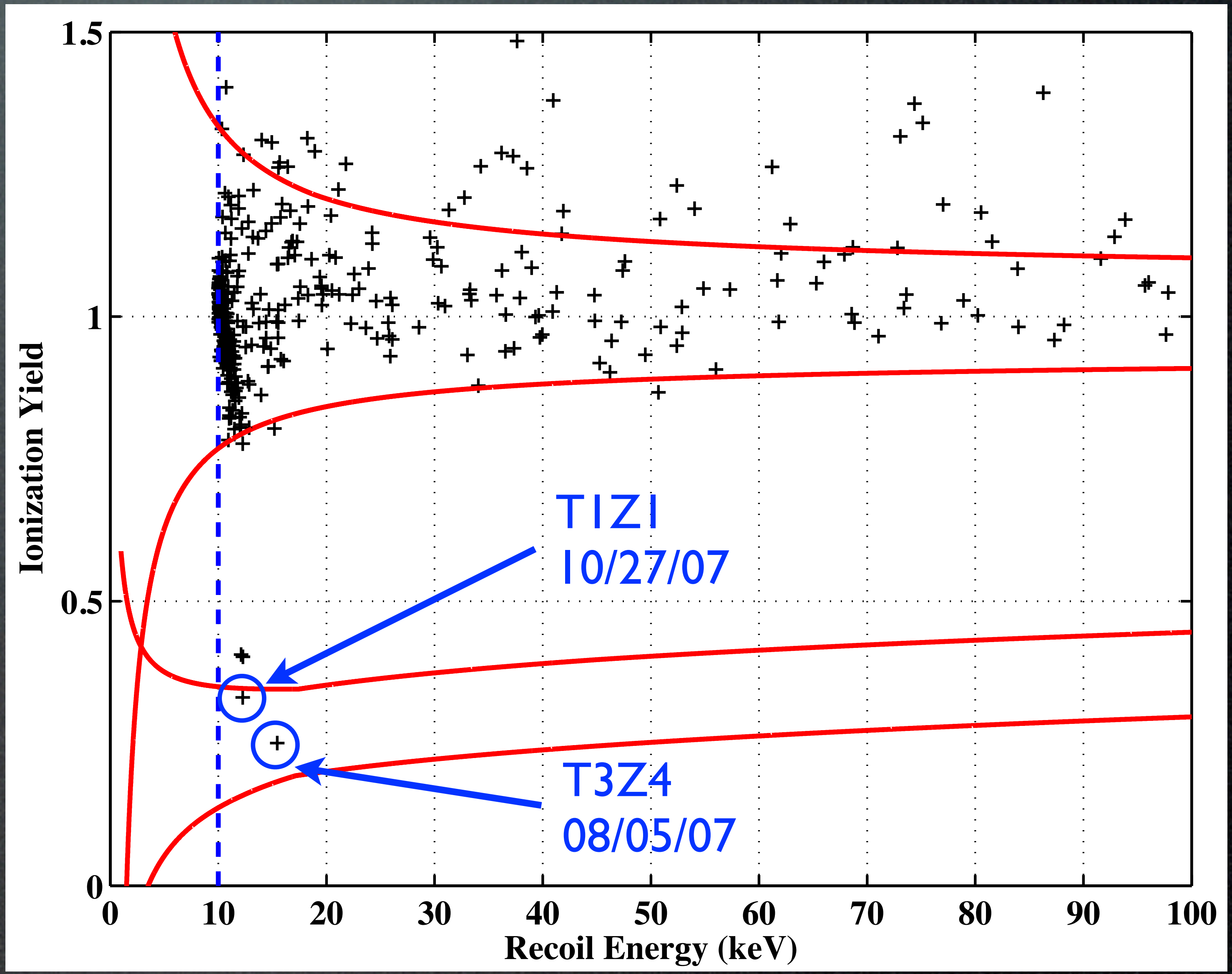

SCDMS iZIP Detector

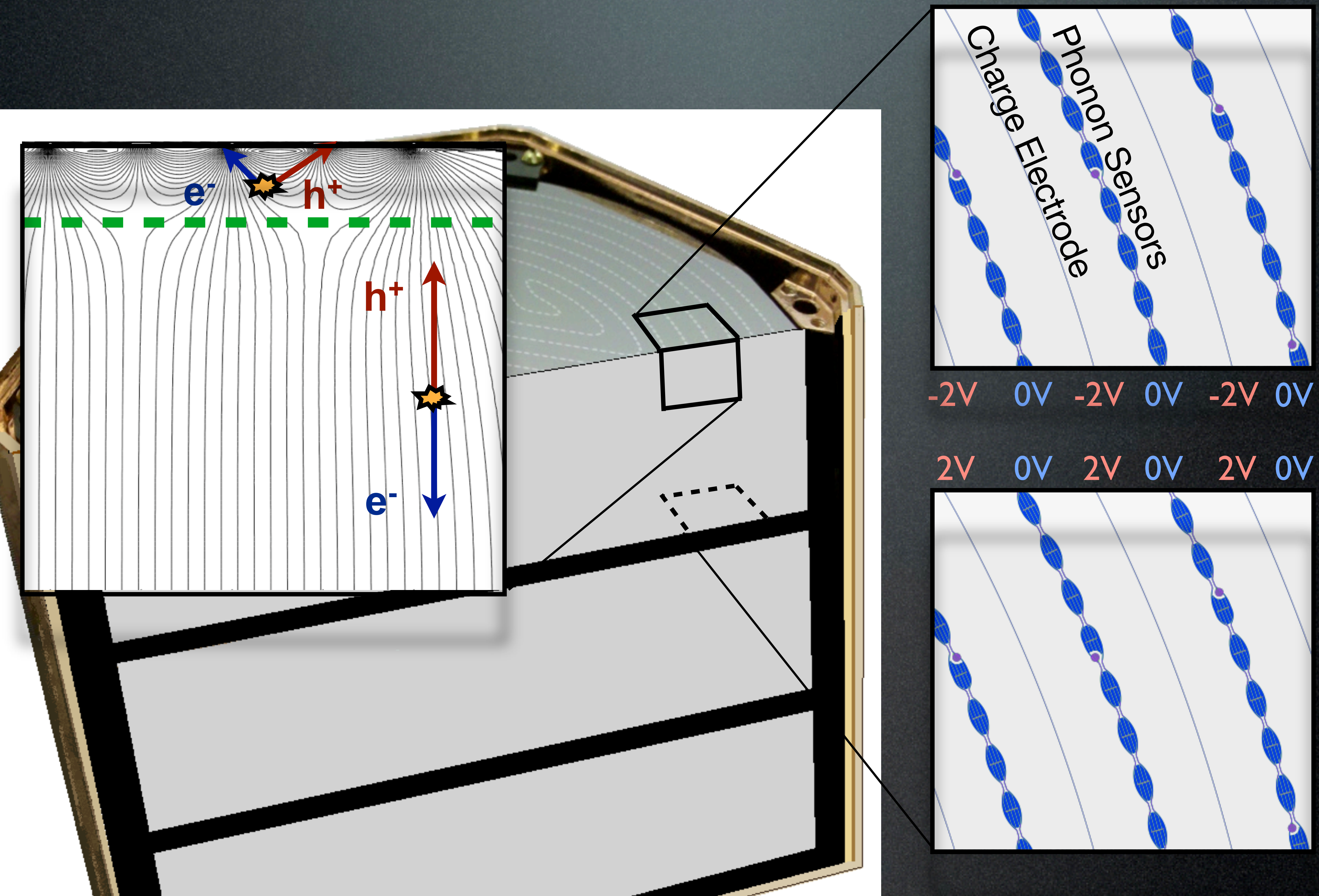

CDMS Members

California Institute of Technology
Z. Ahmed, J. Filippini, S.R. Golwala, D. Moore, R. Nelson, R.W. Ogburn

Case Western Reserve University
D. Akerib, C.N. Bailey, M.R. Dragowsky, D.R. Grant, R. Hennings-Yeomans

Fermi National Accelerator Laboratory
D. A. Bauer, F. DeJongh, J. Hall, D. Holmgren, L. Hsu, E. Ramberg, R. B. Thakur, R.L. Schmitt, J. Yoo

Massachusetts Institute of Technology
A. Anderson, E. Figueroa-Feliciano, **S.A. Hertel**, S.W. Leman, **K.A. McCarthy**

NIST
K. Irwin

Queen's University
P. Di Stefano, C. Crewdson, J. Fox, O. Kamaev, S. Liu, C. Martinez, P. Nadeau, W. Rau, Y. Ricci, M. Verdier

Santa Clara University
B. A. Young

Southern Methodist University
J. Cooley, B. Karabuga, S. Scorza, H. Qiu

SLAC/KIPAC
M. Asai, A. Borgland, D. Brandt, P.L. Brink, W. Craddock, E. do Couto e Silva, G.G. Godfrey, J. Hasi, M. Kelsey, C.J. Kenney, **P.C. Kim**, R. Partridge, R. Resch, D. Wright

Stanford University
B. Cabrera, M. Cherry, R. Moffatt, L. Novak, M. Pyle, M. Razeti, B. Shank, A. Tomada, S. Yellin, J. Yen

Syracuse University
M. Kos, M. Kiveni, R. W. Schnee

Texas A&M
A. Jastram, K. Koch, R. Mahapatra, M. Platt, K. Prasad, J. Sander

University of California, Berkeley
M. Daal, T. Doughty, N. Mirabolfathi, A. Phipps, B. Sadoulet, D. Seitz, B. Serfass, D. Speller, **K.M. Sundqvist**

University of California, Santa Barbara
R. Bunker, D.O. Caldwell, H. Nelson

University of Colorado Denver
B.A. Hines, M.E. Huber

University of Florida
T. Saab, D. Balakishiyeva, B. Welliver

University of Minnesota
J. Beaty, H. Chagani, P. Cushman, S. Fallows, M. Fritts, V. Mandic, X. Qiu, A. Reisetter, J. Zhang

University of Zurich
S. Arrenberg, T. Bruch, L. Baudis, M. Tarka

References

- "Invited Review Article: Physics and Monte Carlo Techniques as Relevant to Cryogenic, Phonon and Ionization Readout of CDMS Radiation-Detectors", S.W. Leman, Review of Scientific Instruments (submitted)
- "Comparison of CDMS [100] and [111] oriented germanium detectors", S.W. Leman, S.A. Hertel, P. Kim, et al, Low Temperature Physics Journal (accepted)
- "Validation of Phonon Physics in the CDMS Detector Monte Carlo", K.A. McCarthy, S.W. Leman, P. Kim, et al, Proceedings of the 14th International Workshop on Low Temperature Detectors, Low Temperature Physics Journal (submitted)
- "Simulations of Noise in Phase-Separated Transition-Edge Sensors for SuperCDMS", A.J. Anderson, S.W. Leman, et al, Low Temperature Physics Journal (accepted)
- "Modeling phase-separated transition-edge sensors in SuperCDMS detectors", A.J. Anderson, S.W. Leman, et al, Nuclear Instruments and Methods A (submitted)
- "Monte Carlo Comparisons to a Cryogenic Dark Matter Search Detector with low Transition-Edge-Sensor Transition Temperature", S.W. Leman, K.A McCarthy, P. Kim, et al, Journal of Applied Physics 110, 094515 (2011)
- "Phonon Quasidiffusion in CDMS Large Germanium Detectors", S.W. Leman, K.A. McCarthy, et al, Chinese Journal of Physics, vol 49 (2011) p. 349 (PHONONS 2010 conference proceedings)

Event Classification

Charge vs Lattice Interactions

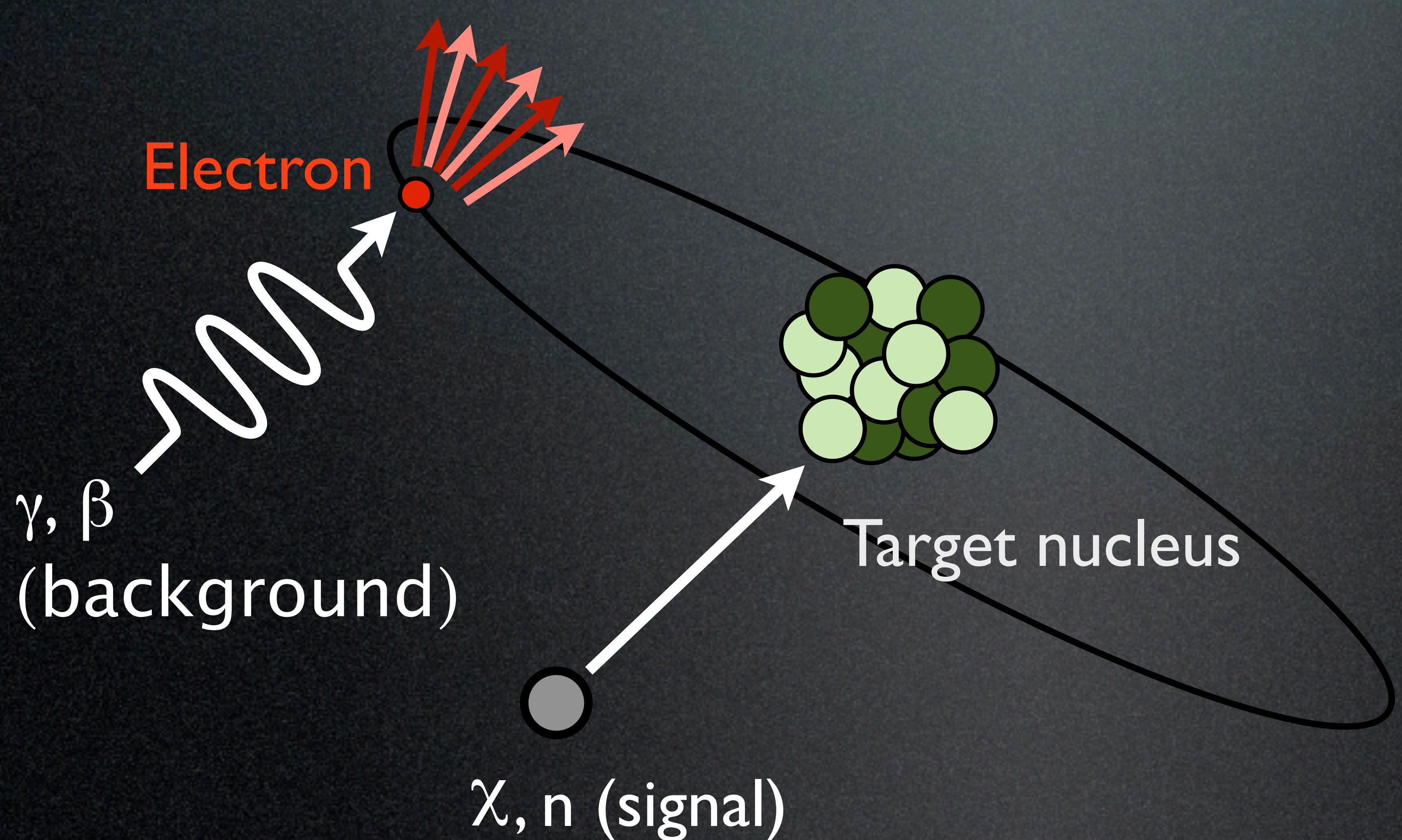

Charge vs Lattice Interactions

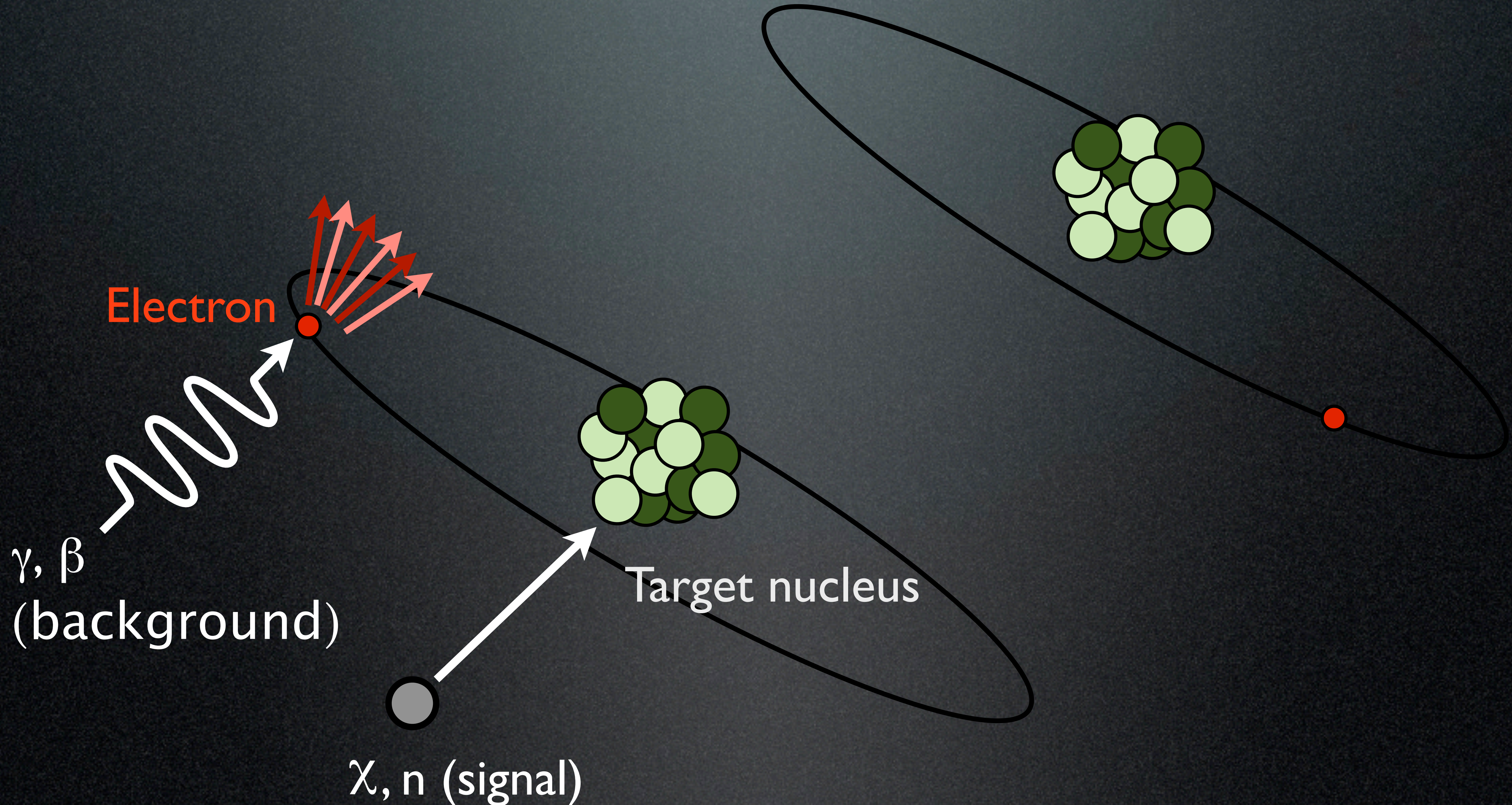

Charge vs Lattice Interactions

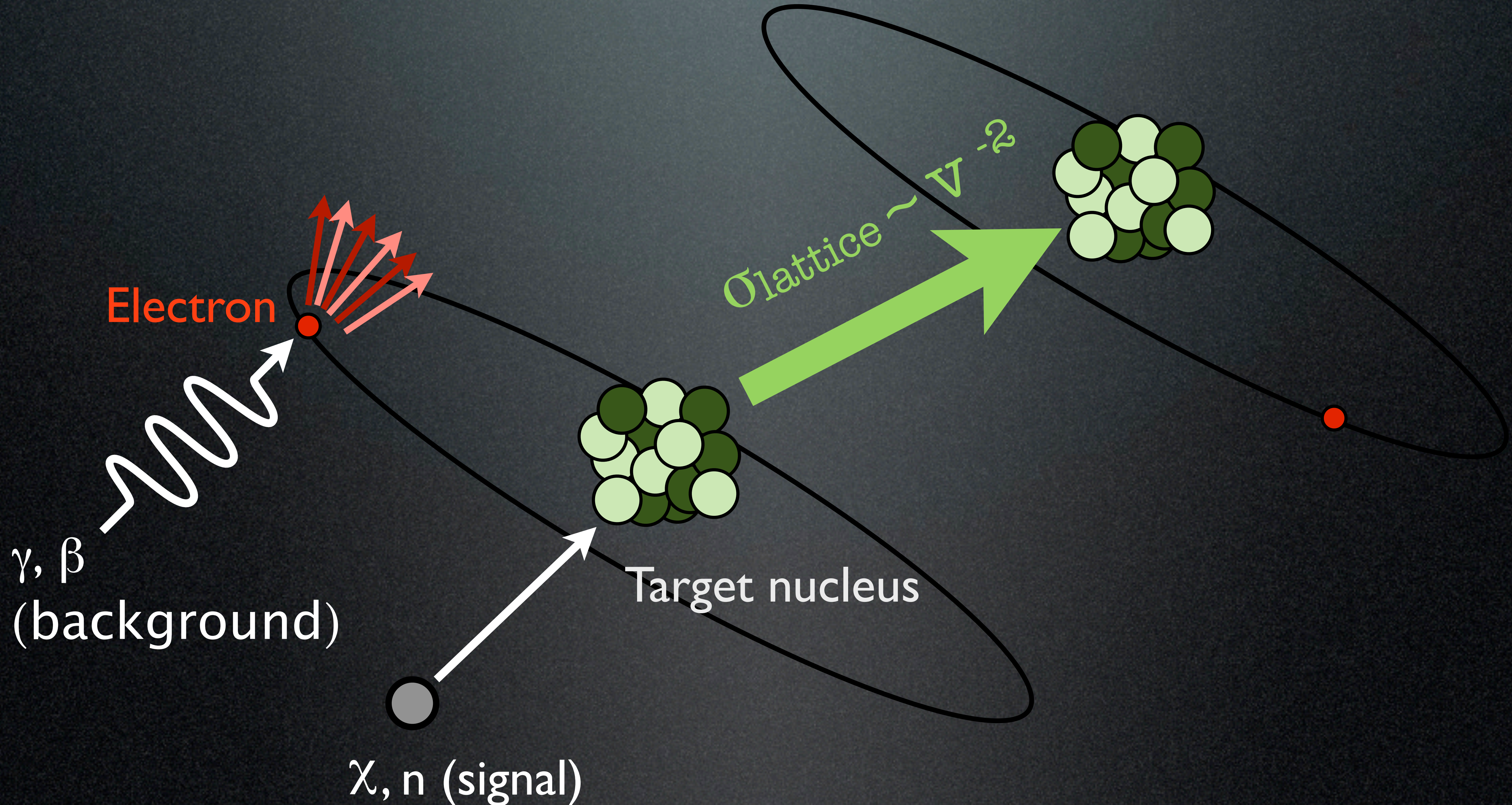

Charge vs Lattice Interactions

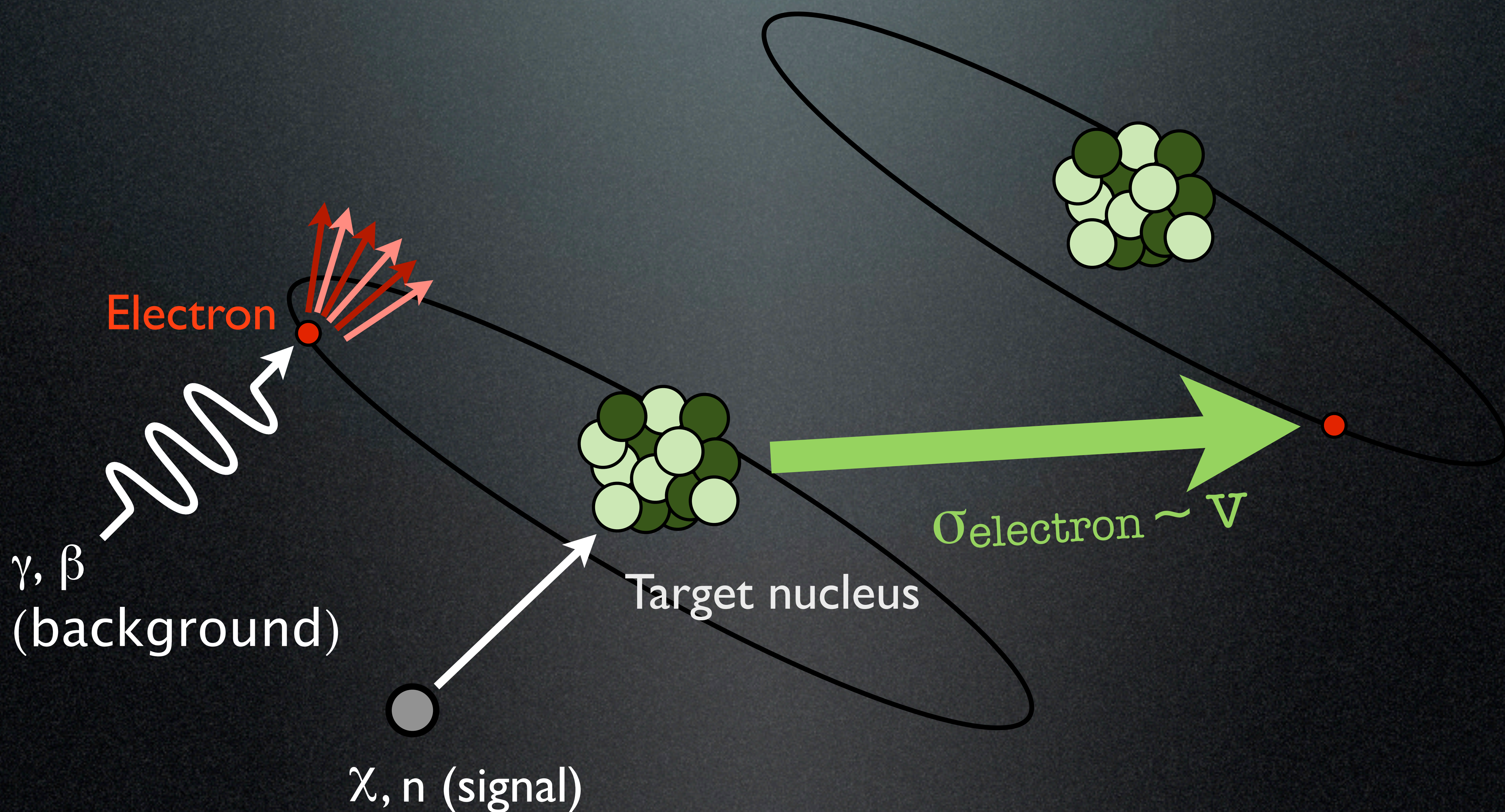

Electron-Ion Interaction

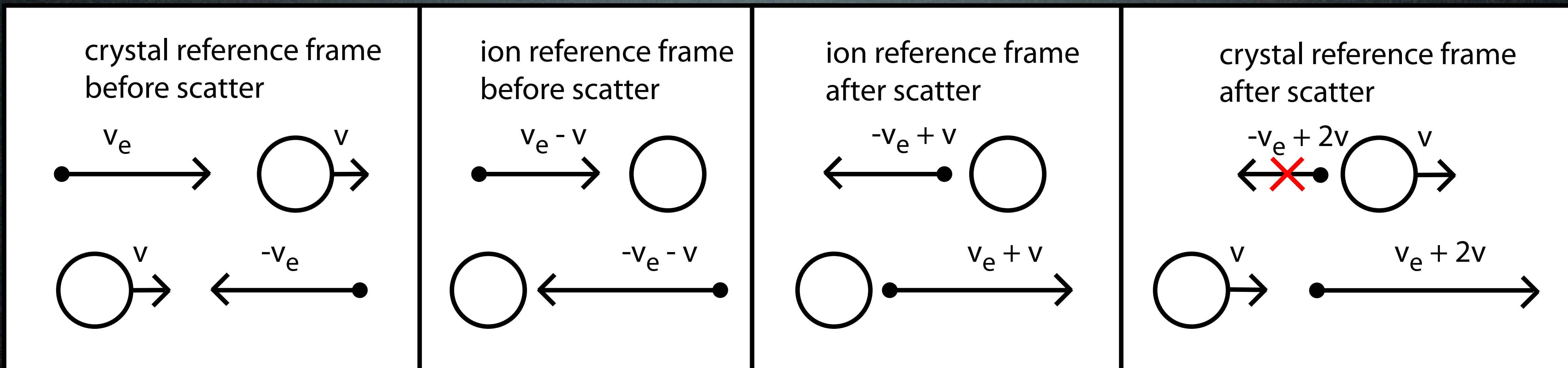

● electron

○ ion

Ion-electron interactions are via a potential and hence can only change the direction of the electron velocity in the ion reference frame.

Two hypothetical ion-electron interactions, shown before and after the scatter and in the crysal and ion reference frames. In the parallel interaction, the final electron velocity is too small to scatter to an unoccupied region outside of the Fermi sphere and is forbidden. In the anti-parallel process, the electron can be scatterd to an unoccupied state outside of the Fermi sphere.

Green: Region in Fermi sphere in which ion-electron interaction can scatter electrons to unoccupied region outside of sphere (allowed)

Red: Region in Fermi sphere in which ion-electron interaction can scatter electrons to occupied region inside of sphere (fobidden)

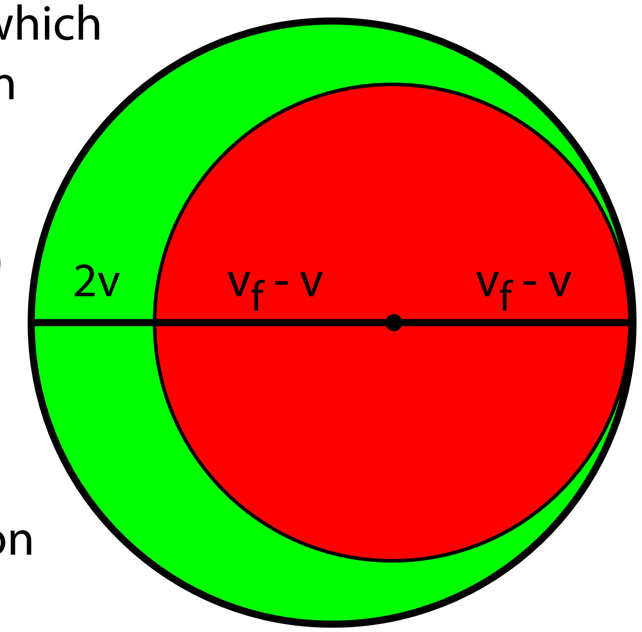

Lindhard Theory

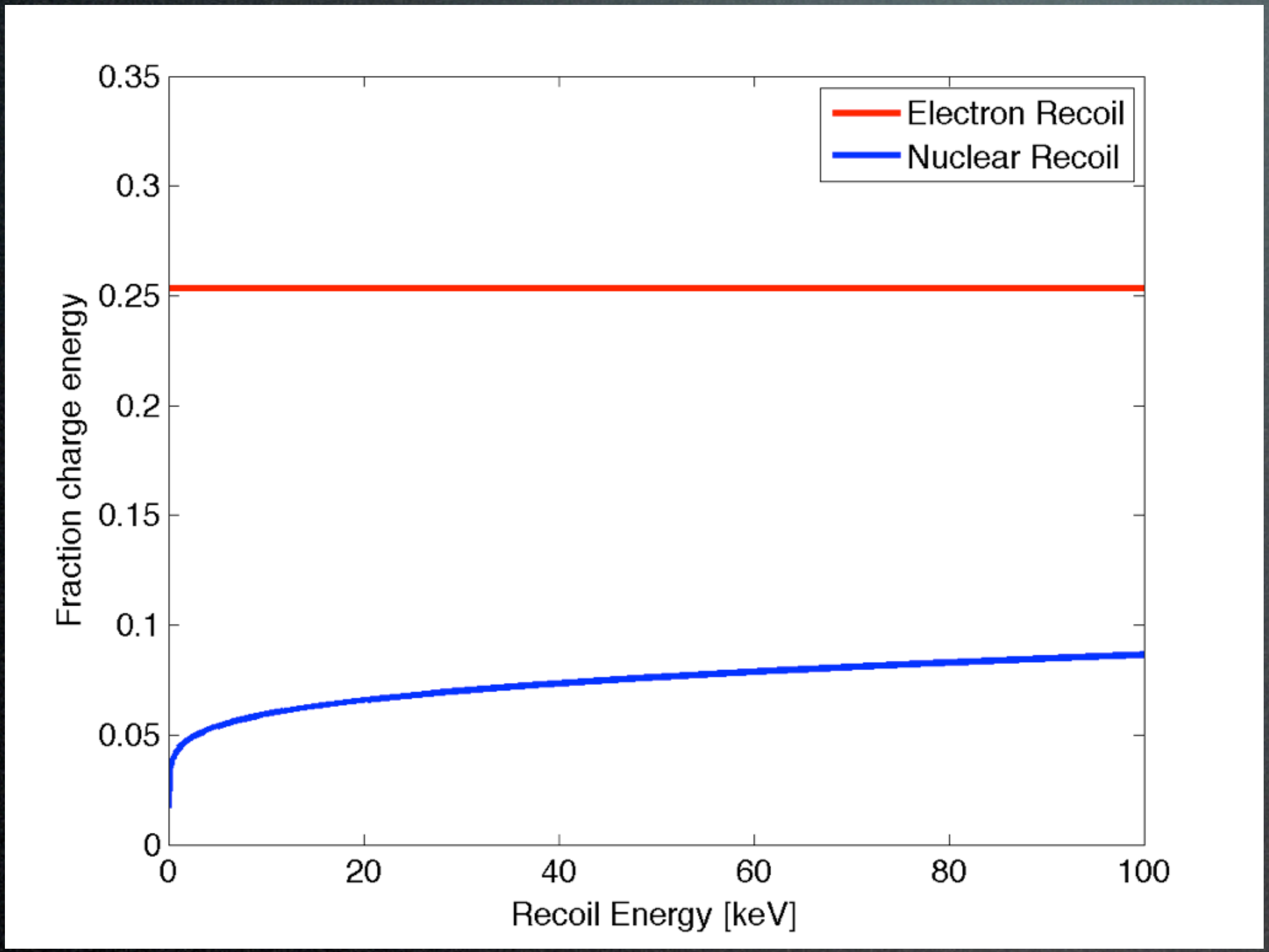

- $\sigma_{lattice} \sim V^{-2}$ (Rutherford scattering)
- $\sigma_{electron} \sim V$ (Accessible electron states)

Charge Transport

100x33 mm iZIP
E-Field

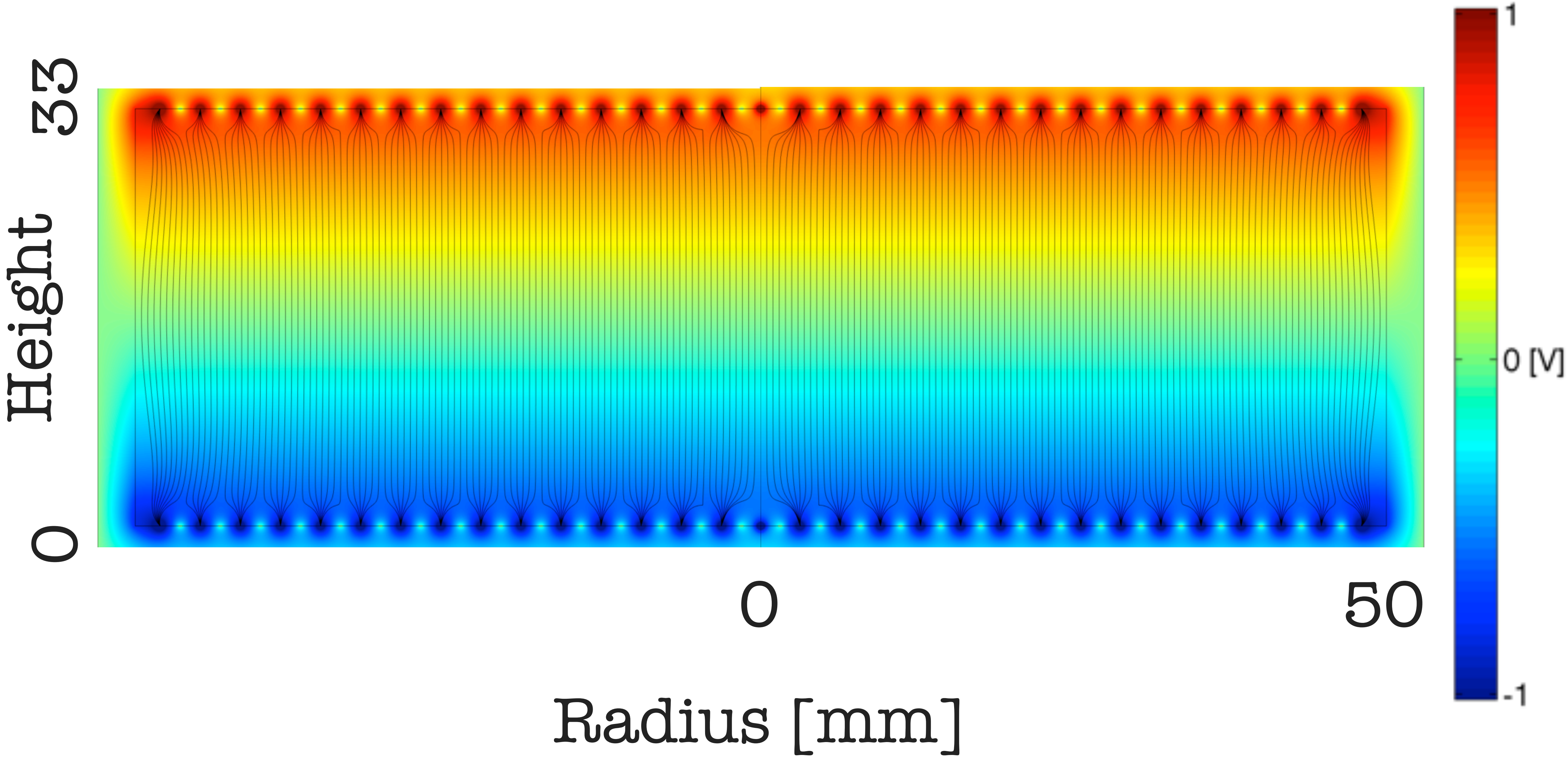

Germanium Band Structure

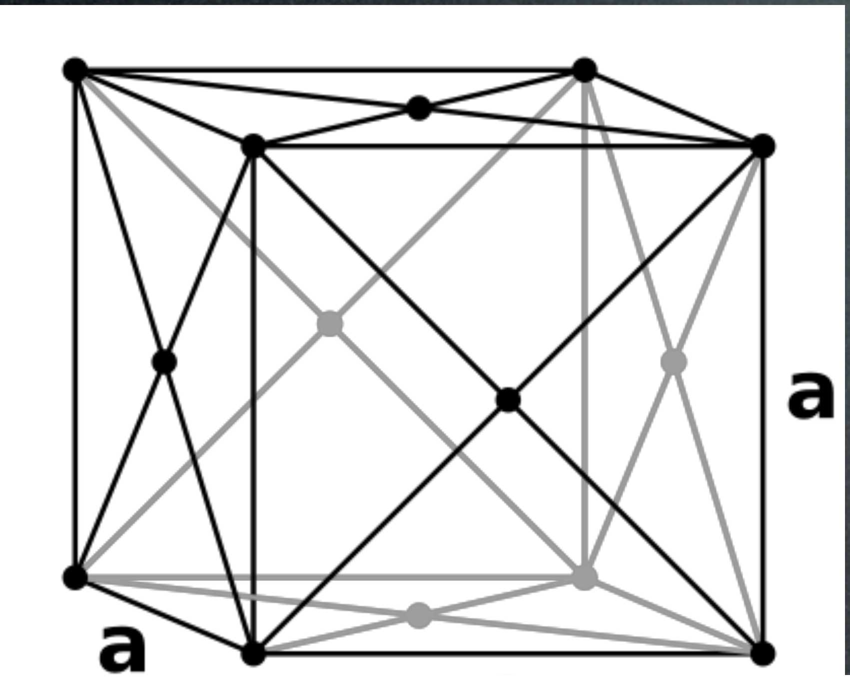

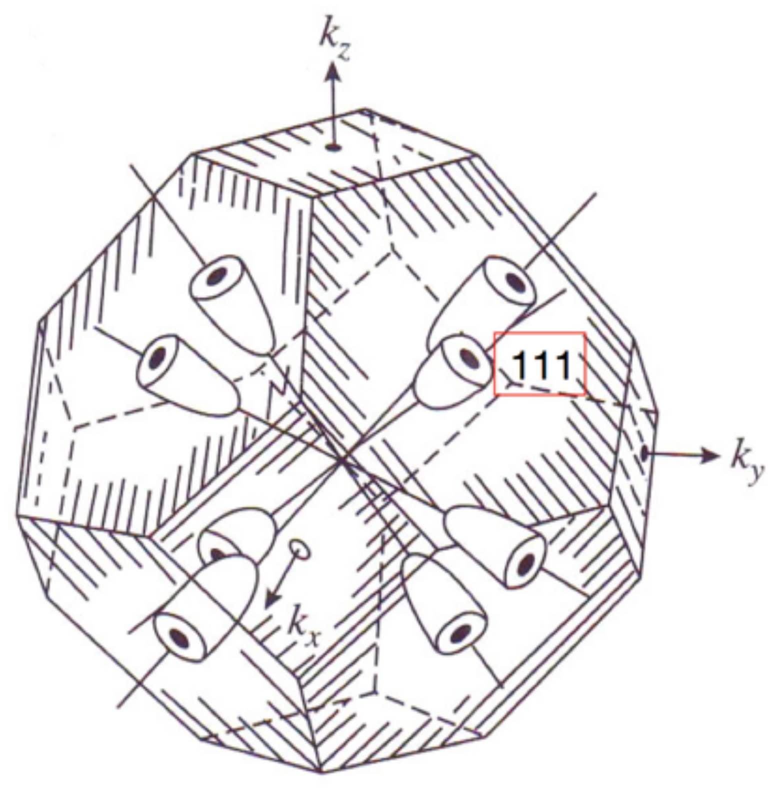

L valleys of Ge

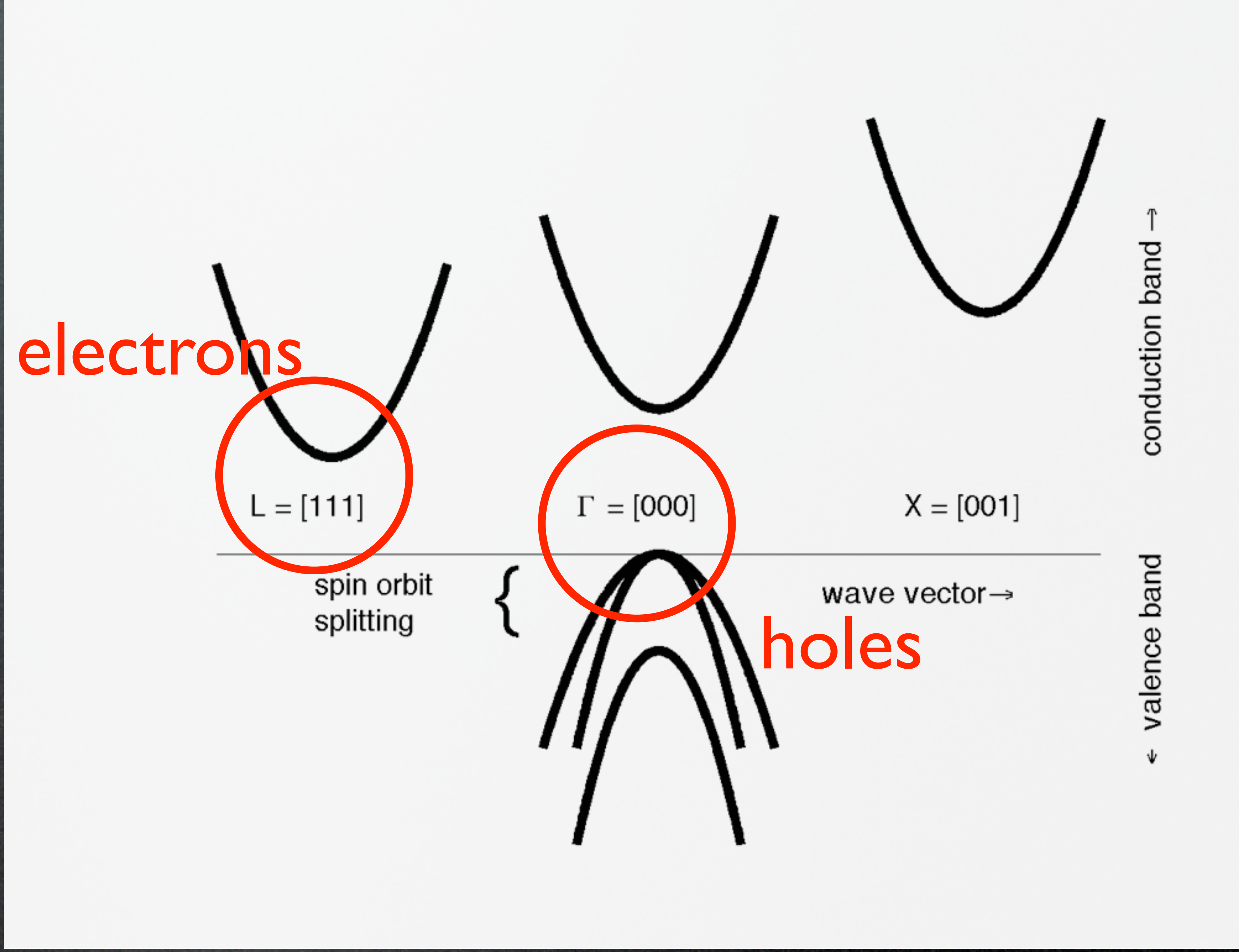

Electron Mass Tensor

- Holes exist in the Γ band with mass scalar, $m = 0.35\ m_e$
- In germanium, electrons exist in the L band with mass tensor

$$m = \begin{pmatrix} 1.58 & 0 & 0 \\ 0 & 0.081 & 0 \\ 0 & 0 & 0.081 \end{pmatrix} m_e$$

in the longitudinal (111), transverse, transverse basis

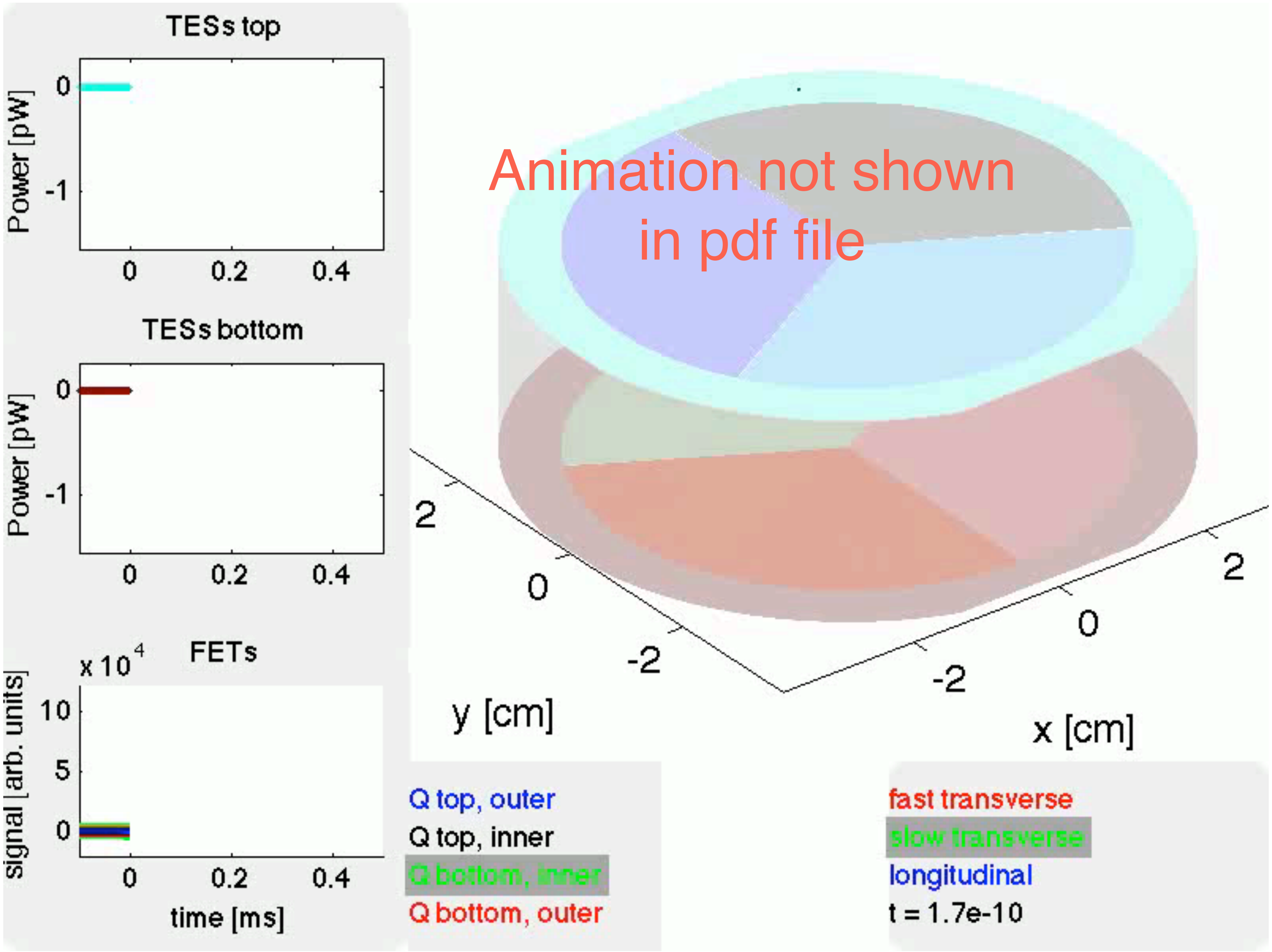

TESs top
Power [pW]
0
-1
0
0.2
0.4
TESs bottom
Power [pW]
0
-1
0
0.2
0.4
FETs
x 10^4
signal [arb. units]
10
5
0
0
0.2
0.4
time [ms]
Animation not shown
in pdf file
2
0
-2
y [cm]
2
0
-2
x [cm]
Q top, outer
Q top, inner
Q bottom, inner
Q bottom, outer
fast transverse
slow transverse
longitudinal
t = 1.7e-10

Inter-valley Scattering

- 4 different valleys $[111]$, $[\bar{1}11]$, $[1\bar{1}1]$, $[\bar{1}\bar{1}1]$
- Can scatter between valleys at high energy or near impurities

Edelweiss Measurement

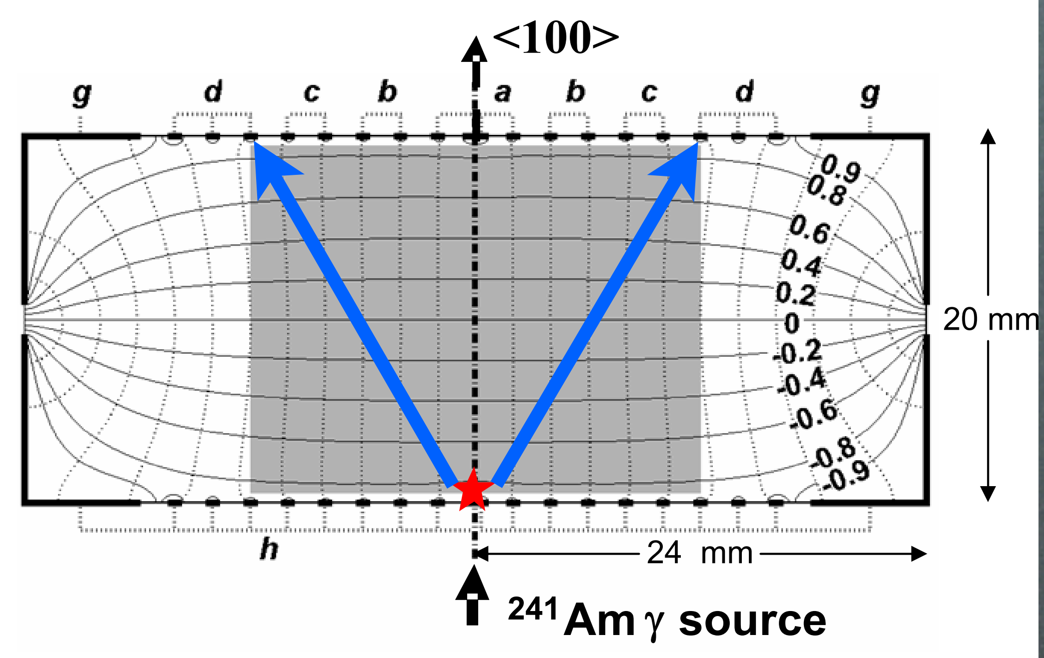

Signal entirely in **d** if no IV scattering

Increased signal in **a** with increased field

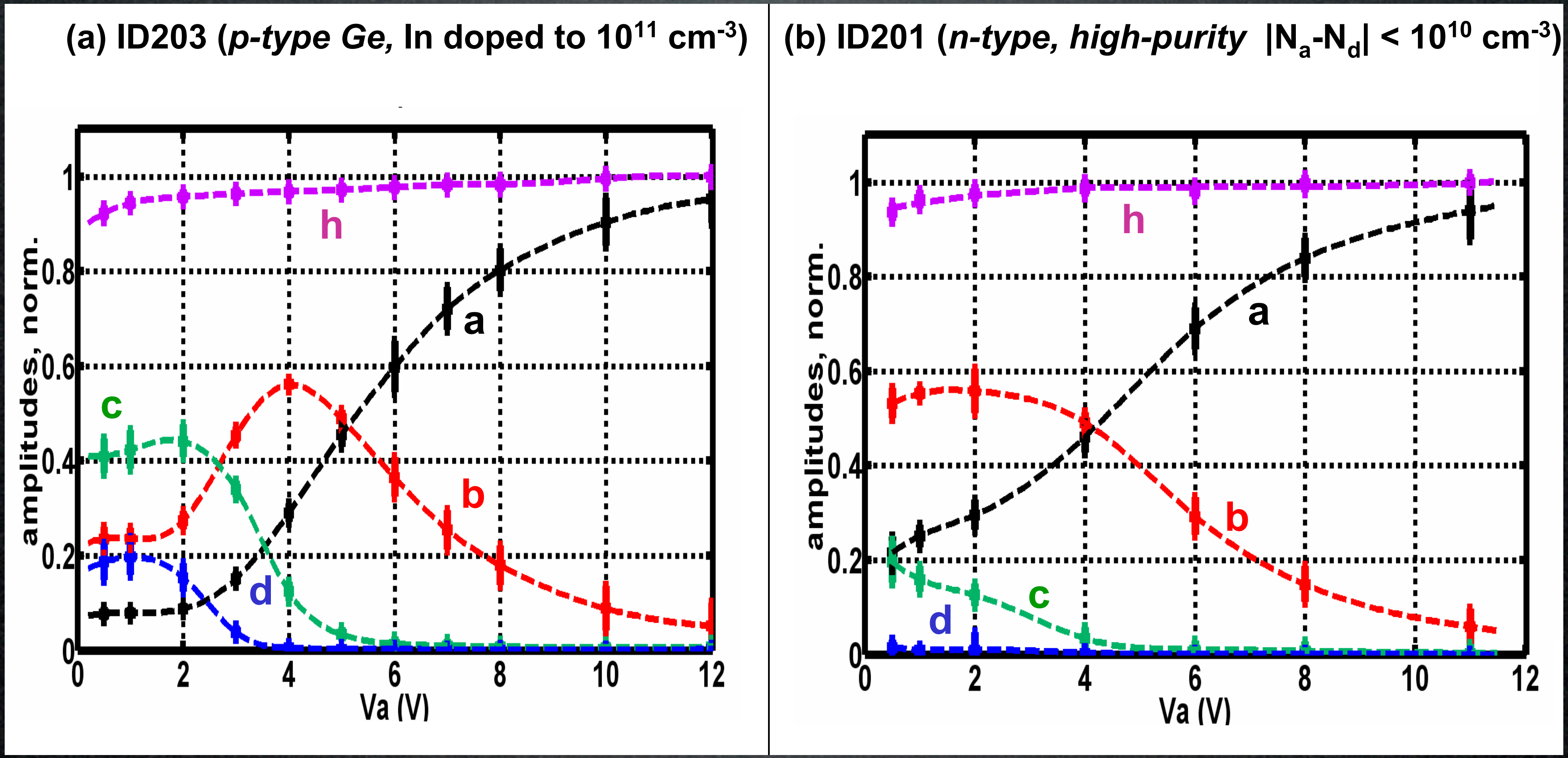

Edelweiss Measurement

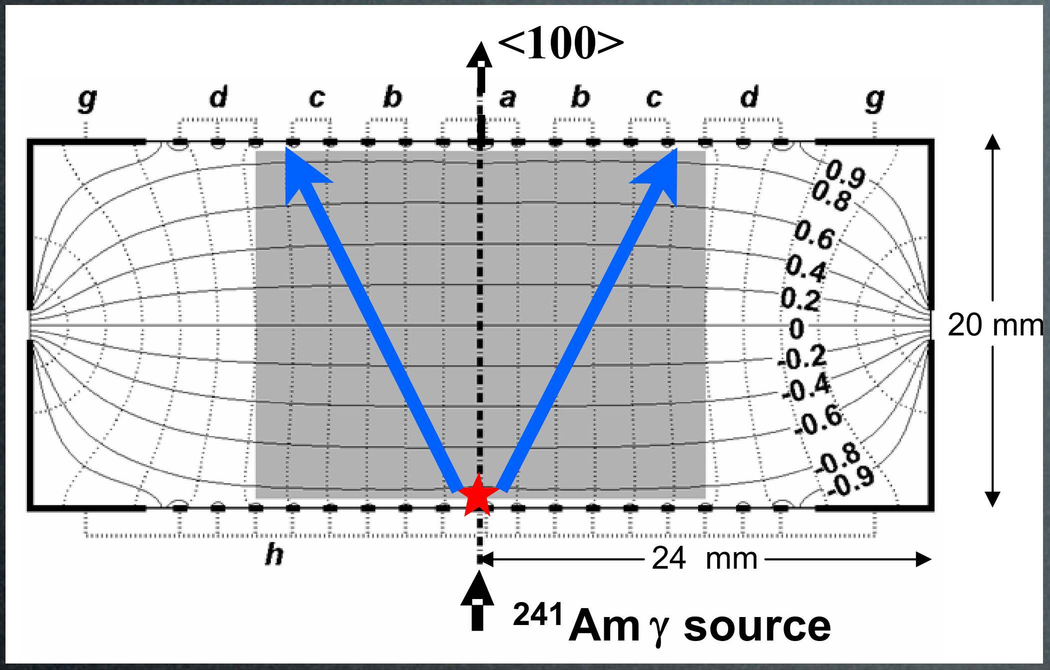

Signal entirely in **d** if no IV scattering

Increased signal in **a** with increased field

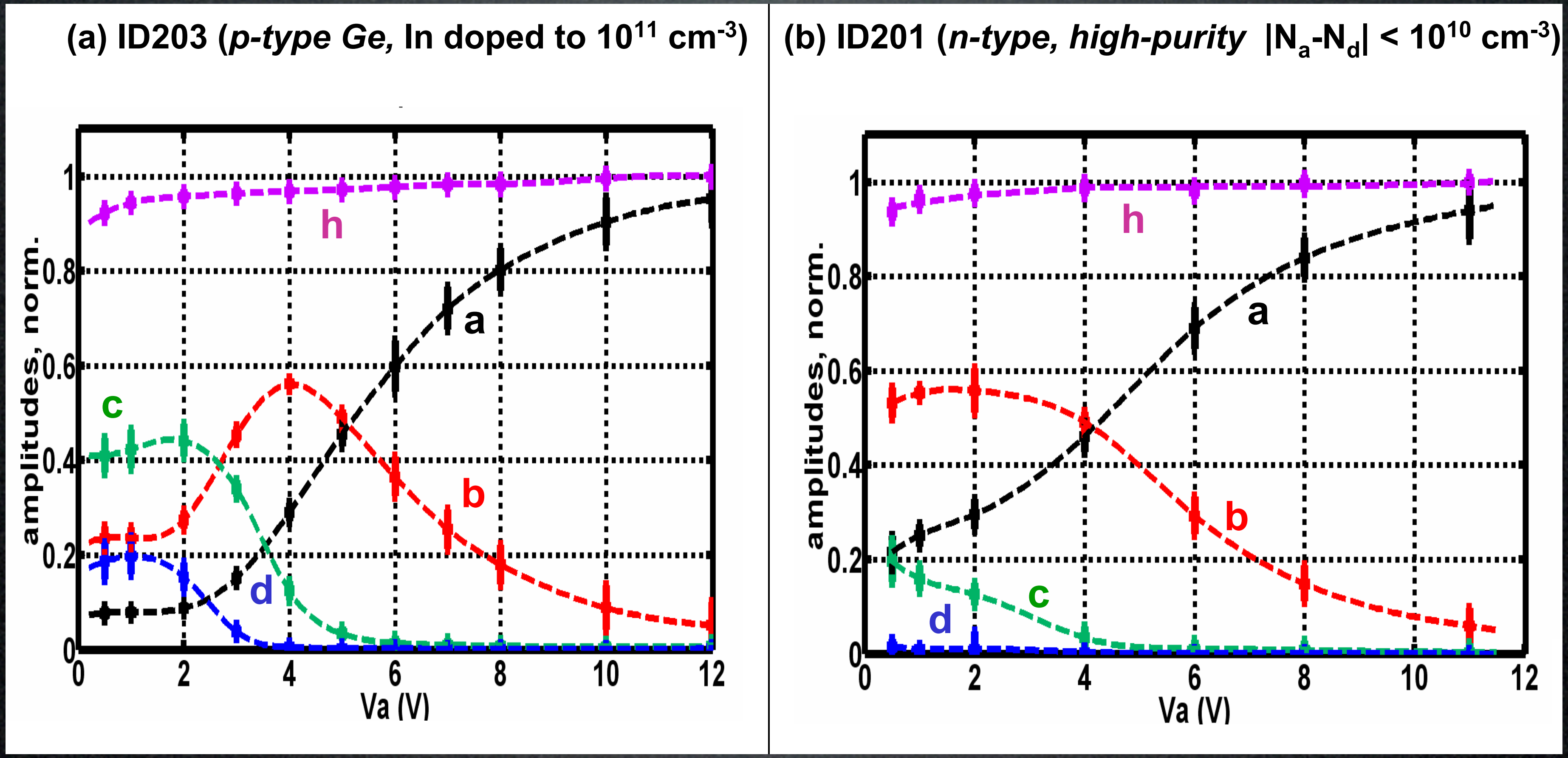

Edelweiss Measurement

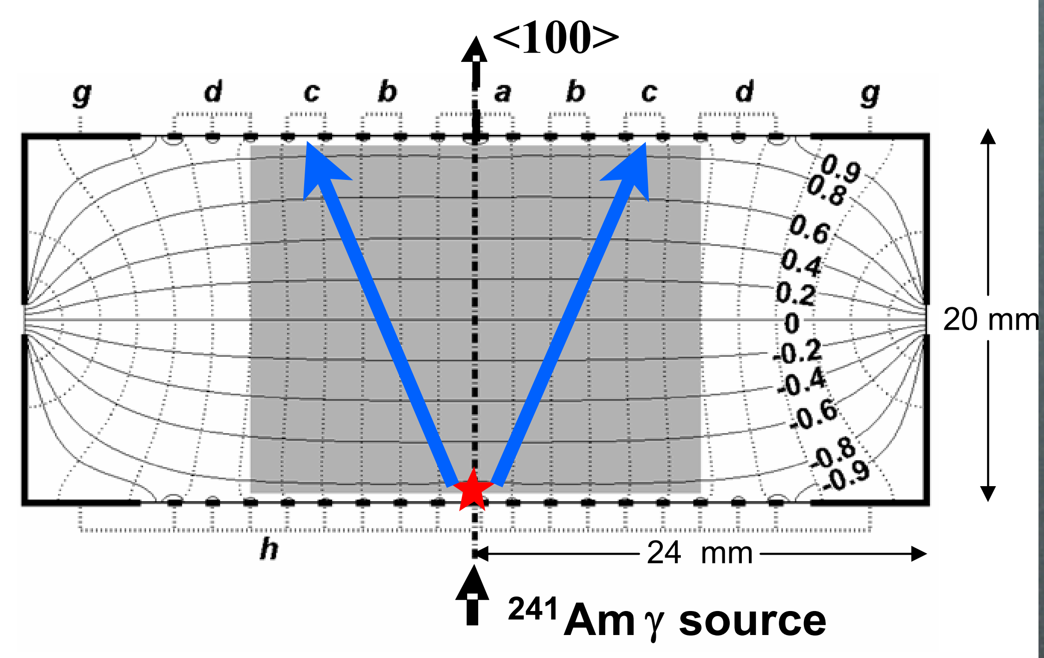

Signal entirely in **d** if no IV scattering

Increased signal in **a** with increased field

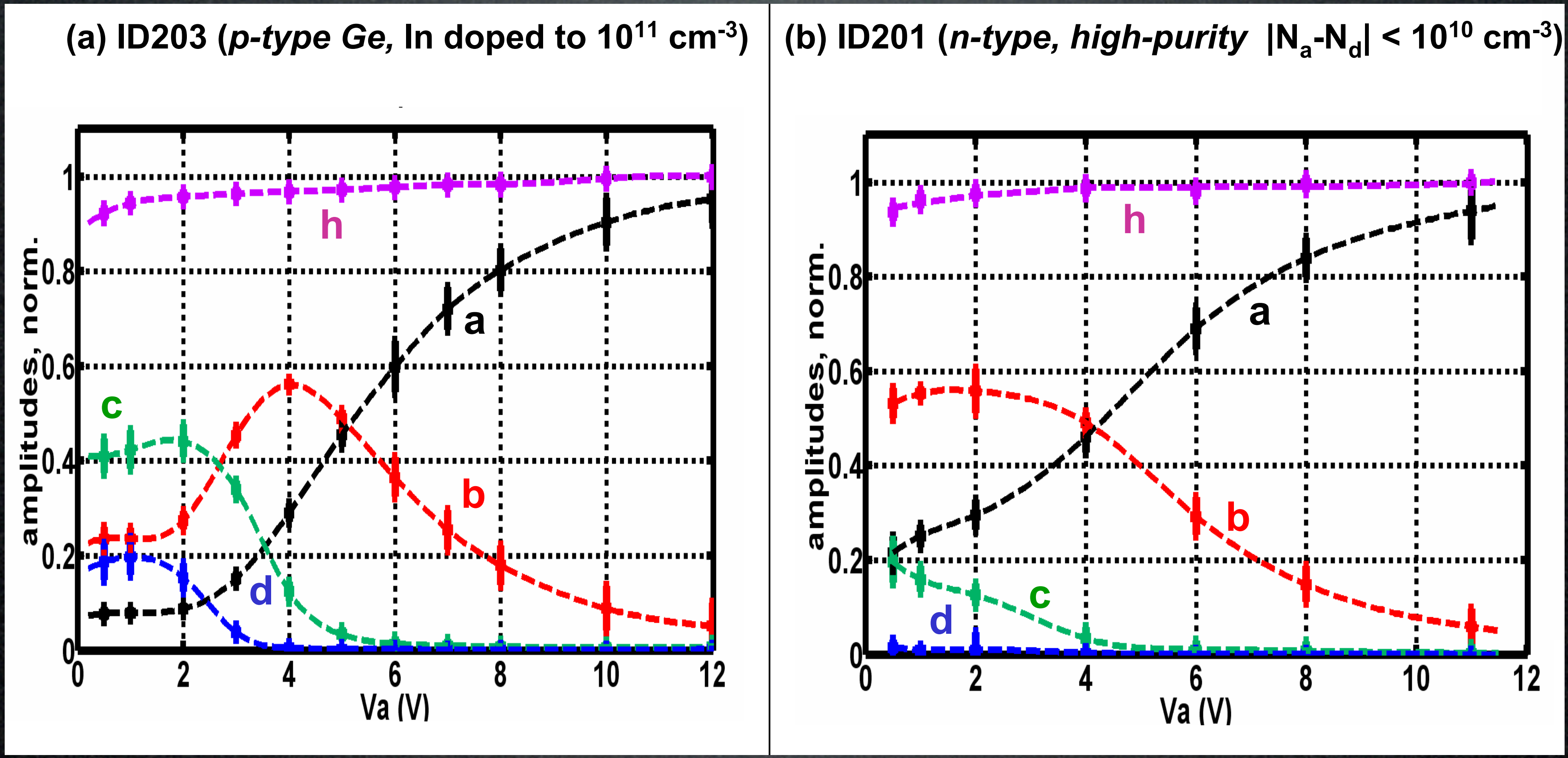

Edelweiss Measurement

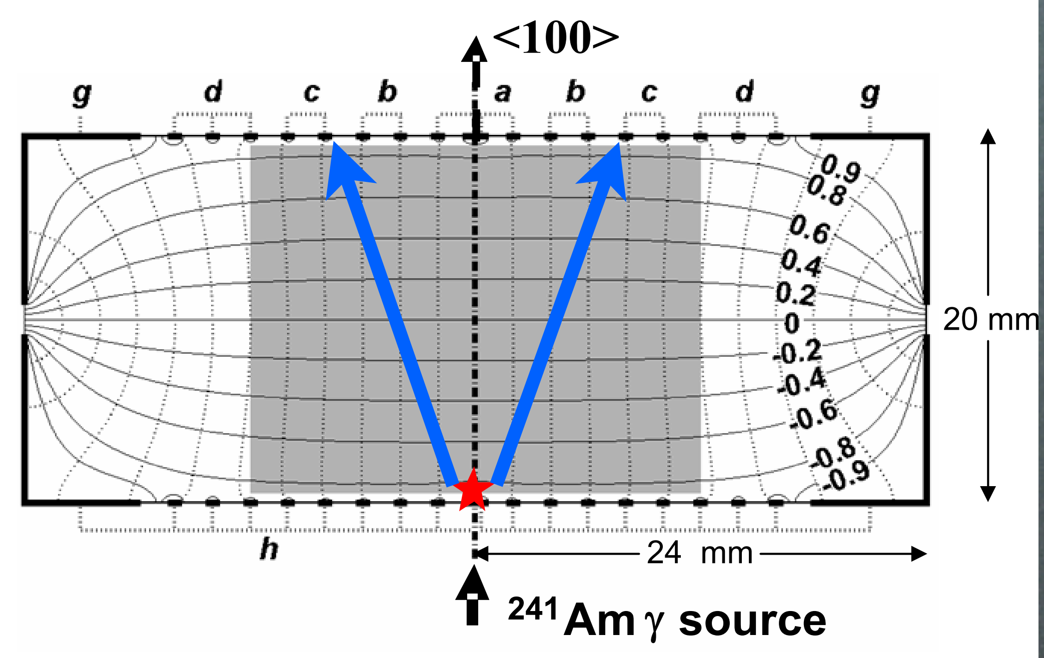

Signal entirely in **d** if no IV scattering

Increased signal in **a** with increased field

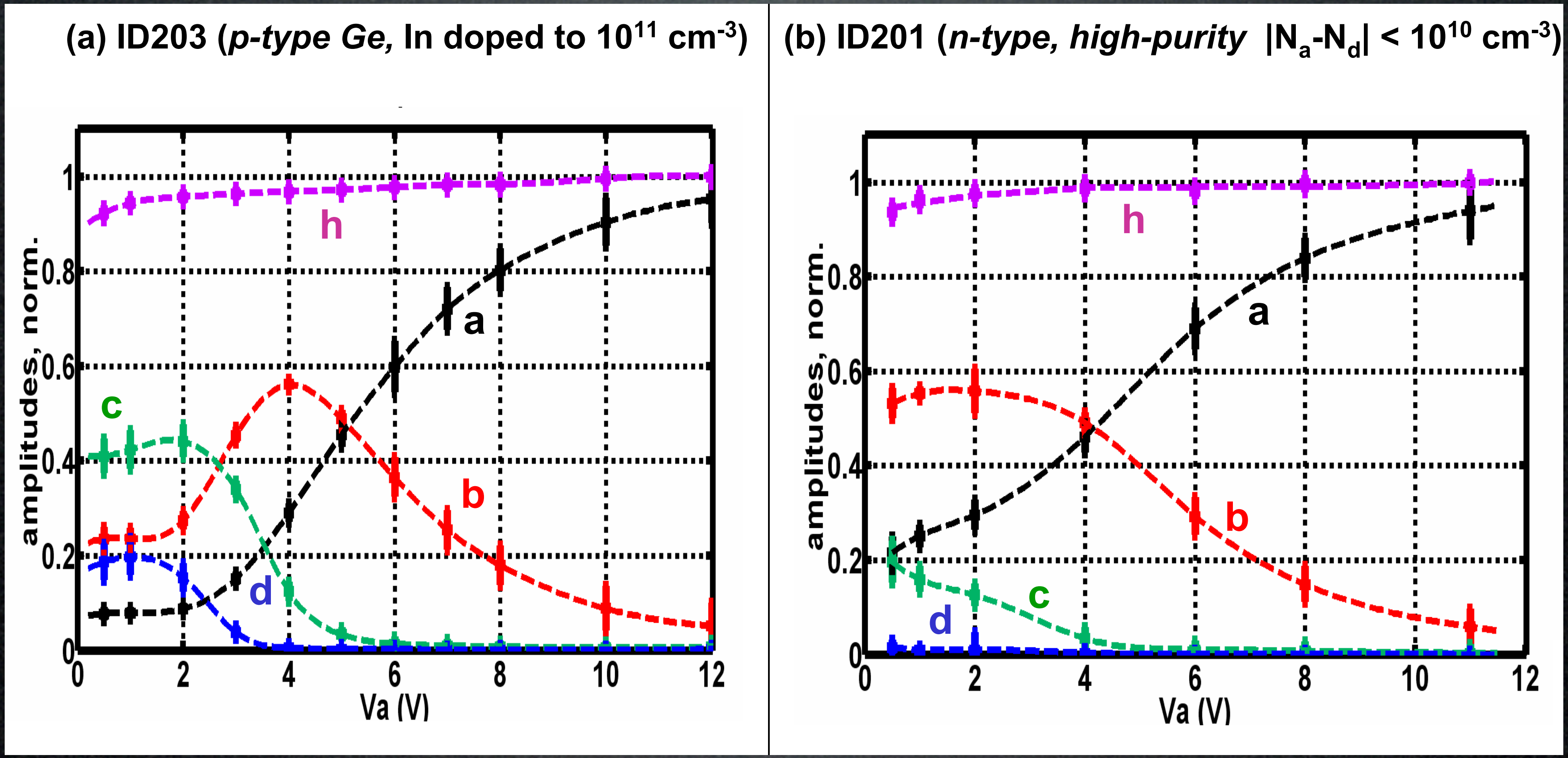

Edelweiss Measurement

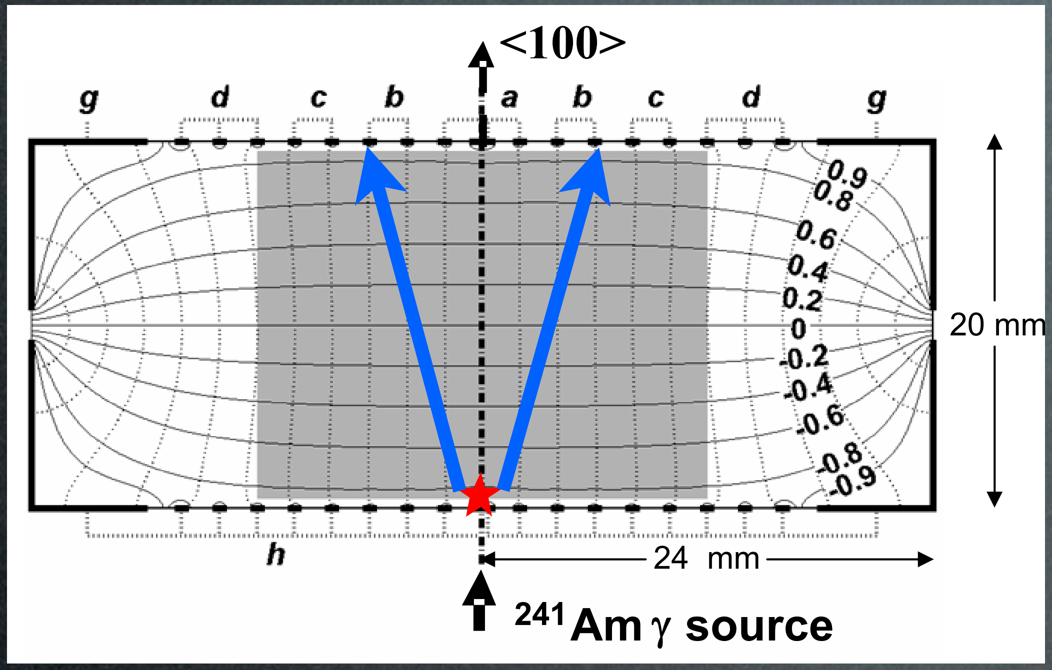

Signal entirely in **d** if no IV scattering

Increased signal in **a** with increased field

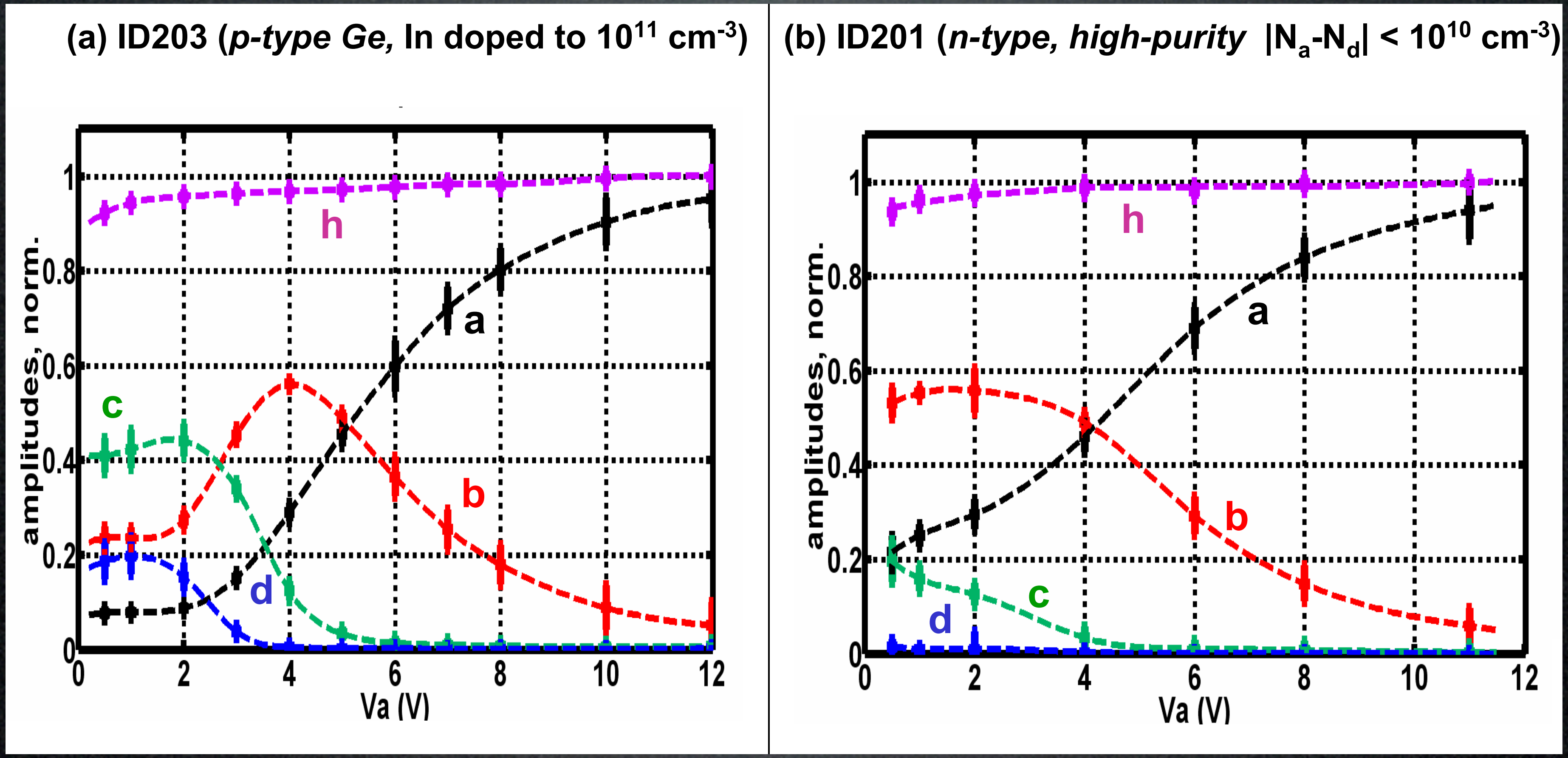

Edelweiss Measurement

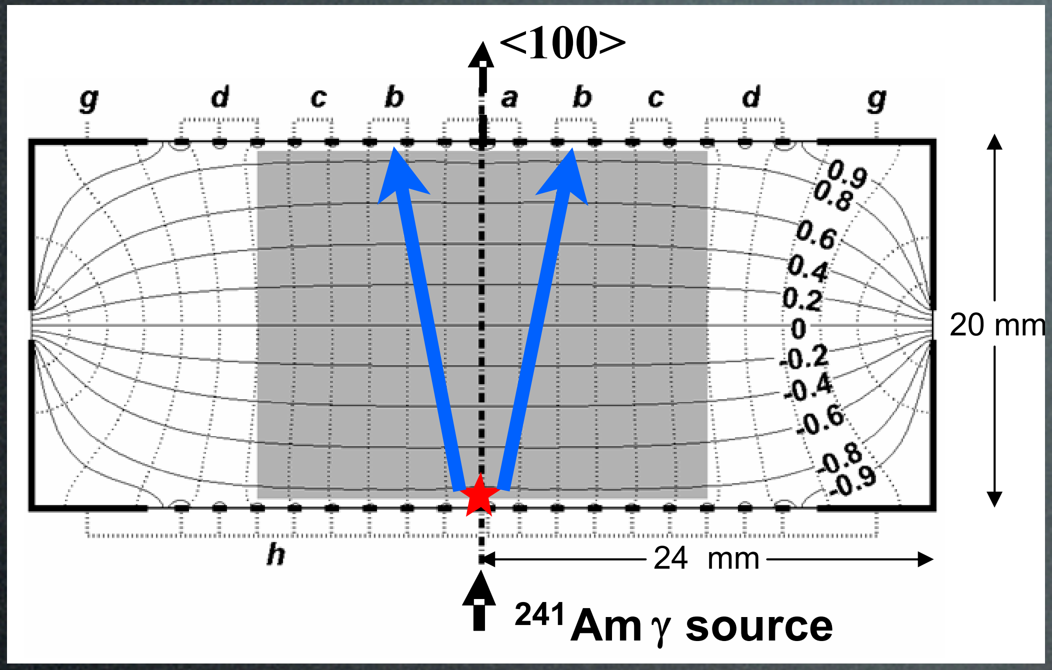

Signal entirely in **d** if no IV scattering

Increased signal in **a** with increased field

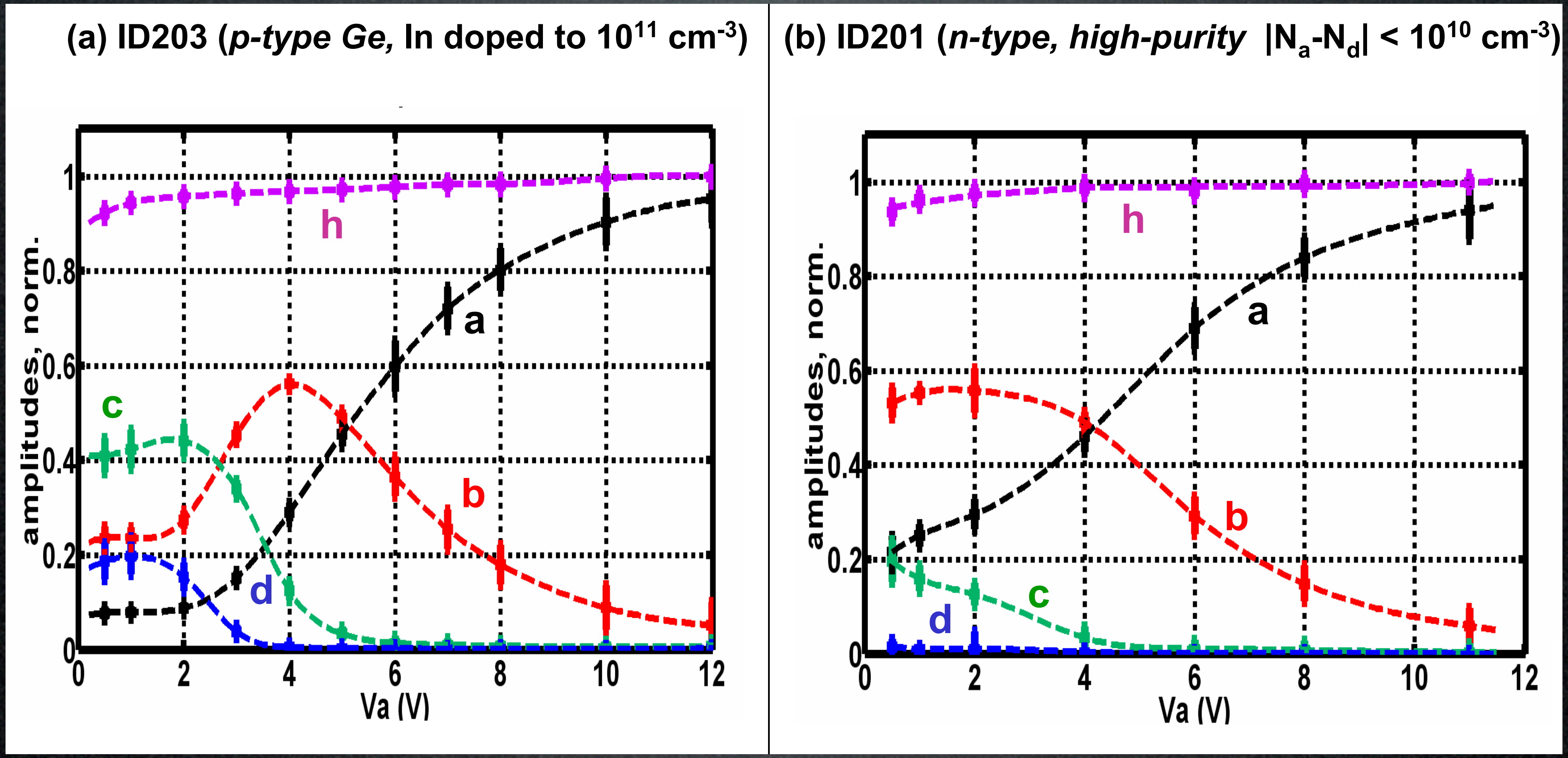

Edelweiss Measurement

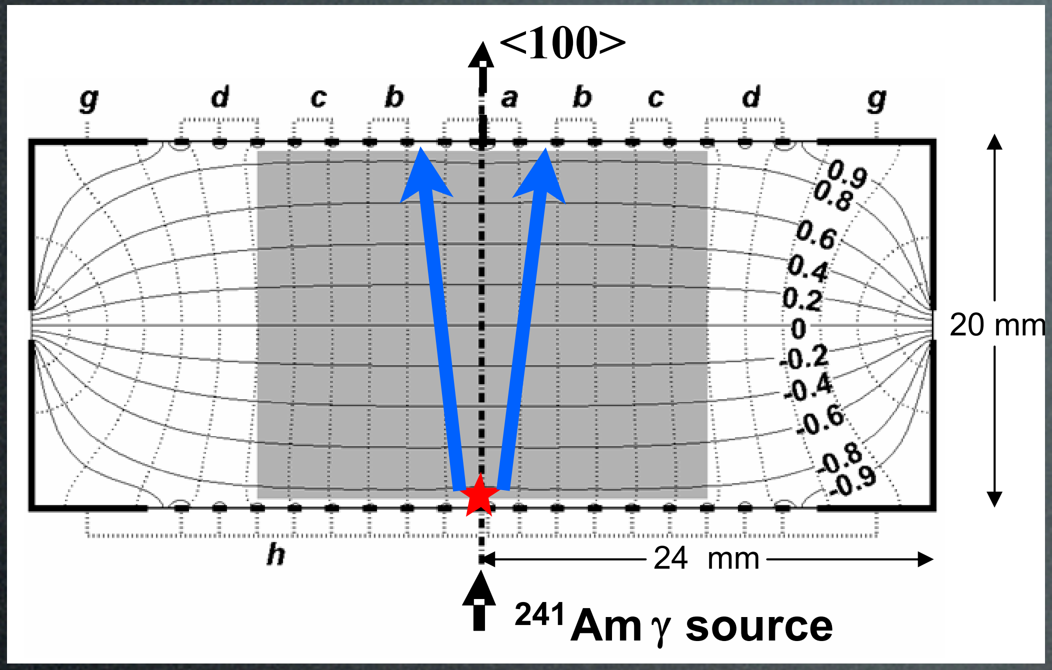

Signal entirely in **d** if no IV scattering

Increased signal in **a** with increased field

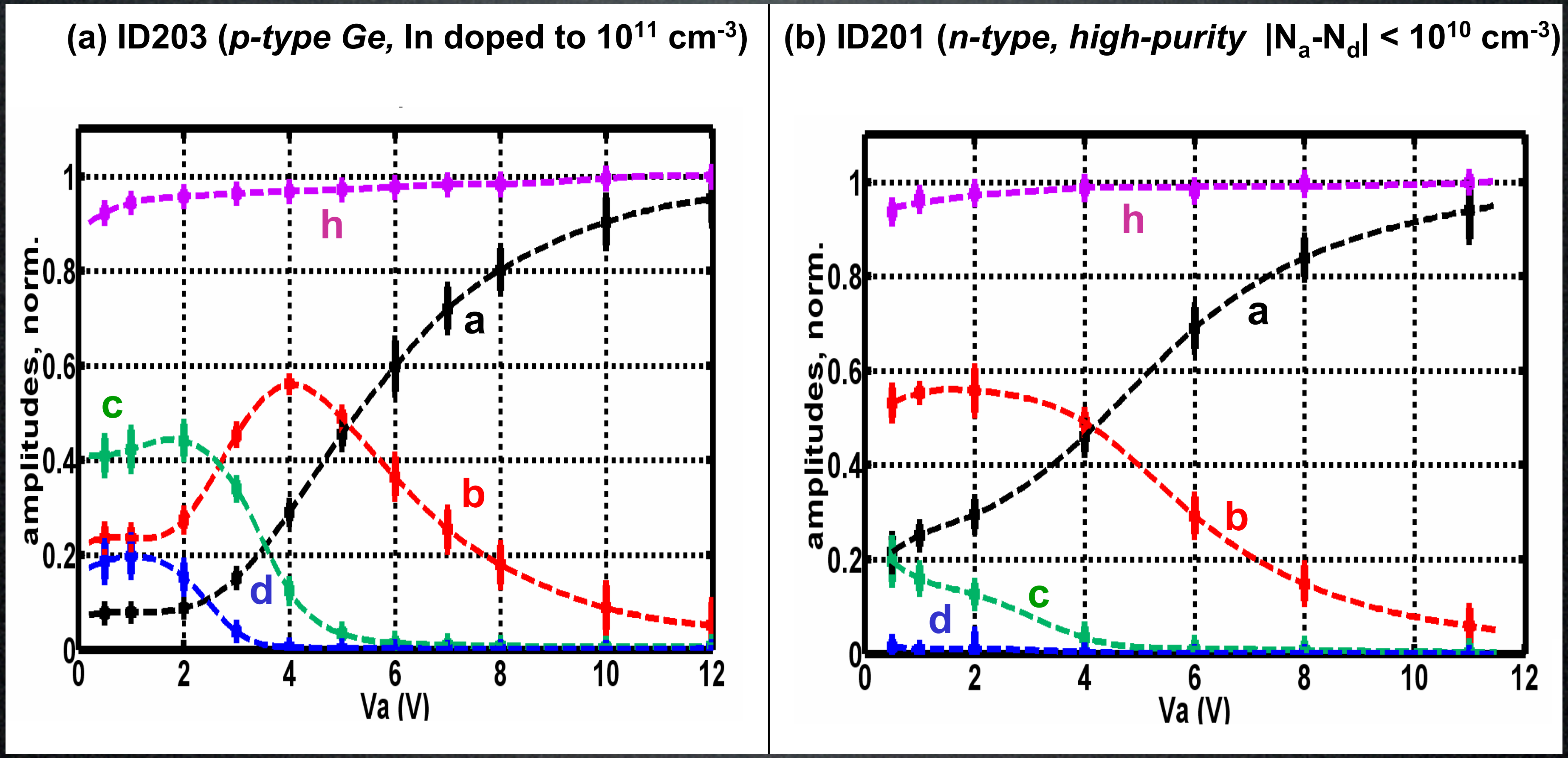

Edelweiss Measurement

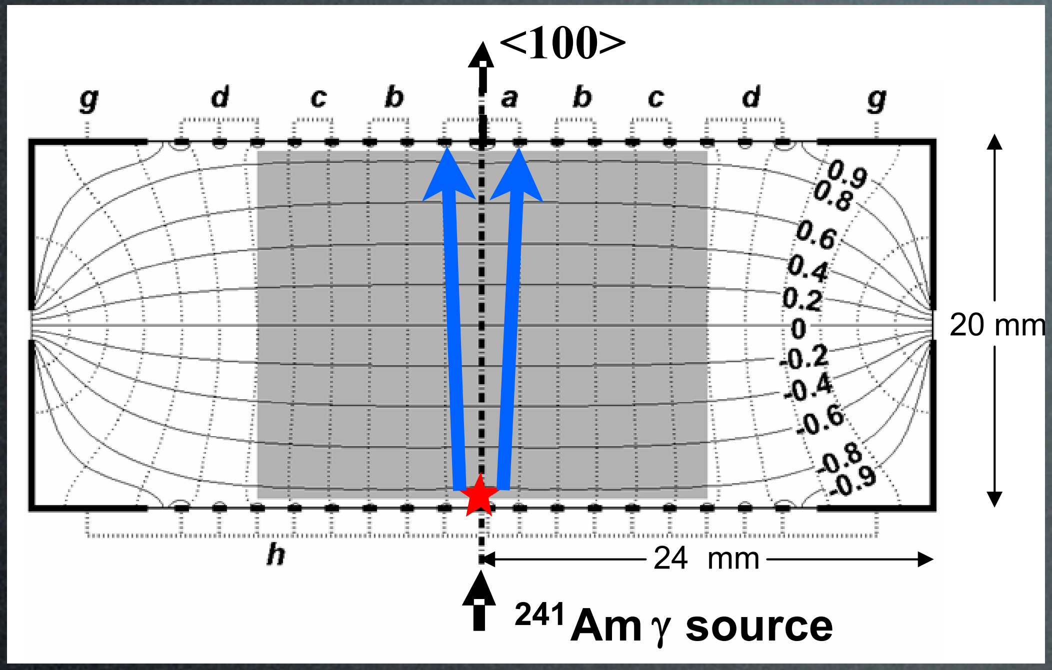

Signal entirely in **d** if no IV scattering

Increased signal in **a** with increased field

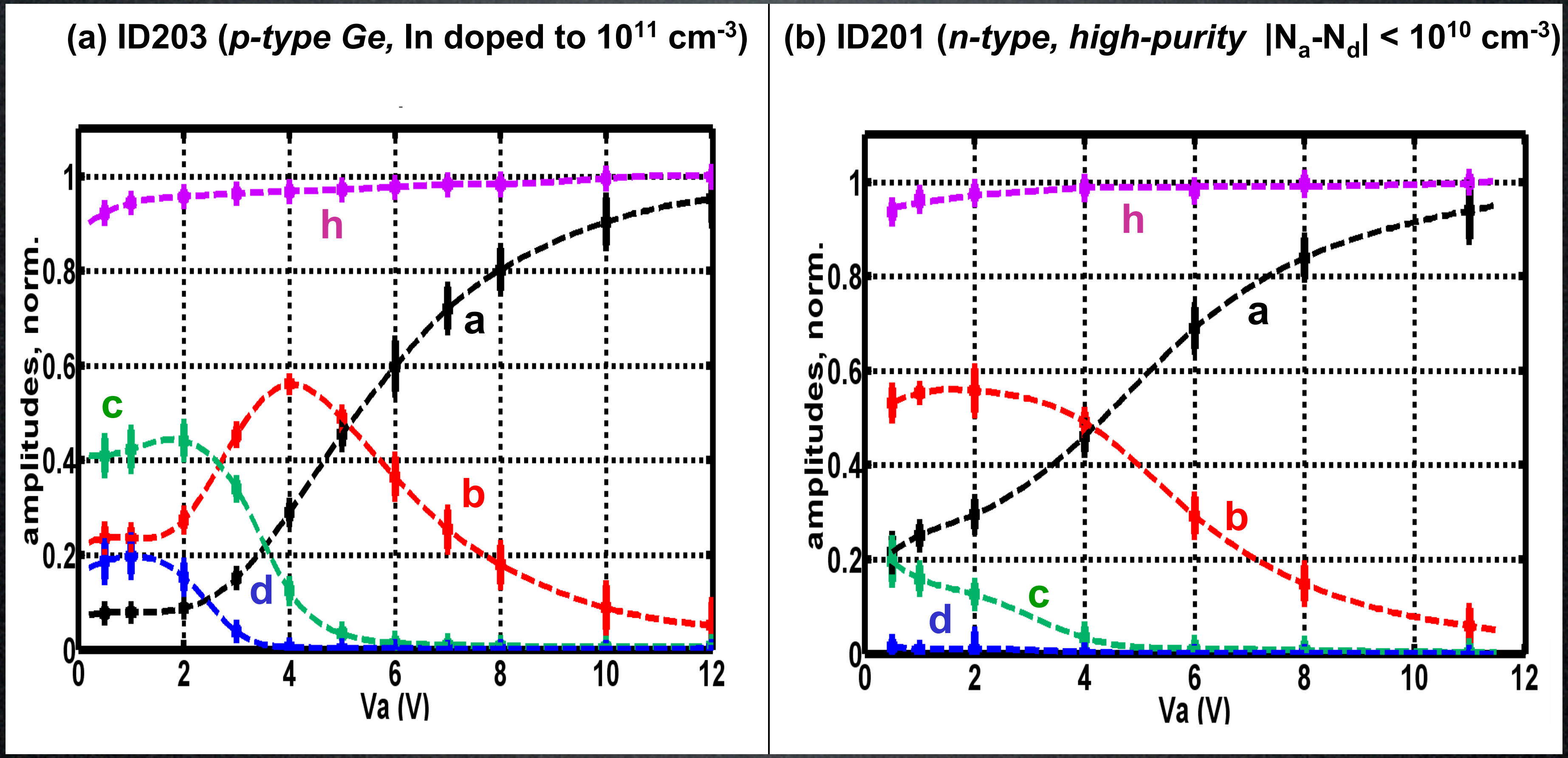

Signal vs Bias Voltage

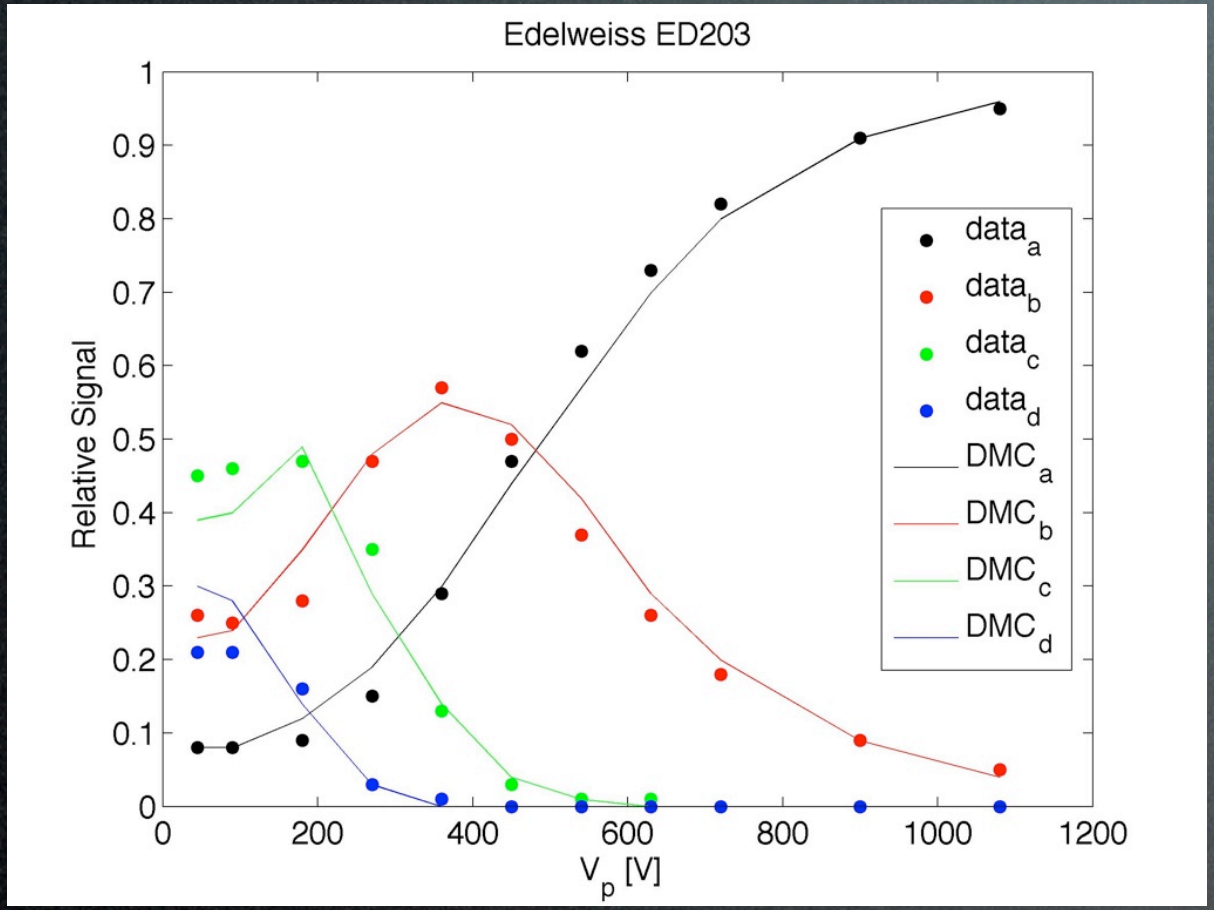

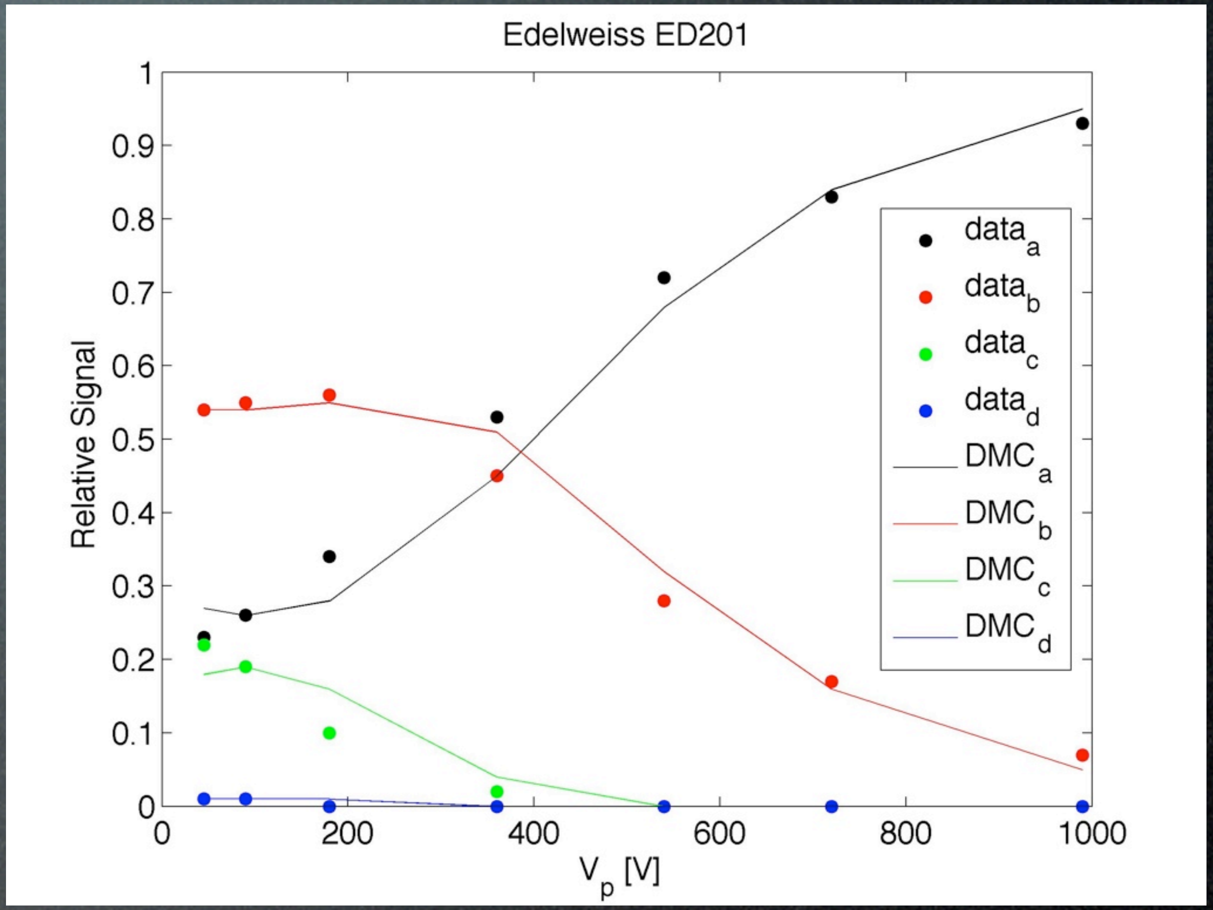

- $\sigma = 6.72\text{e-}2\ [s^{-1}]\ (E_0{}^2 + |E_{HV}|^2)^{3.24/2}$
- $E_{0,ED203} = 217$, $E_{0,ED201} = 352$

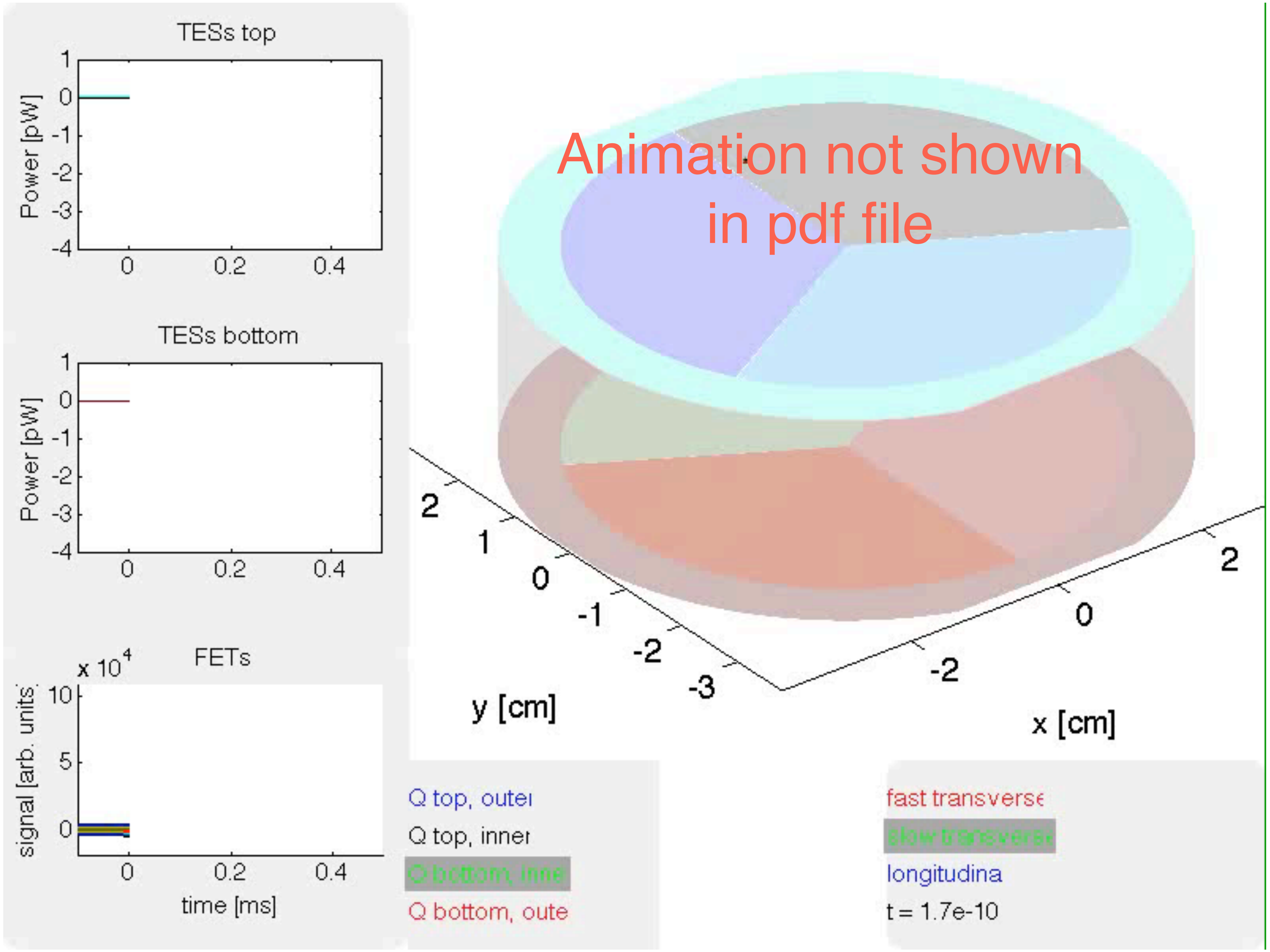

TESs top
Power [pW]
TESs bottom
Power [pW]
FETs
x 10^4
signal [arb. units]
time [ms]
Animation not shown
in pdf file
y [cm]
x [cm]
Q top, outer
Q top, inner
Q bottom, inne
Q bottom, oute
fast transverse
slow transverse
longitudina
t = 1.7e-10

Charge Readout

Ramo-Shockley Potentials

$$\text{signal}_i(t) = \sum_j V_{i,\text{hole}_j}(t) - V_{i,\text{electron}_j}(t)$$

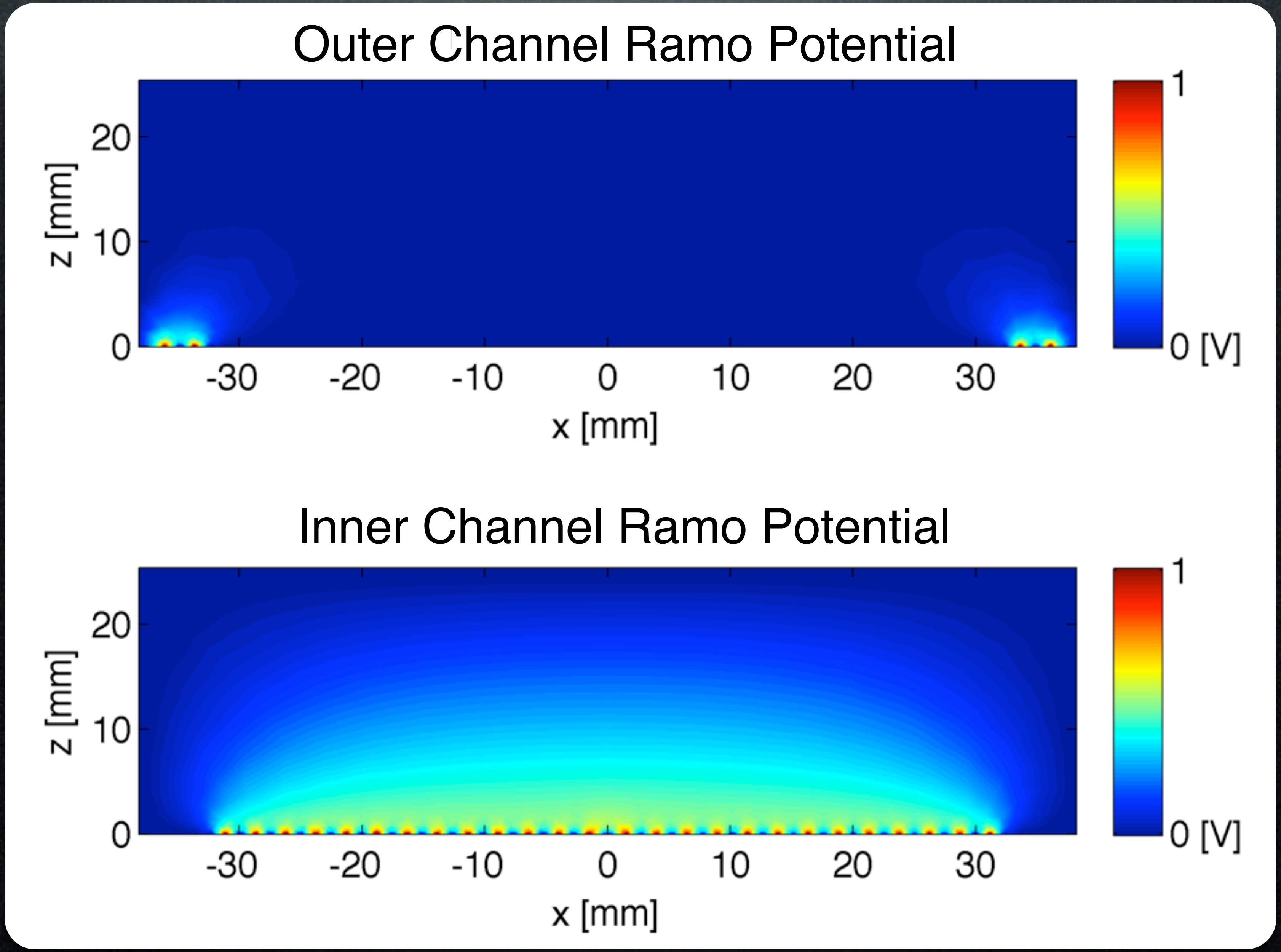

Tracking of Charges Through Ramo-Shockley Potentials

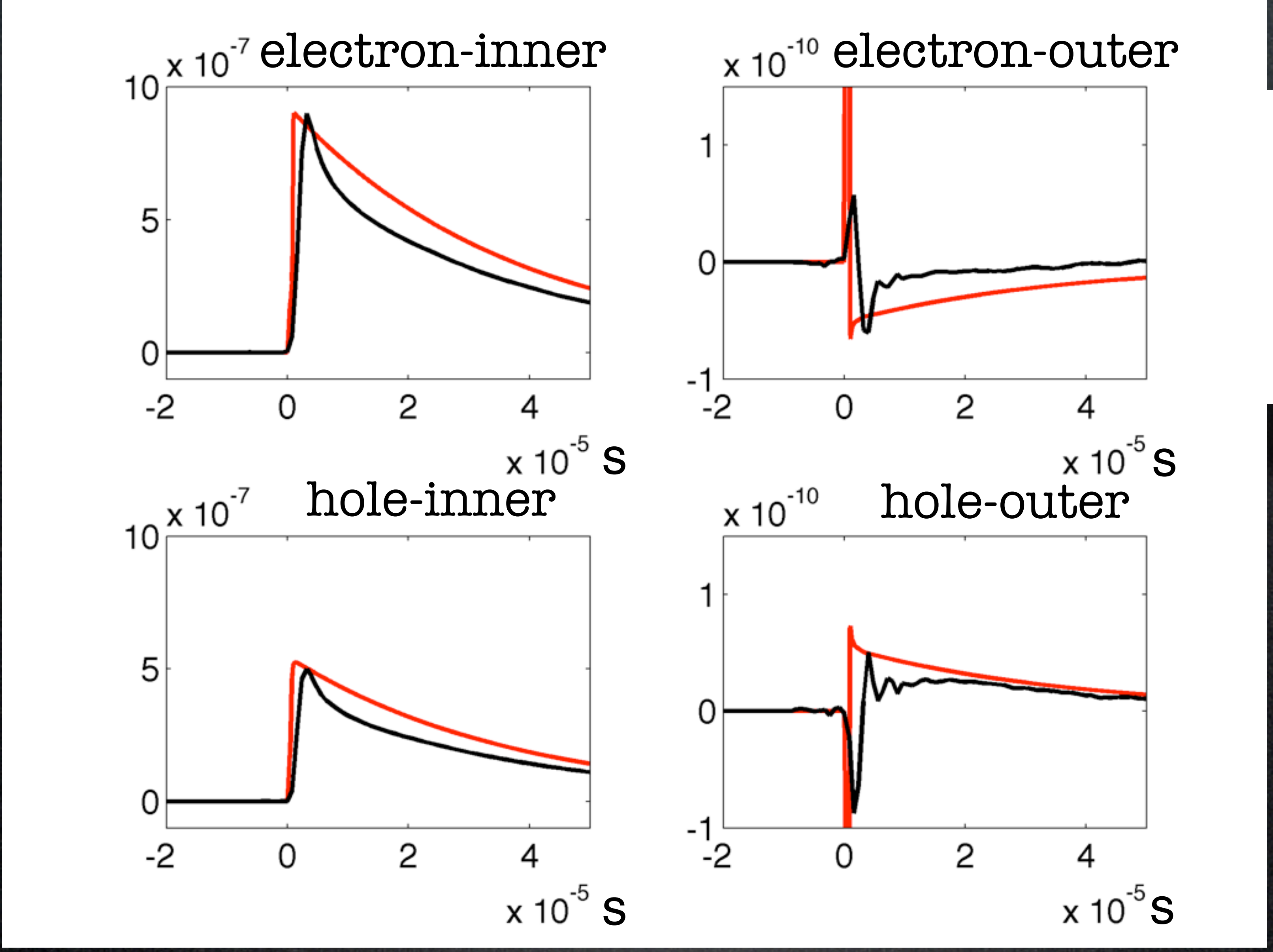

calibration

MC

Phonon Production

Lindhard Theory

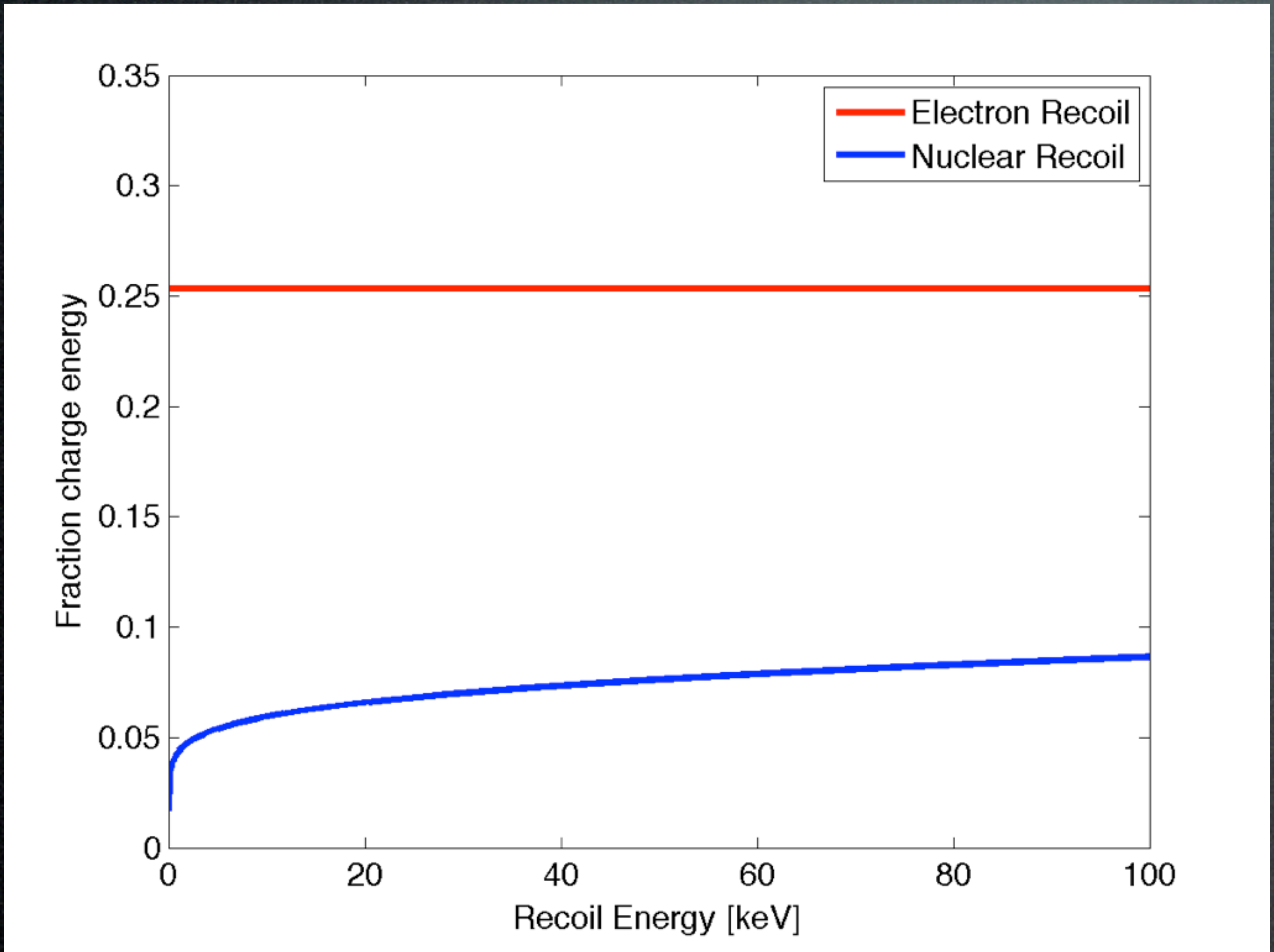

- Prompt phonons produced at Debye frequency.
- Details quickly wash out due to downconversion.

Neganov-Luke Phonons

$$P_{k,k'\pm q} = \frac{2\pi V}{\hbar}\left|< \overrightarrow{k} \pm \overrightarrow{q}|H|\overrightarrow{k} >\right|^2 \delta(E - E' \mp \hbar\omega)$$

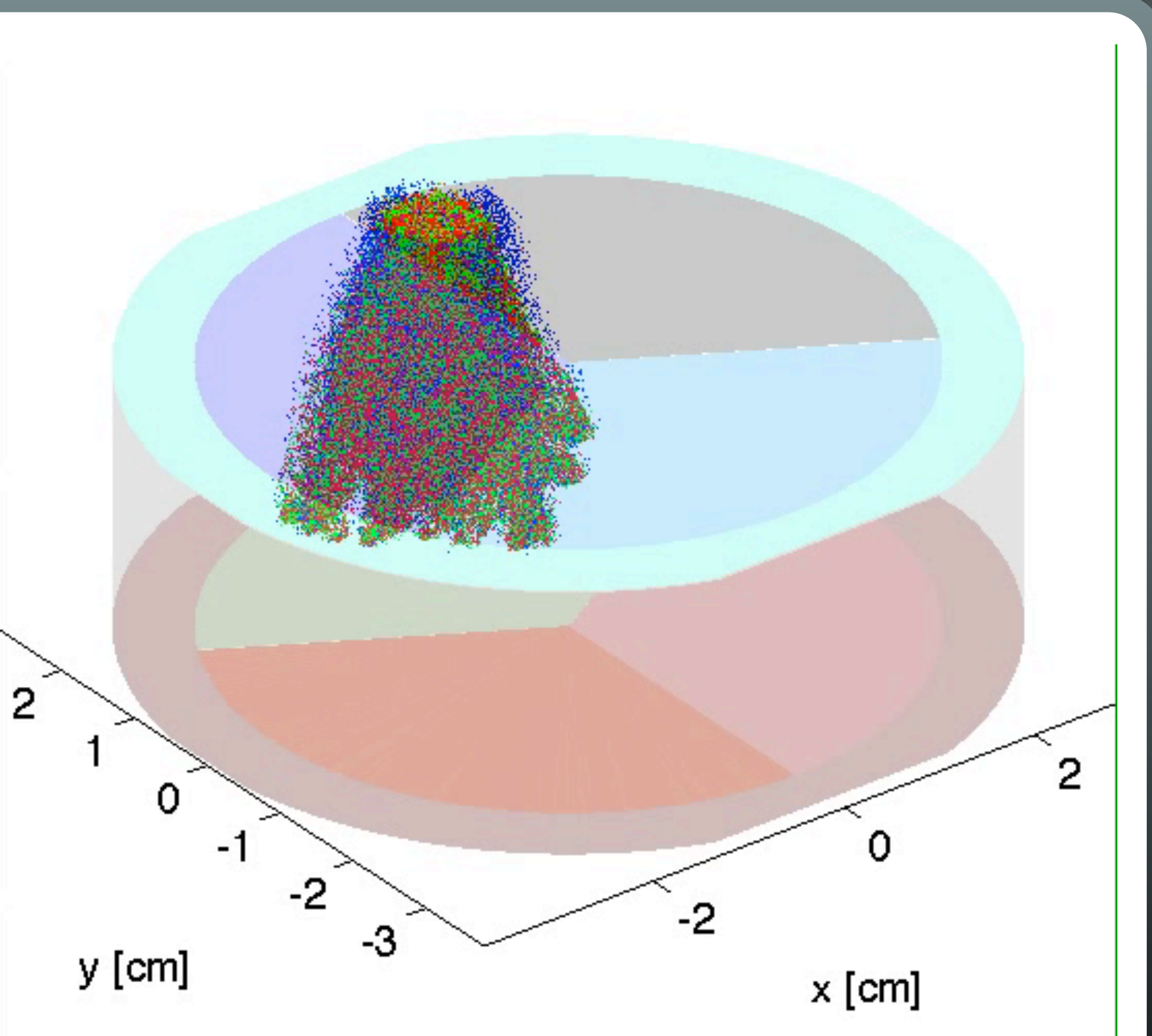

From Fermi's Golden Rule

Angles given by energy - momentum conservation

Neganov-Luke Phonons

- Ballistic and directed in ±z direction

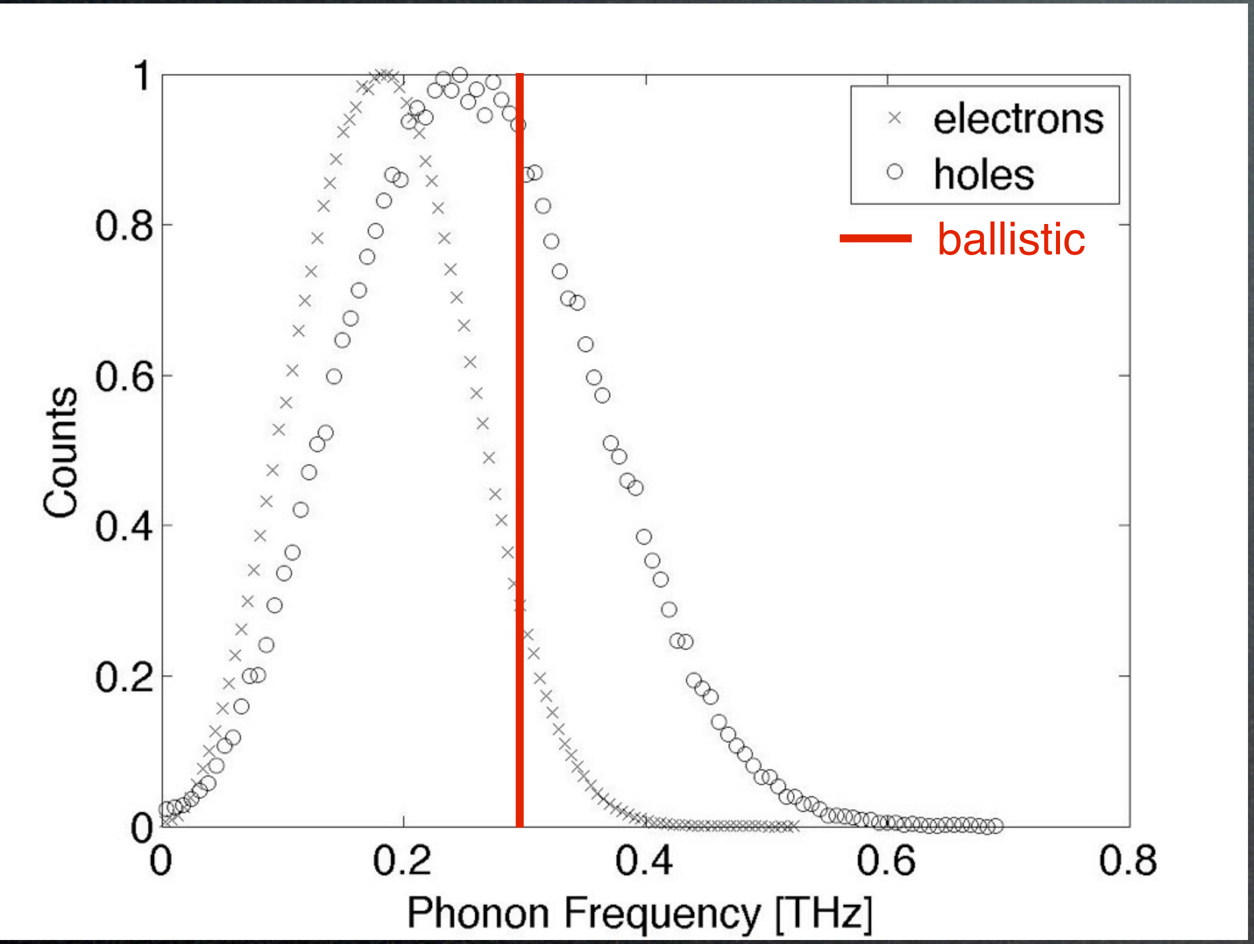

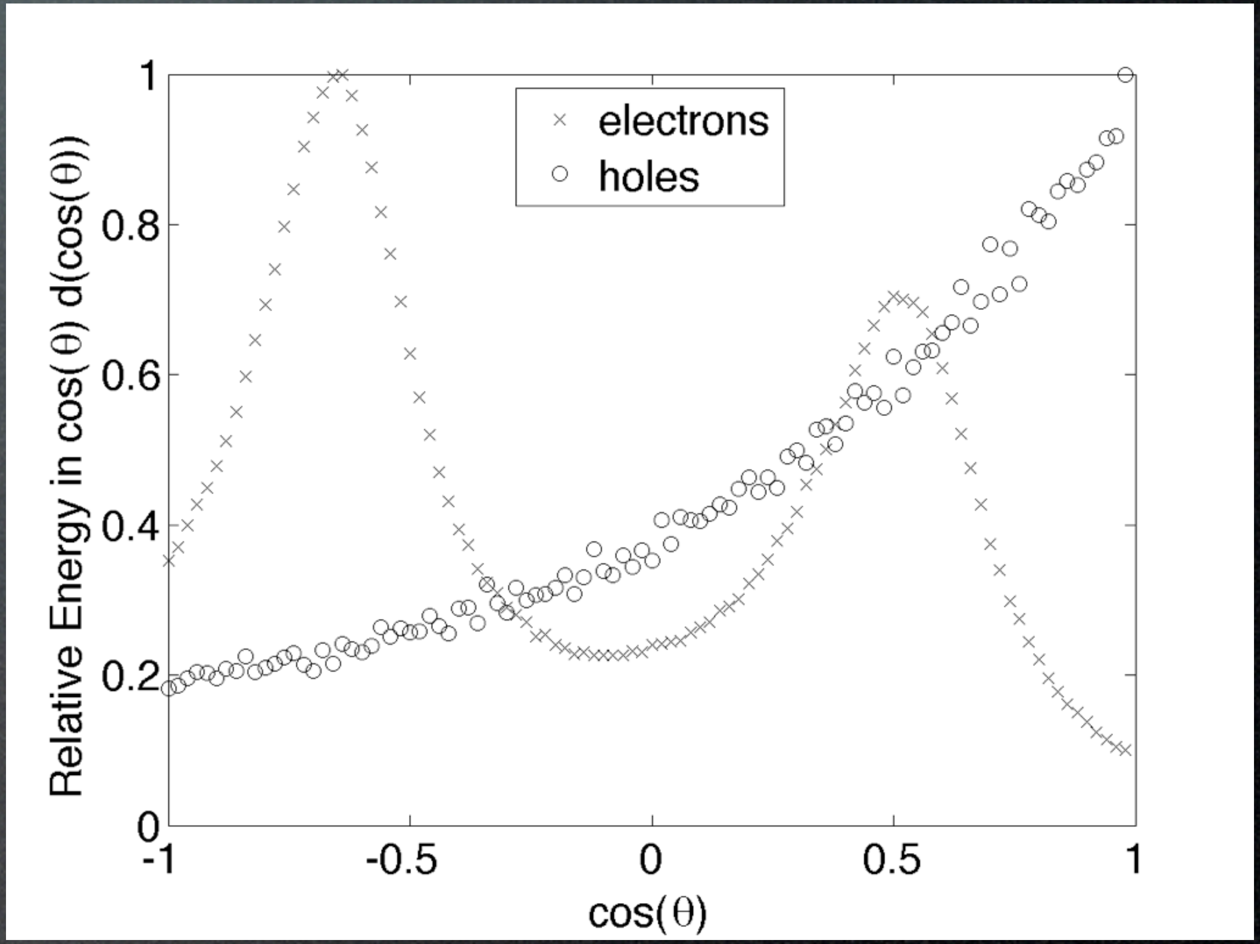

Phonon Transport

Phase Velocities

$$\rho\omega^2\epsilon_\mu = \sum_\tau\Big(\sum_{\sigma\nu} c_{\mu\sigma\nu\tau}k_\sigma k_\nu\Big)\epsilon_\tau$$

ϱ = density
ω = phonon frequency
ϵ = polarization vector
c = elastic constants
k = wave vector

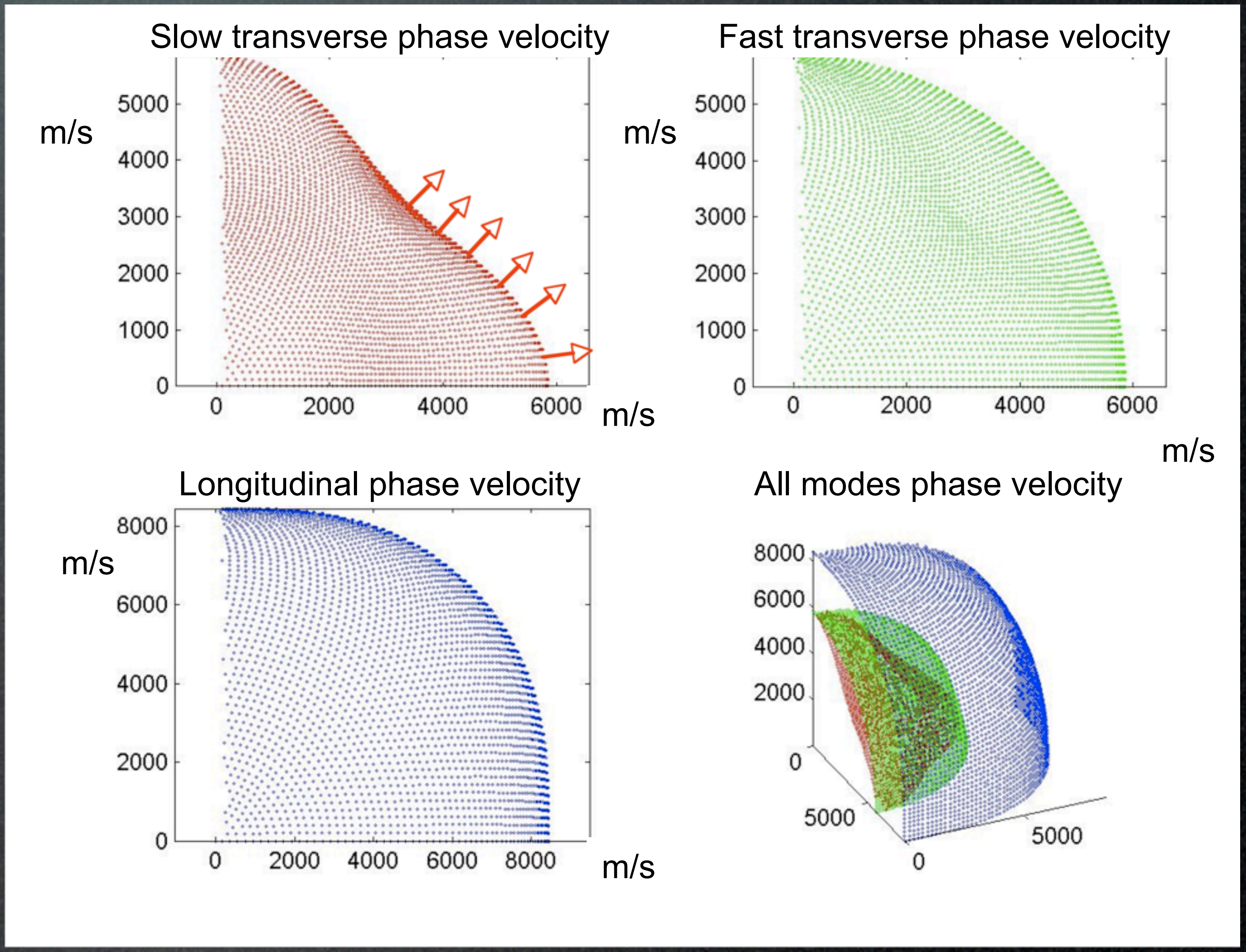

Group Velocity

$$\vec{v}_p = \frac{\omega(\theta, \phi)}{\vec{k}}$$

$$\vec{v}_g = \frac{d\omega(\theta, \phi)}{d\vec{k}}$$

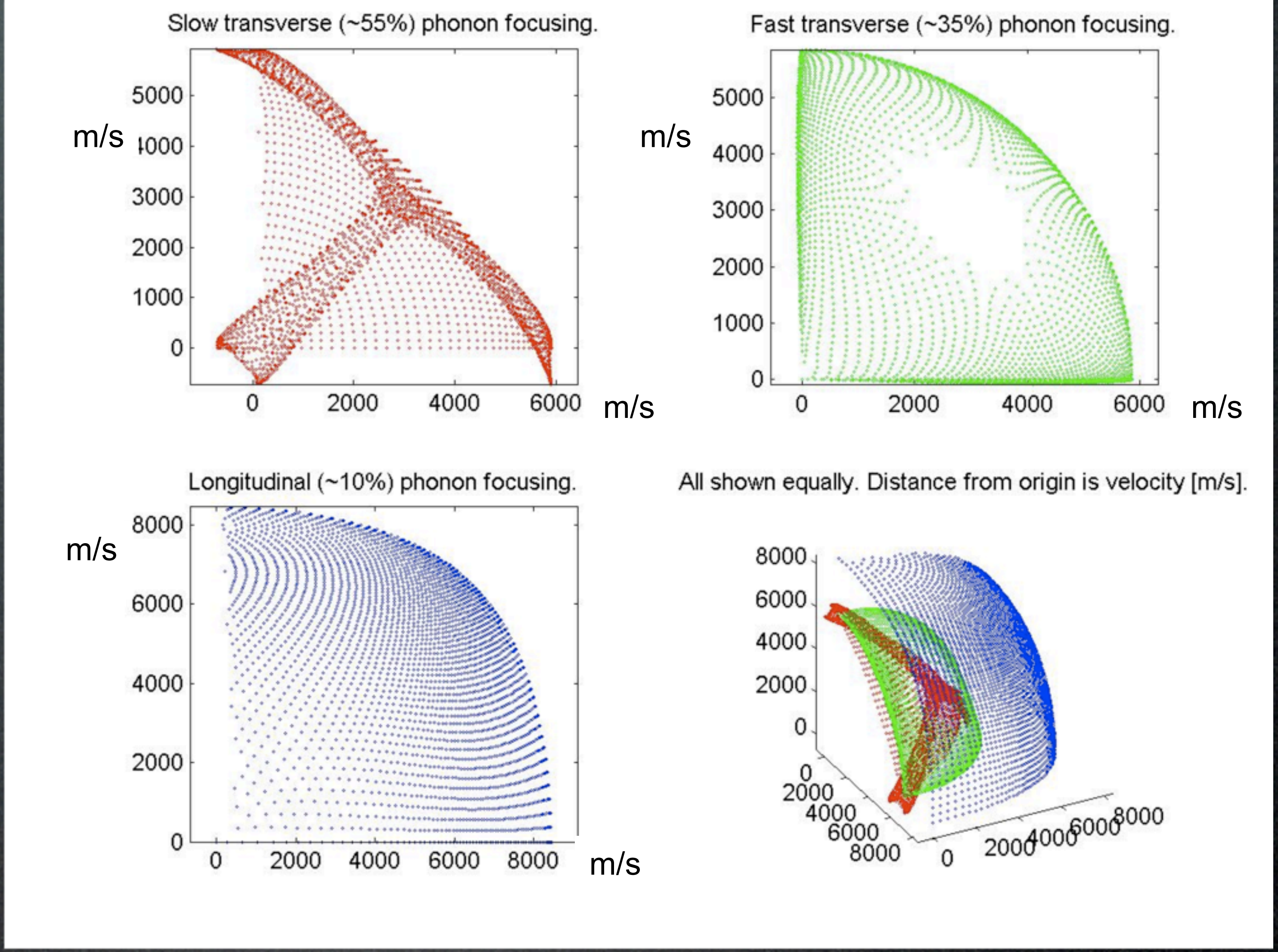

Anisotropic Isotope Scattering

$$\Gamma_{B,Ge} = 3.67 \times 10^{-41}[s^3]\nu^4$$

$$\gamma = \frac{|\vec{e}_\lambda \cdot \vec{e}_{\lambda'}|^2}{v_{\lambda'}^3}$$

Intrinsic mass defects due to natural abundance

Gives rise to phonon diffusion

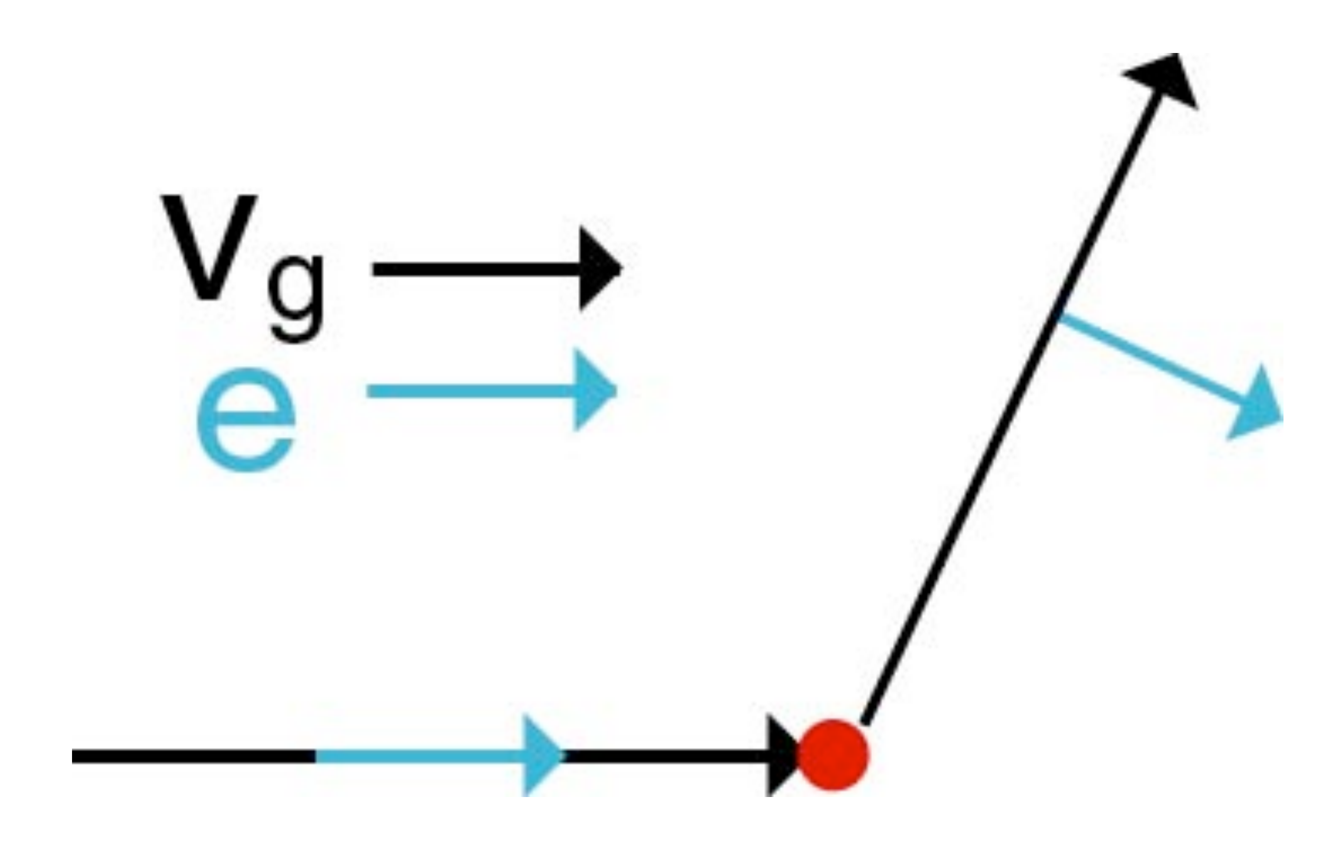

Anharmonic Decay

$$\Gamma_{A(LA),Ge} = 1.62 \times 10^{-54}[s^4]\nu^5$$

Diffusion length increases with time.

Three body problem, difficult to solve due to non-isotropic dispersion relation.

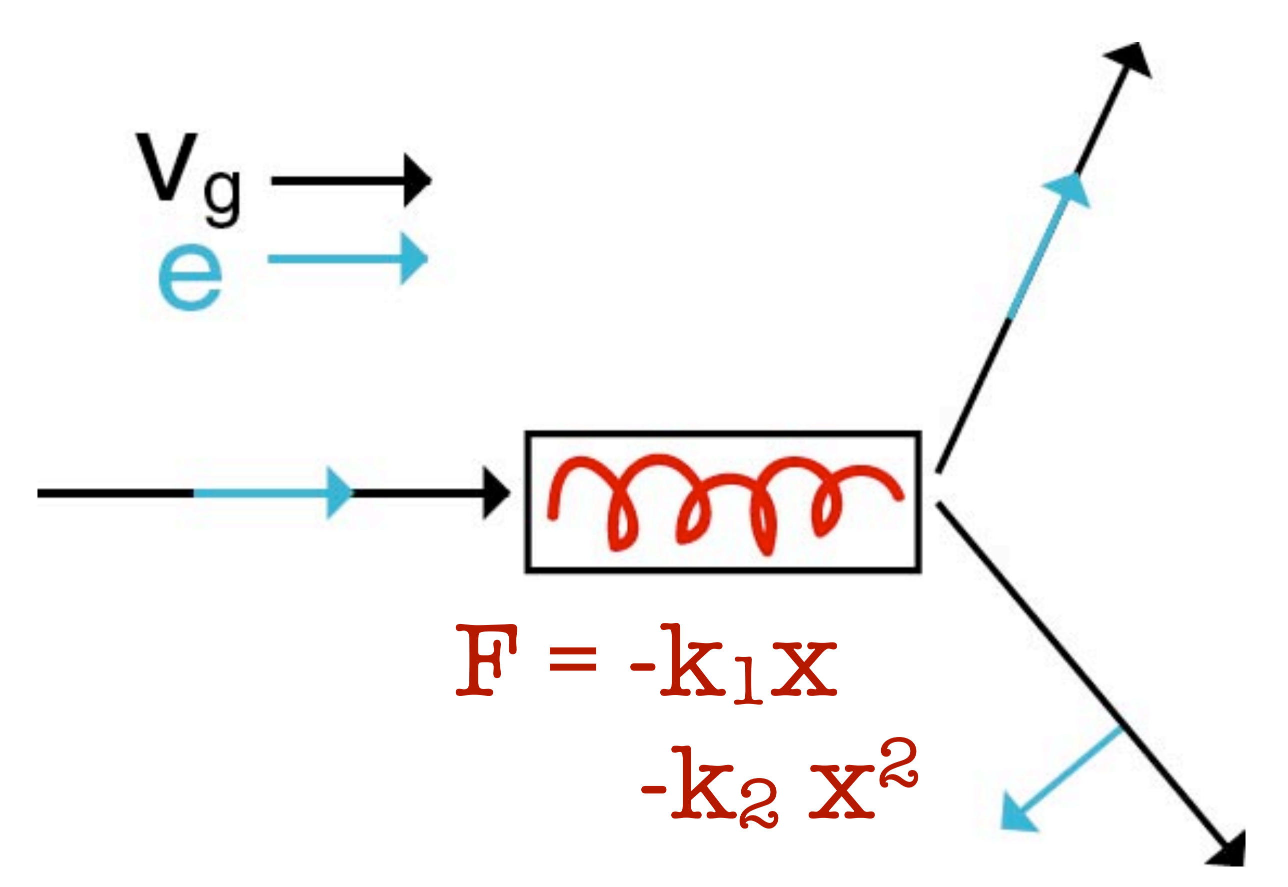

Anharmonic Decay Distributions

L->T+T (74%)
L->L+T (26%)

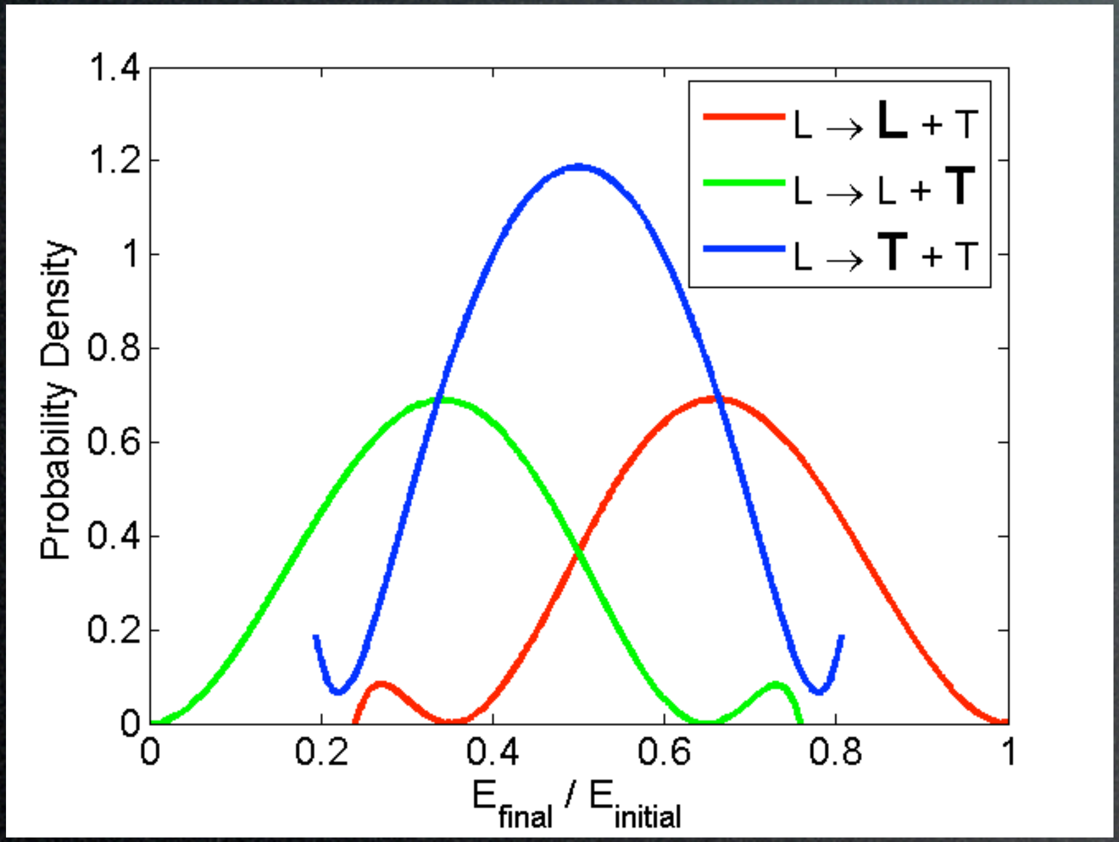

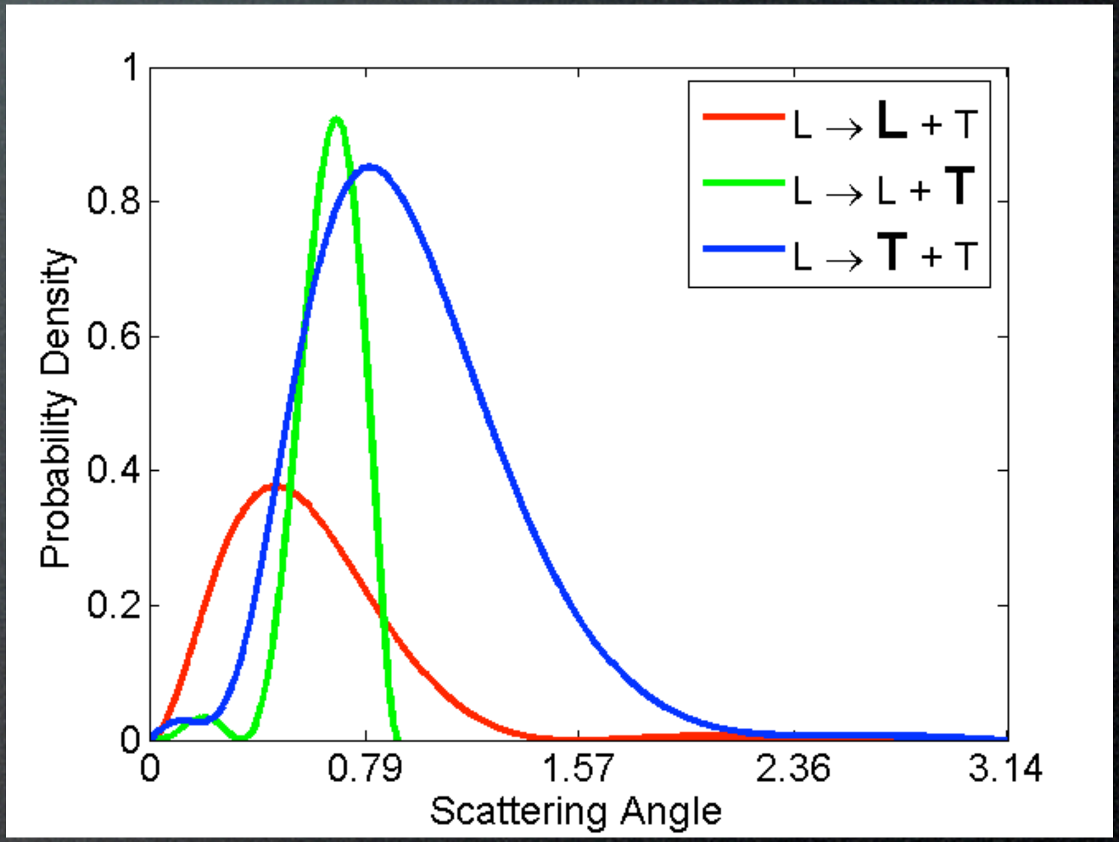

SCDMS iZIP Detector

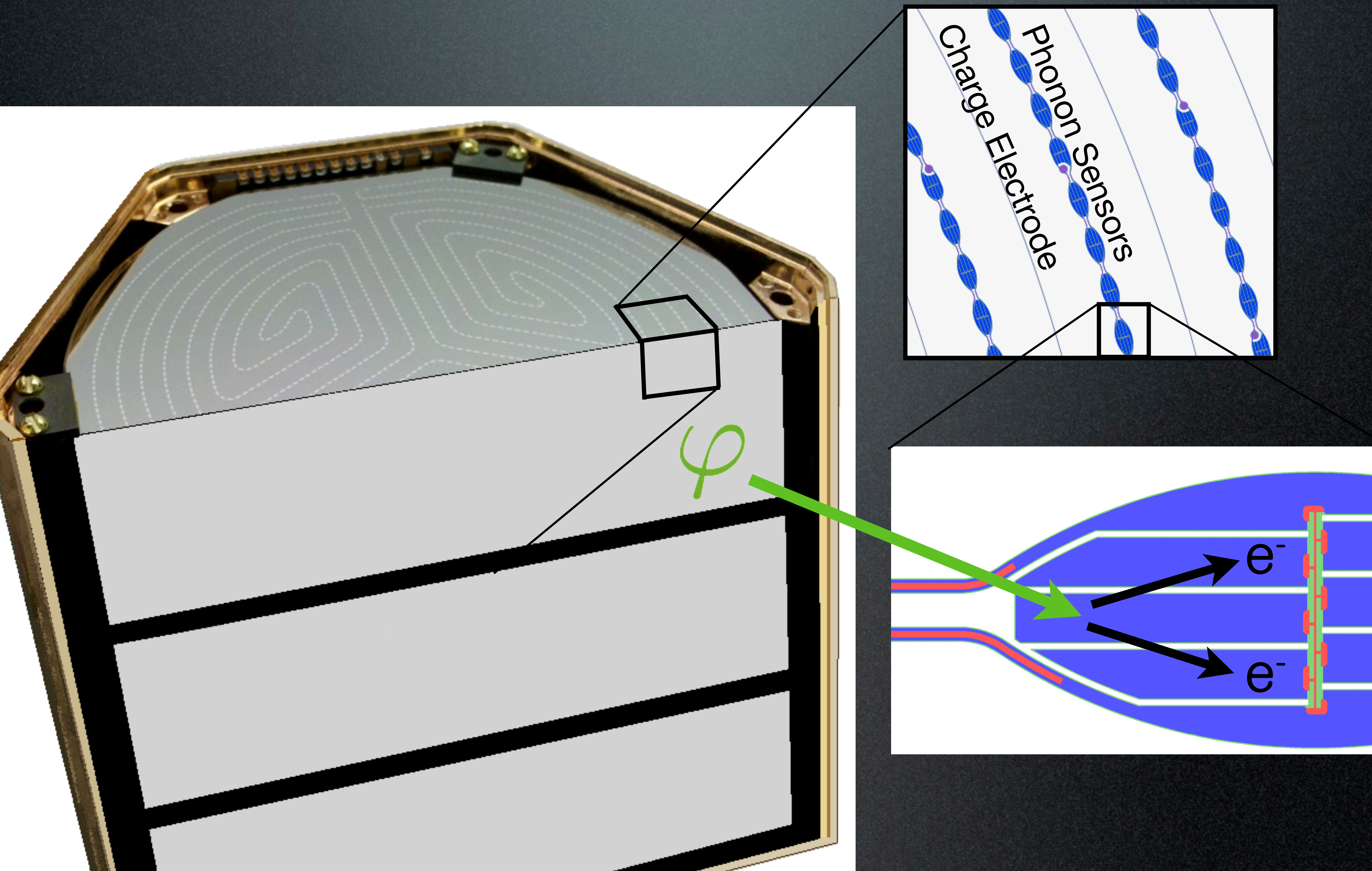

Quasiparticle / Phonon Downconversion

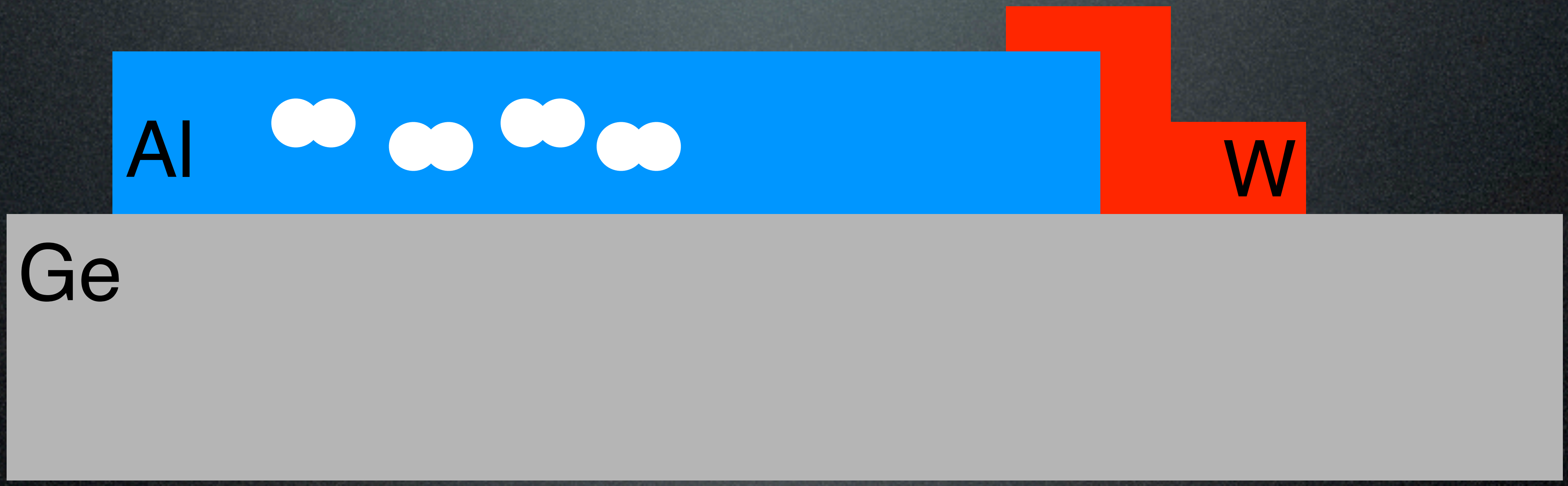

- Downconversion process
  - Production of quasiparticles
  - Phonon energy escapes back to crystal

Quasiparticle / Phonon Downconversion

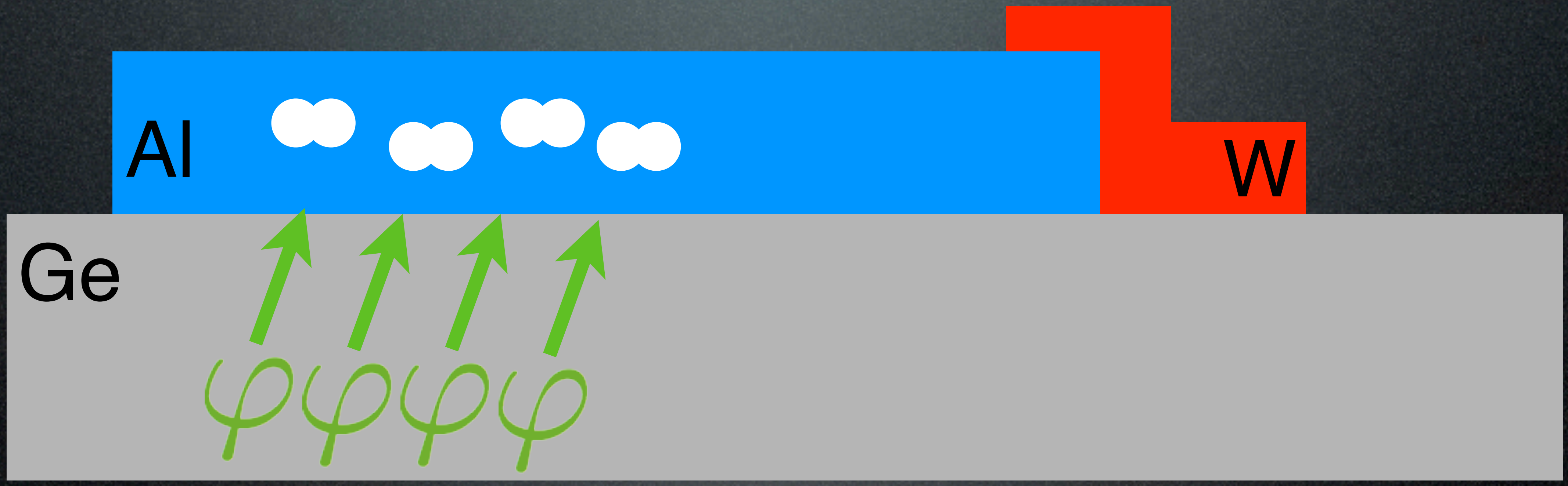

- Downconversion process
  - Production of quasiparticles
  - Phonon energy escapes back to crystal

Quasiparticle / Phonon Downconversion

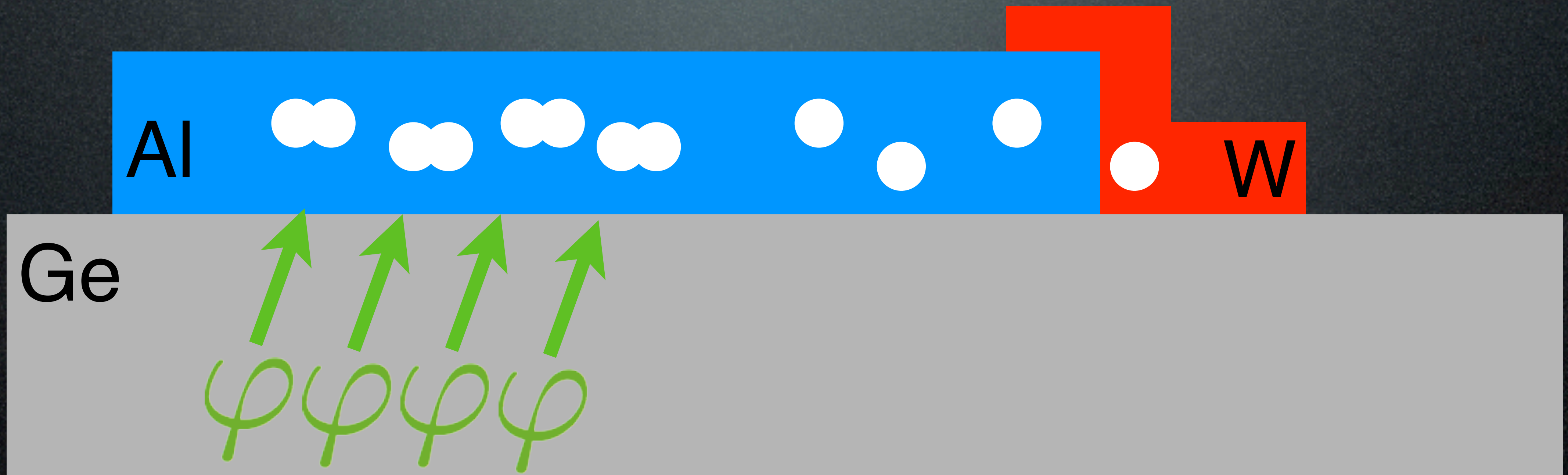

- Downconversion process
  - Production of quasiparticles
  - Phonon energy escapes back to crystal

Quasiparticle / Phonon Downconversion

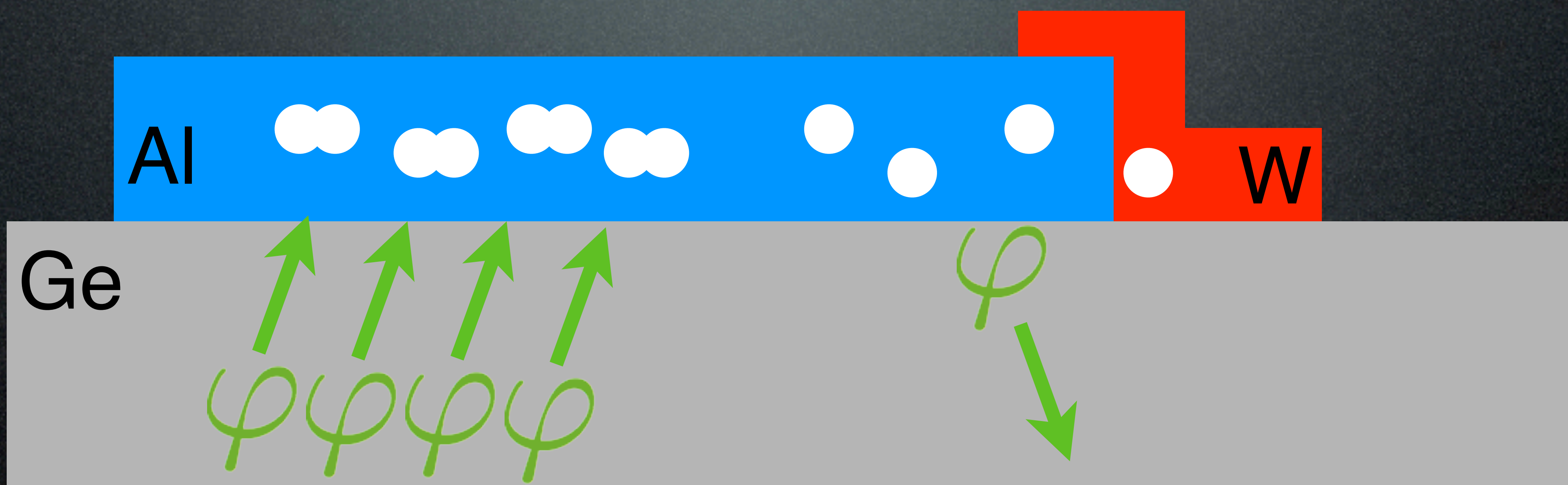

- Downconversion process
  - Production of quasiparticles
  - Phonon energy escapes back to crystal

Quasiparticle Cascade

- Cascade until phonon energy < 2 gap or phonon escapes Al

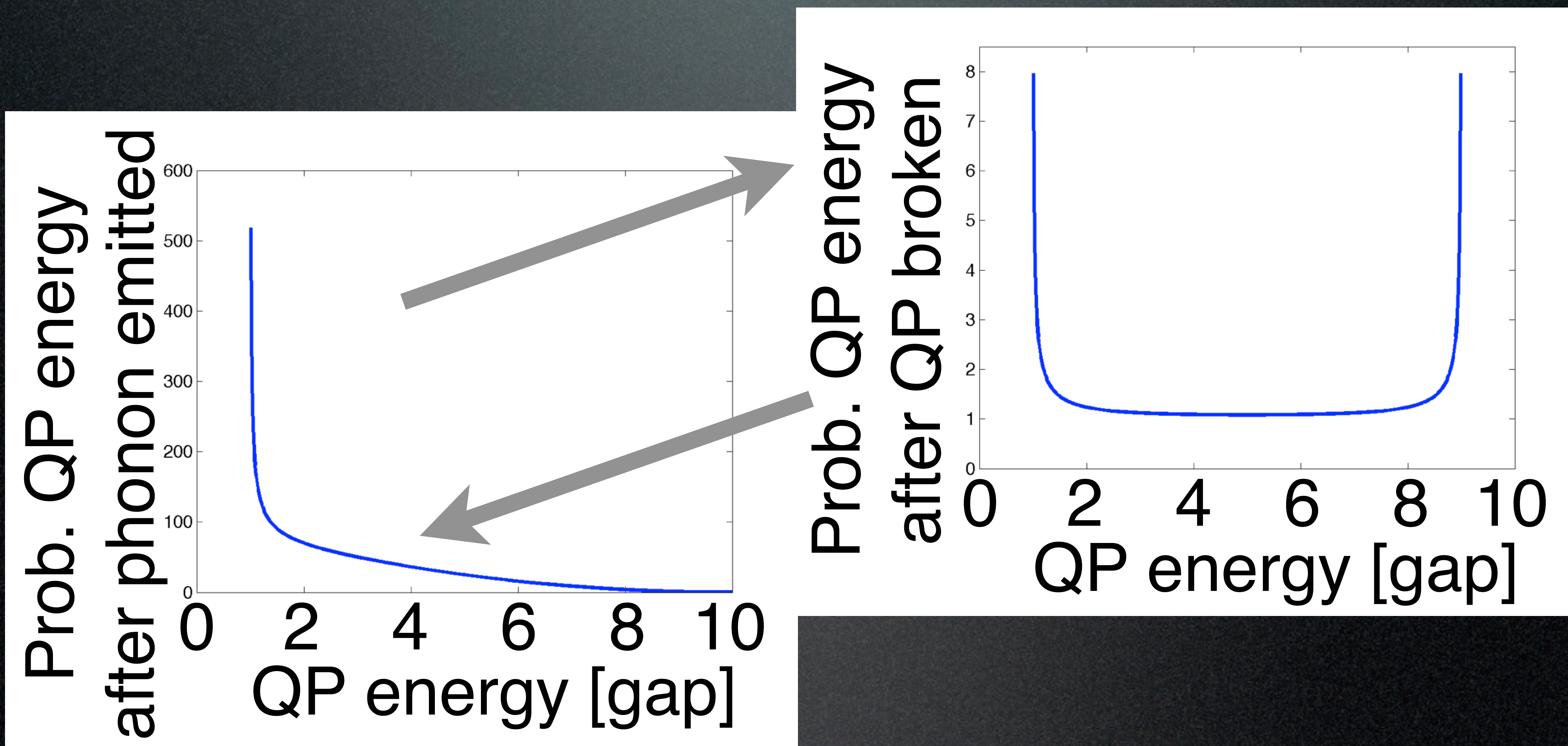

Phonon Readout

Transition Edge Sensors

TES Layout

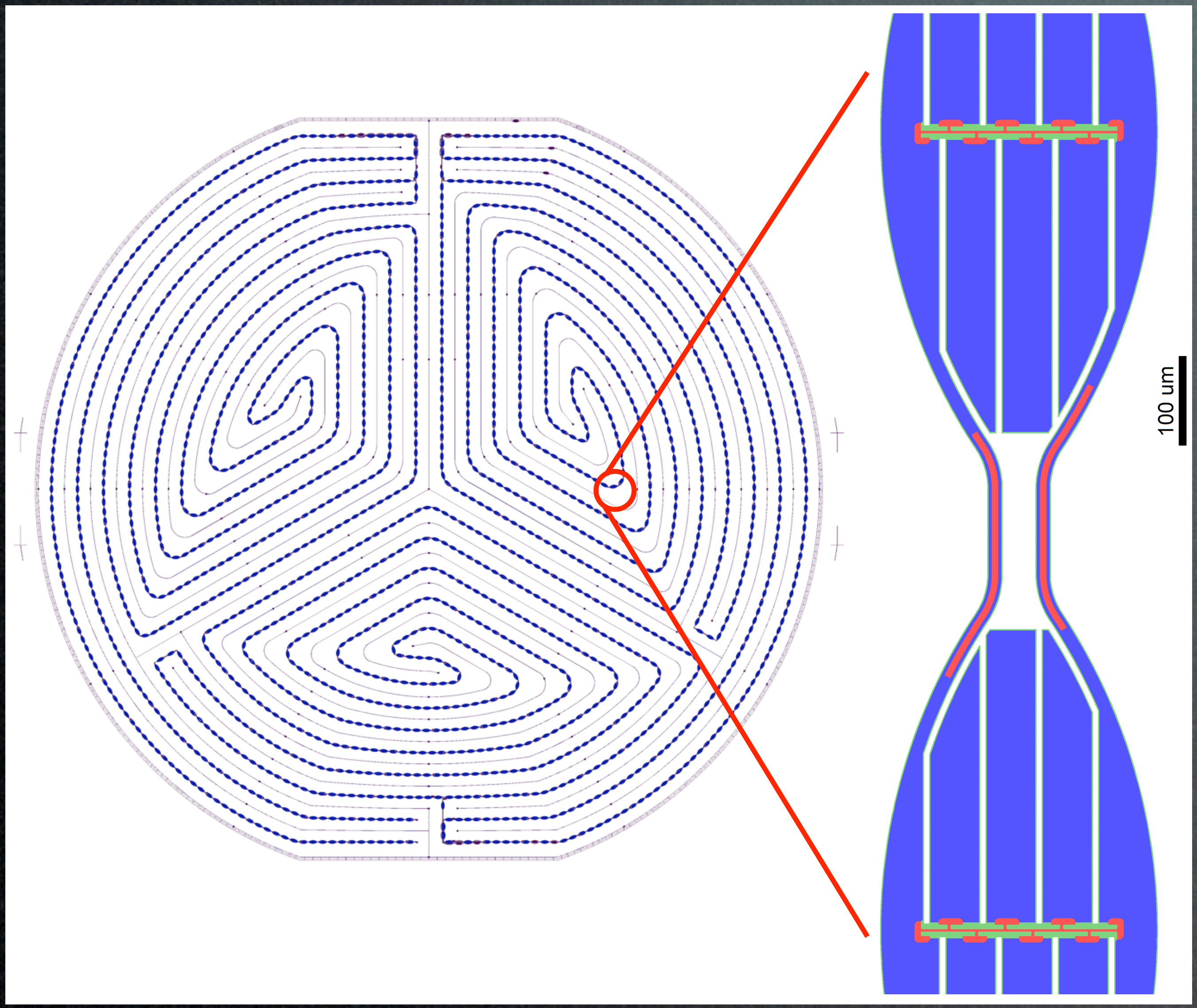

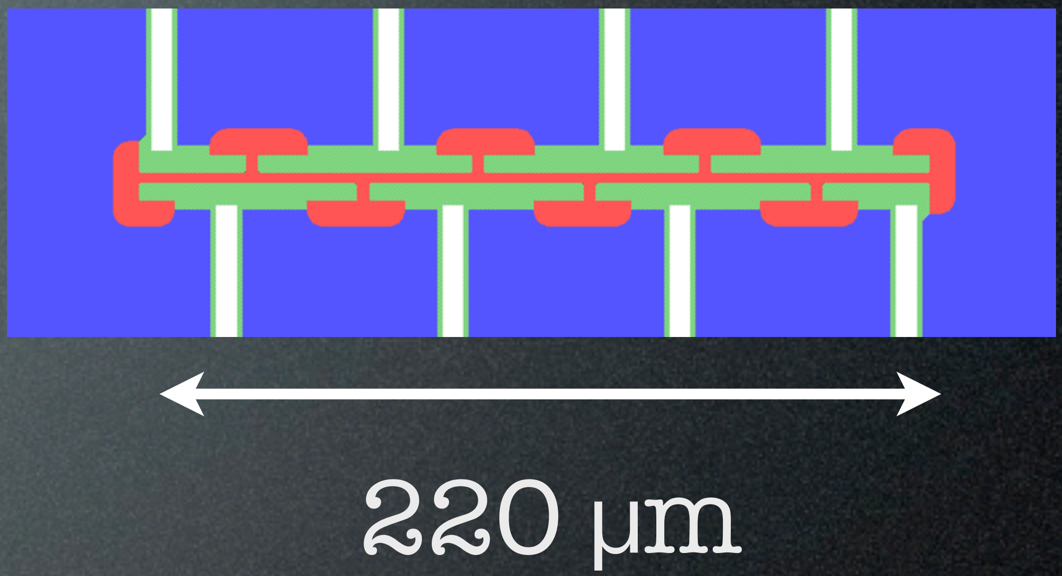

TES Joule Power

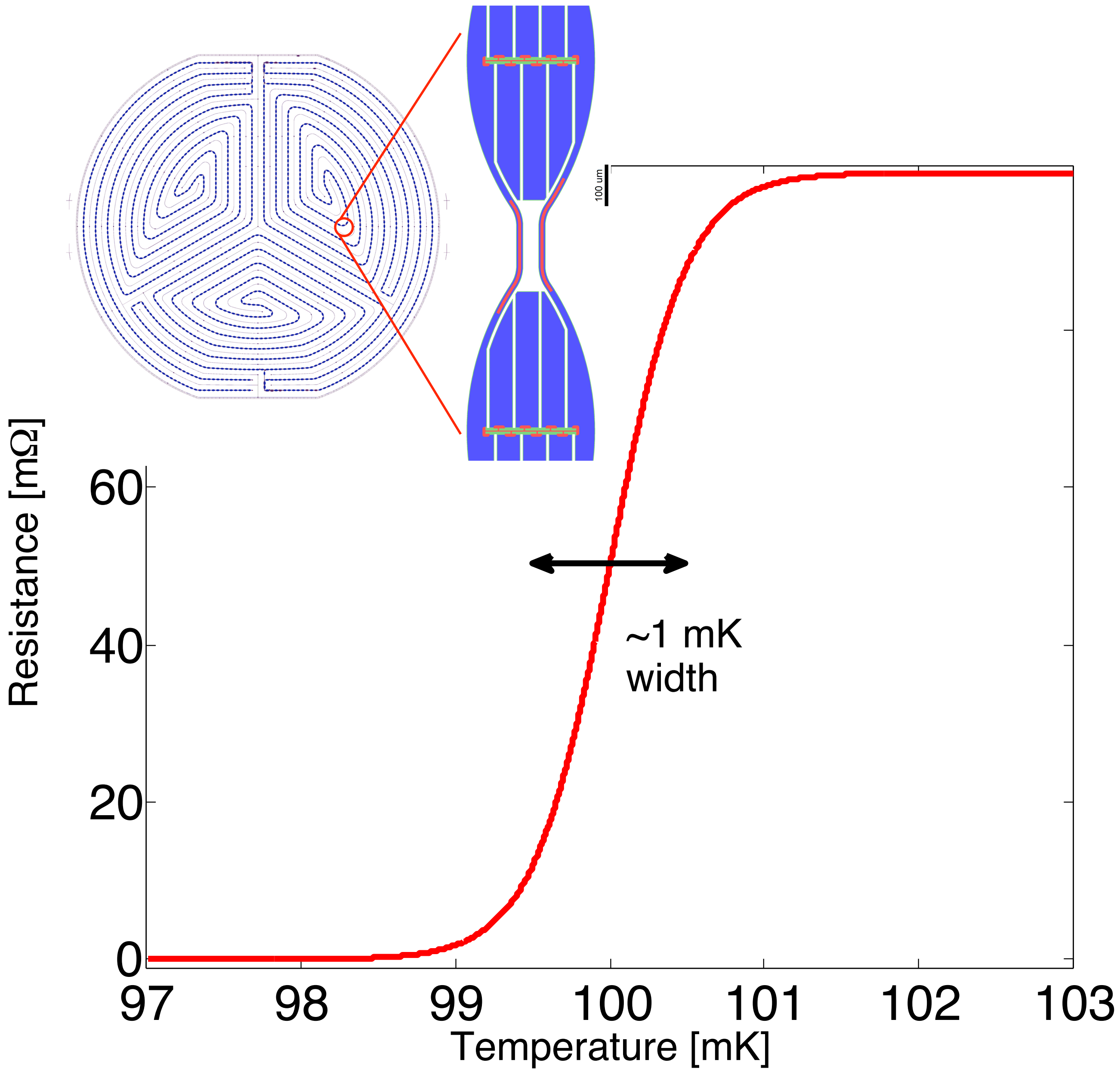

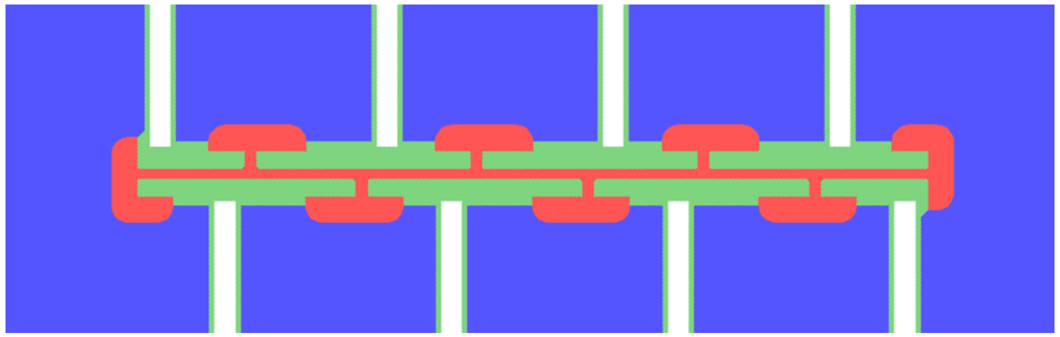

$$P_{\text{Joule}} = \frac{V^2}{R}$$

Negative electro-thermal feedback (stable)

TES Phase Separation

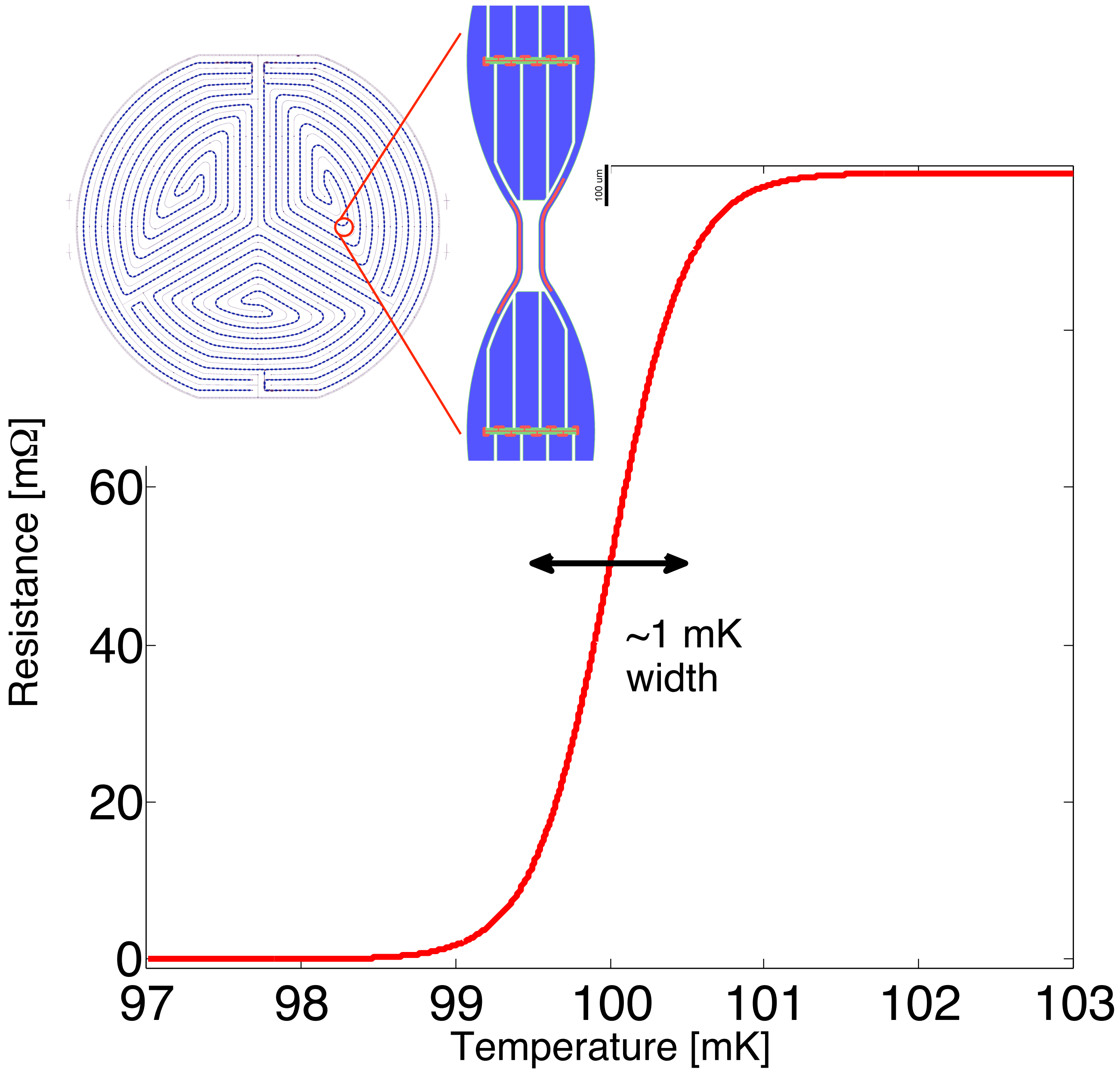

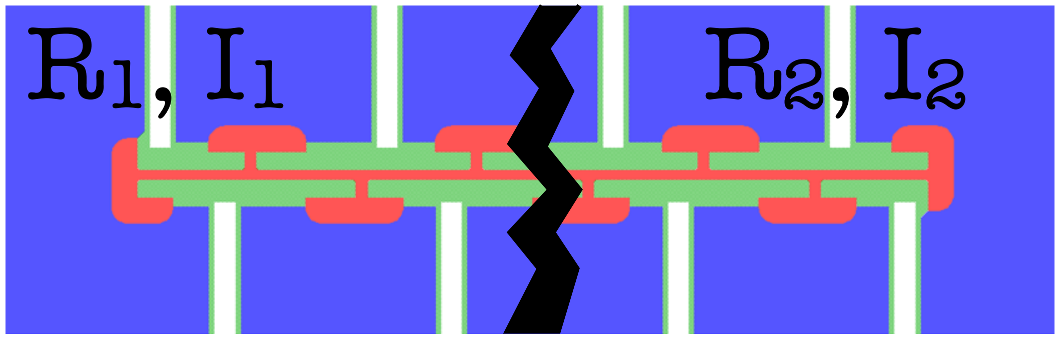

$$P_{\mathrm{Joule},1} = I^2 R_1$$

$$P_{\mathrm{Joule},2} = I^2 R_2$$

Positive electro-thermal feedback between R_1 & R_2 (unstable)

TES I-P Curve

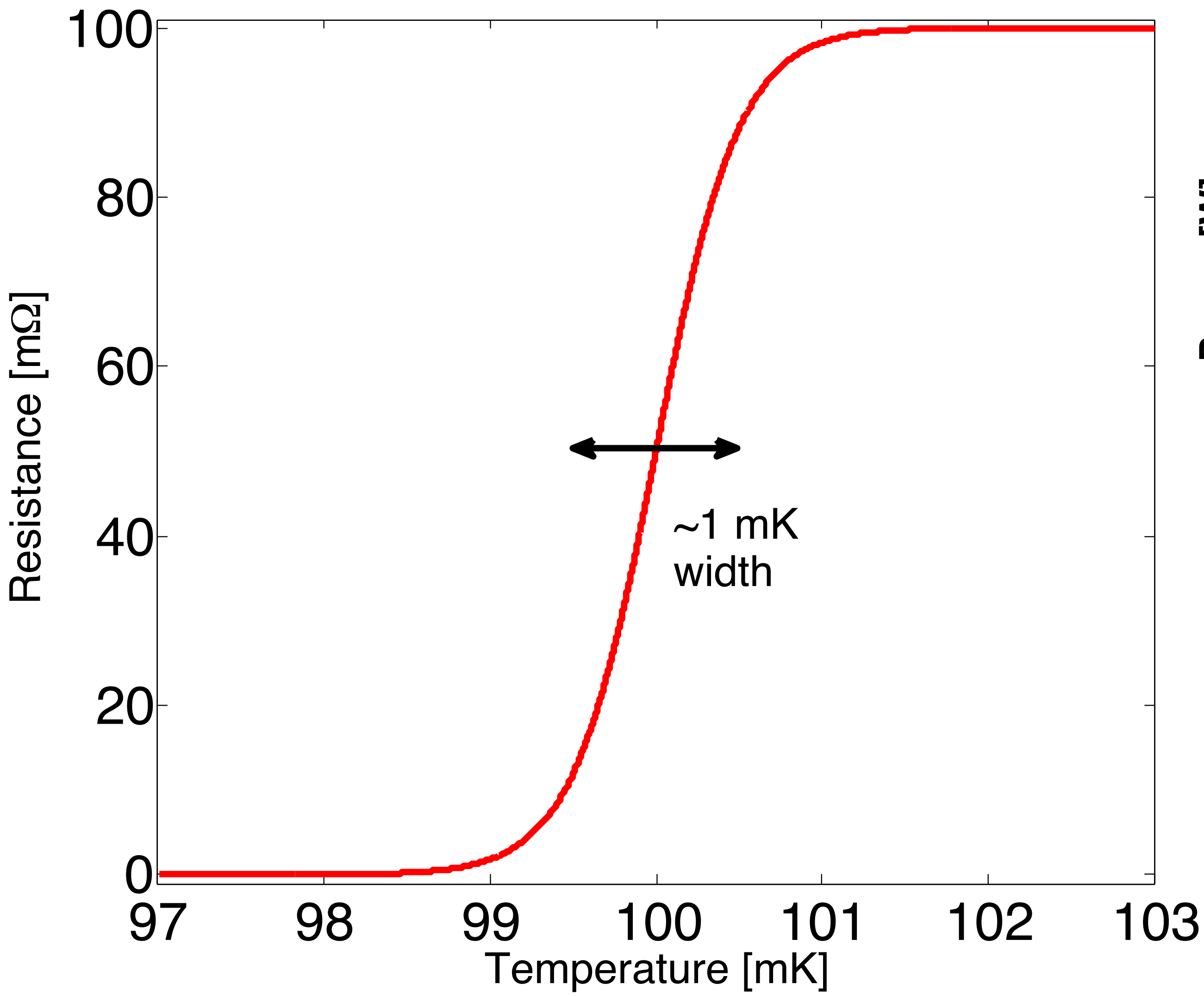

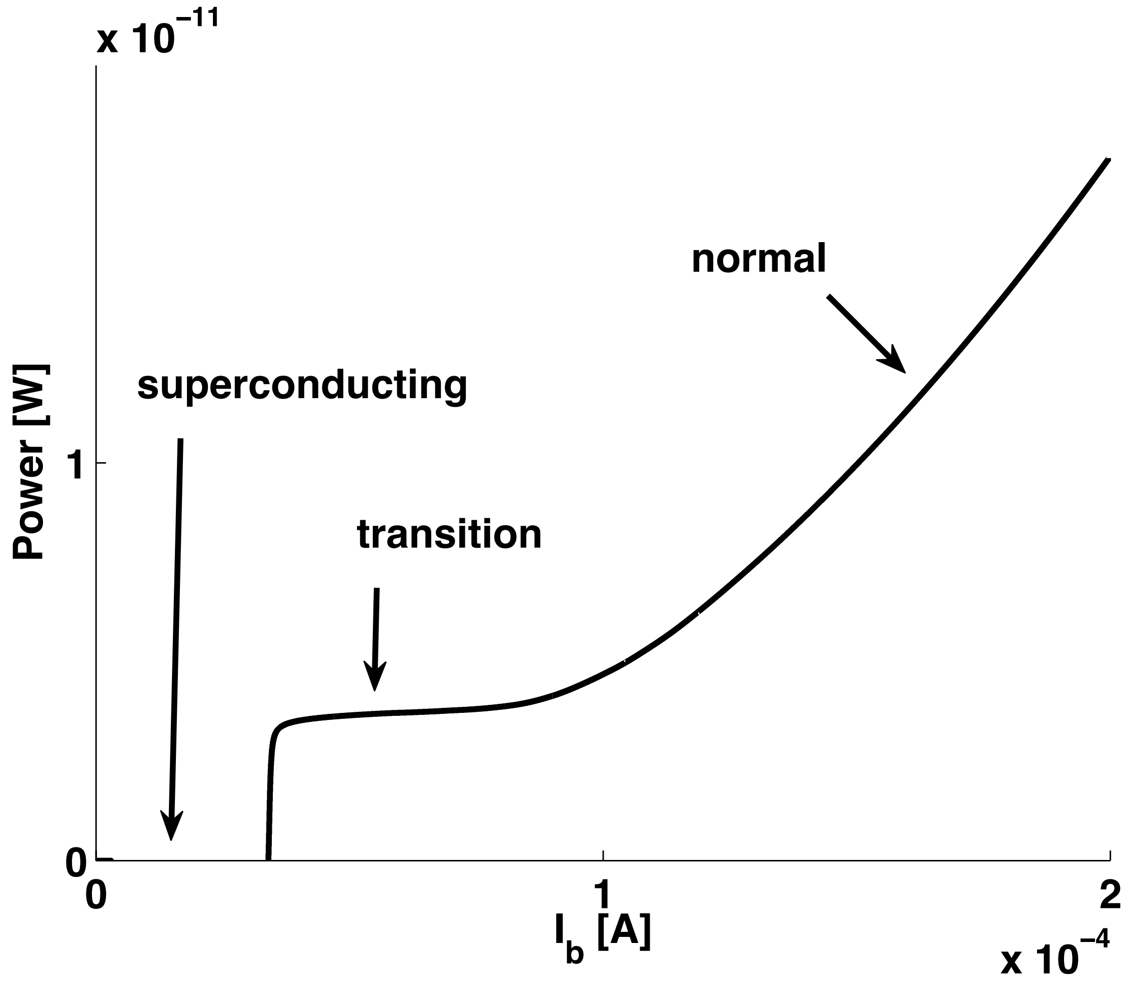

$$P_{\text{Joule}} = P_{\text{TES}\rightarrow\text{substrate}}$$

$$\sim \text{Vol}\left(T_{\text{TES}}^5 - T_{\text{substate}}^5\right)$$

Transition Edge Sensor
I-P Curves

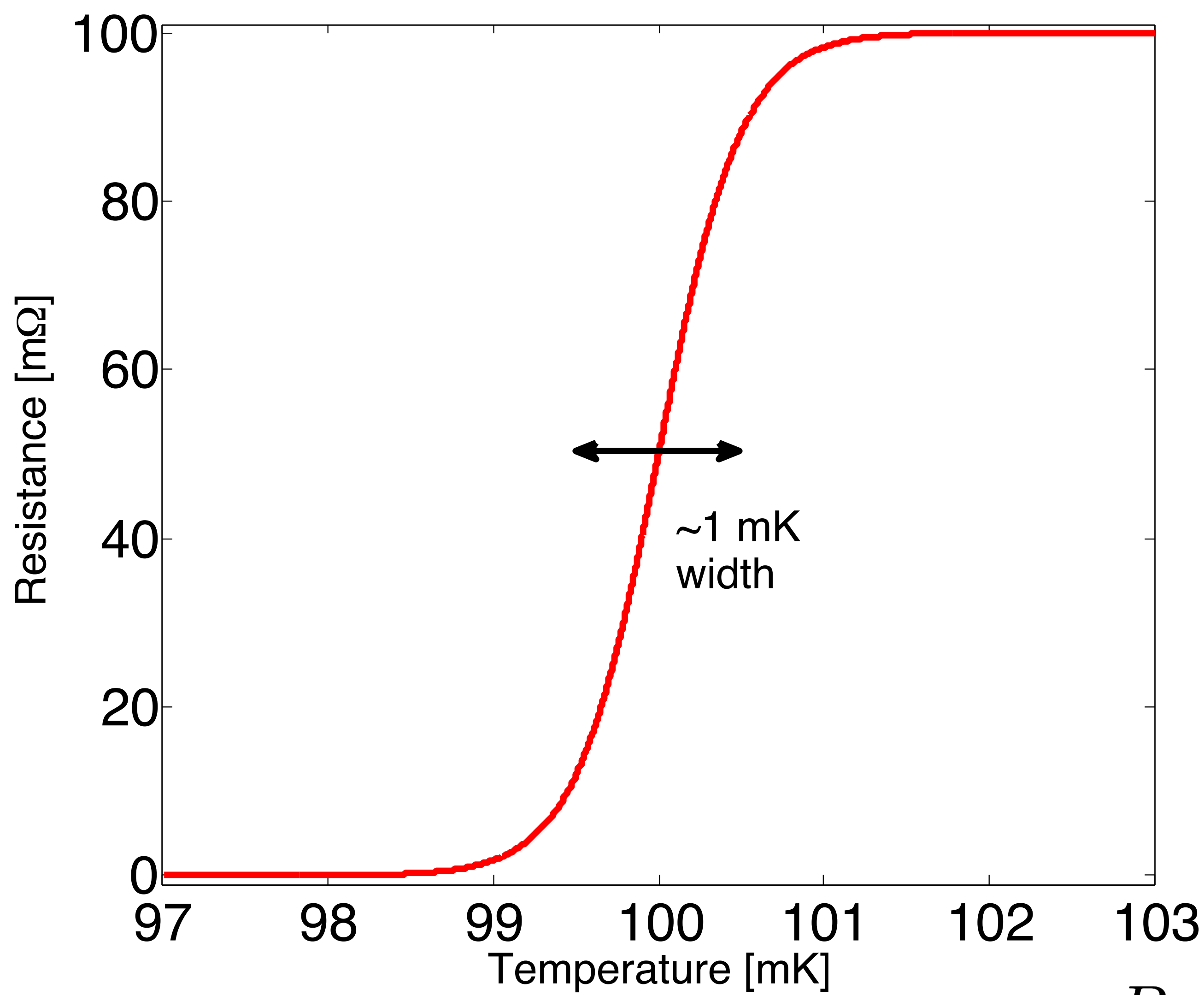

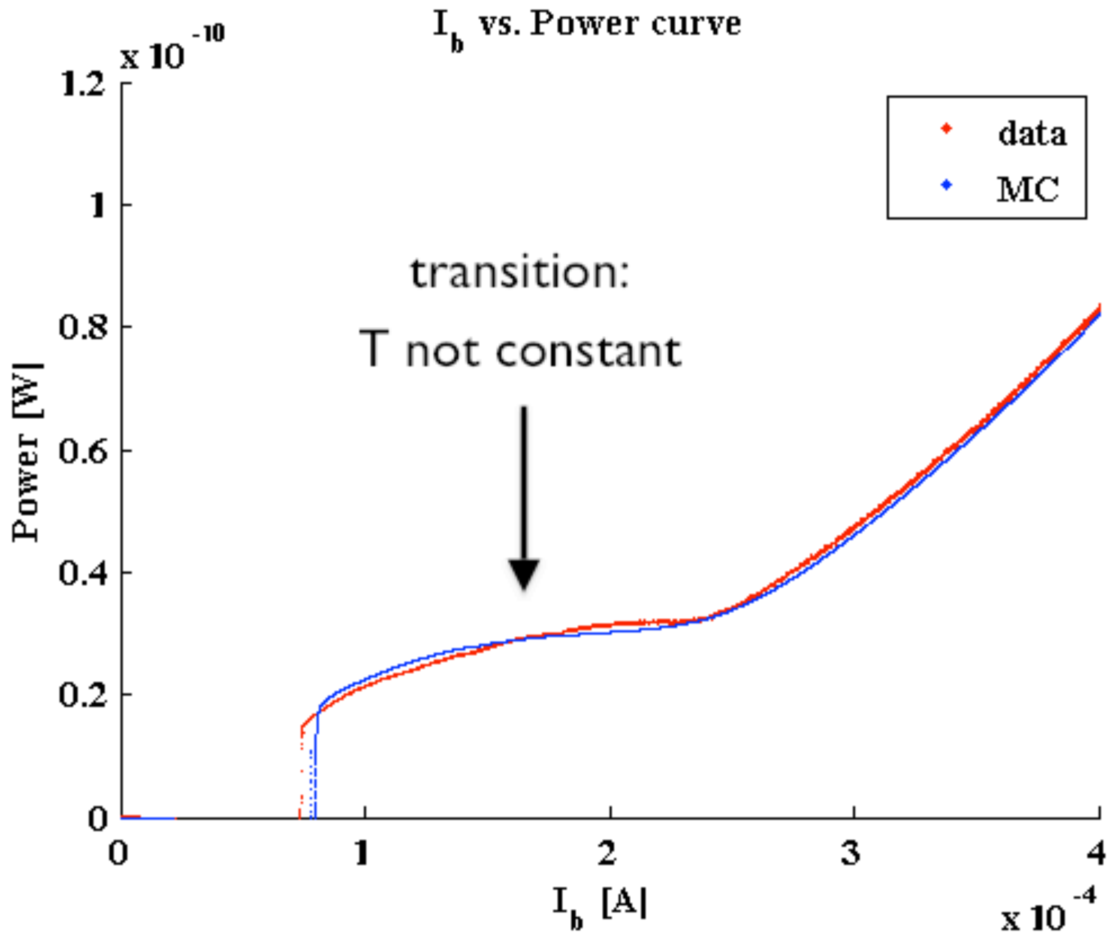

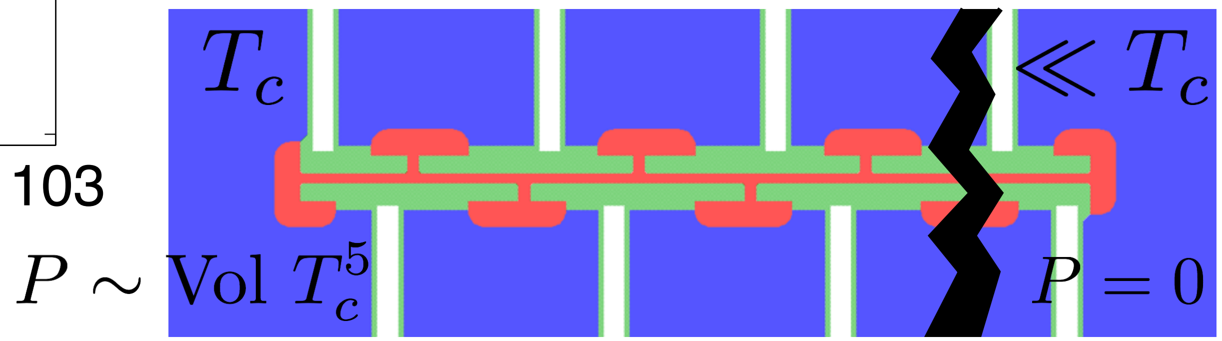

Heat Pulse Transient

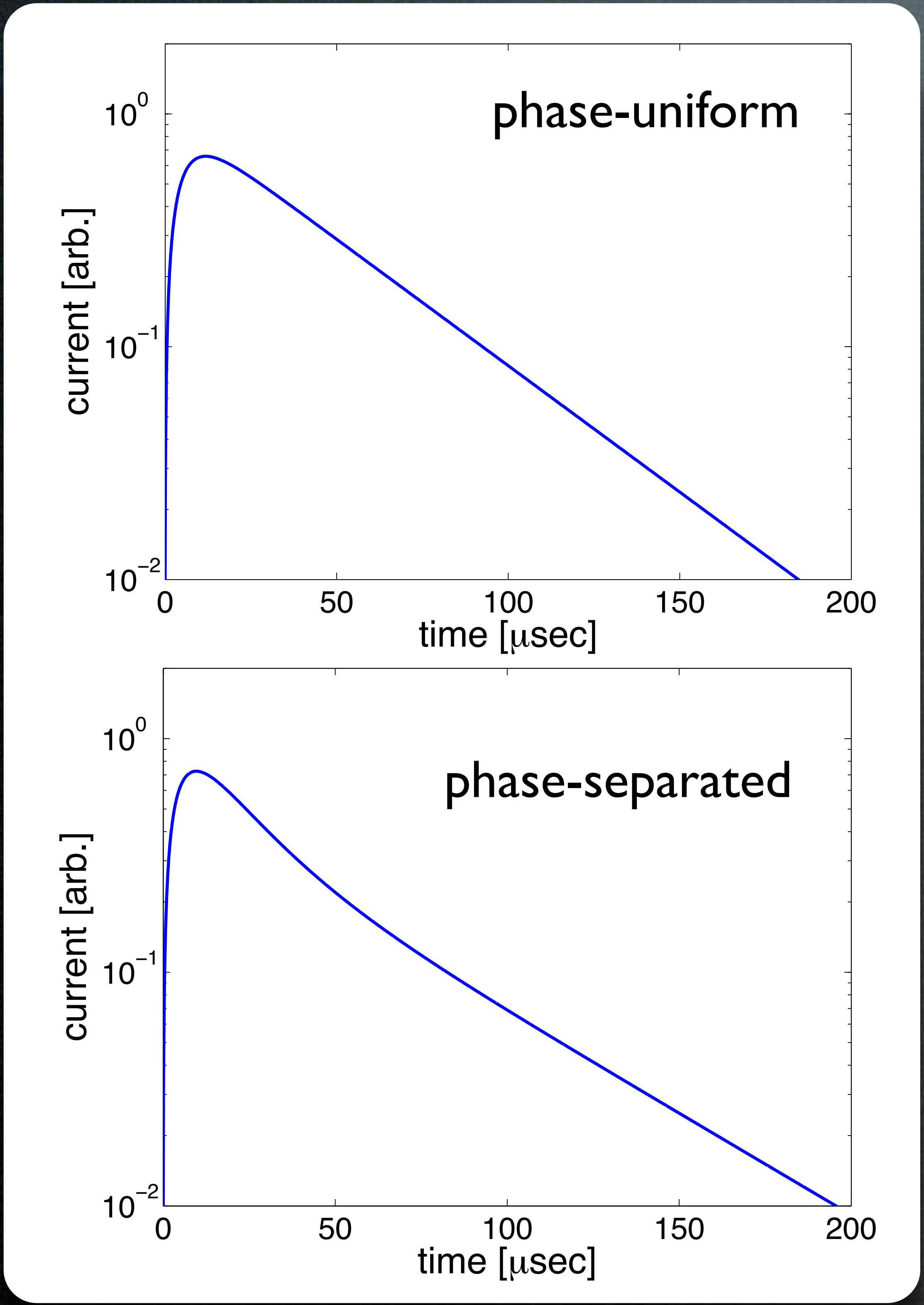

Phase-uniform case time constants

- L/R
- C/G

Phase separated case time constants

- L/R
- thermal diffusion in TES
- C/G

Heat Pulse Transient Model Tuning

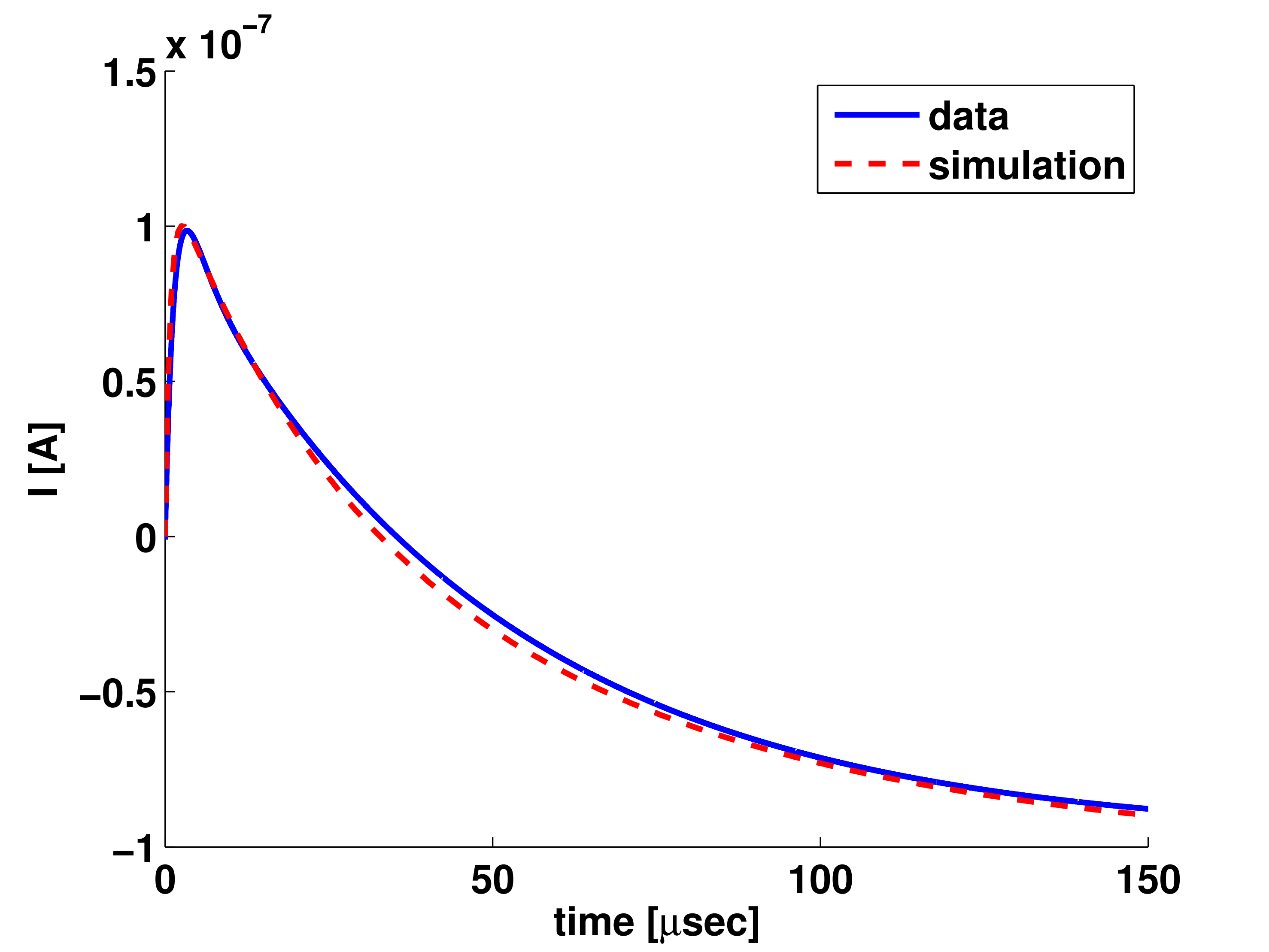

Model Validation :

Charge, Phonon, TES

Position Reconstruction

- Phonon-aluminum interaction probability
    - No QP-phonon downconversion
    - No TES physics

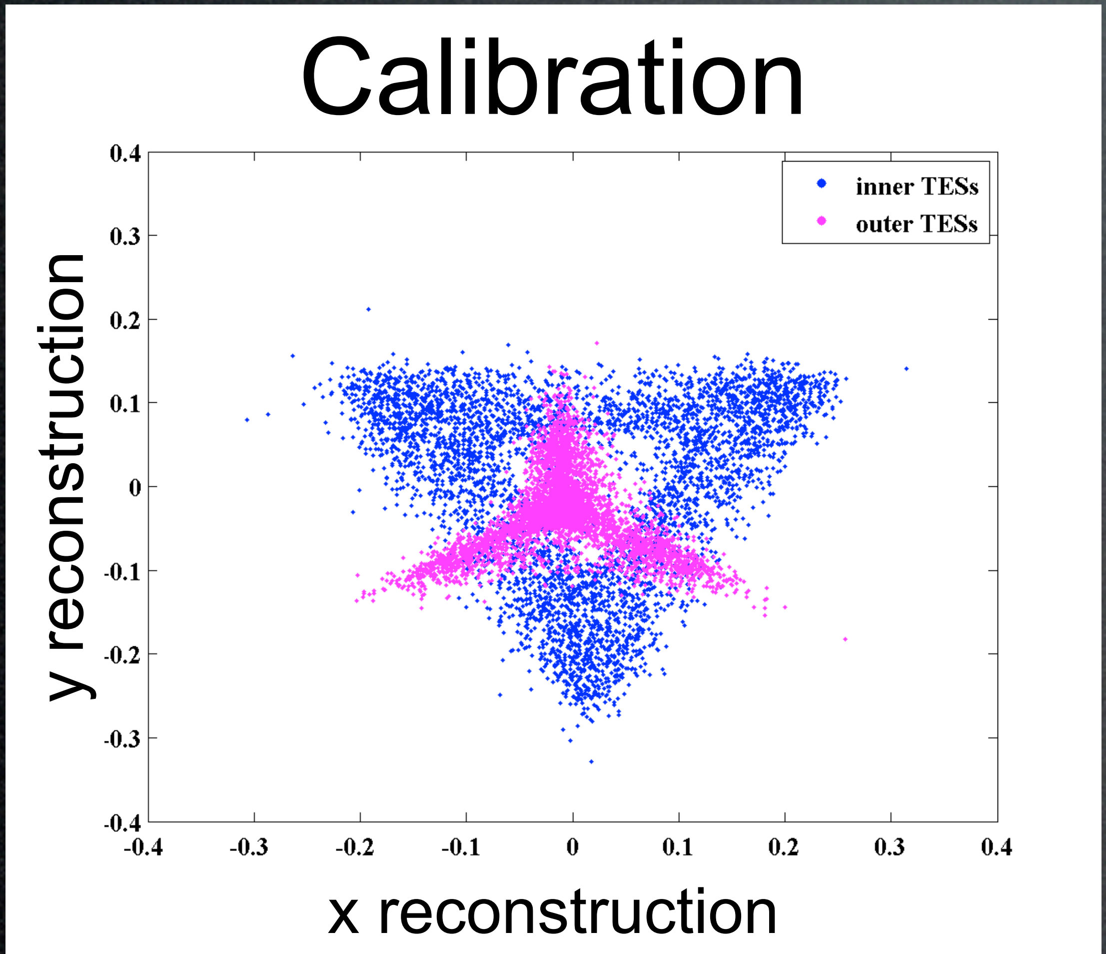

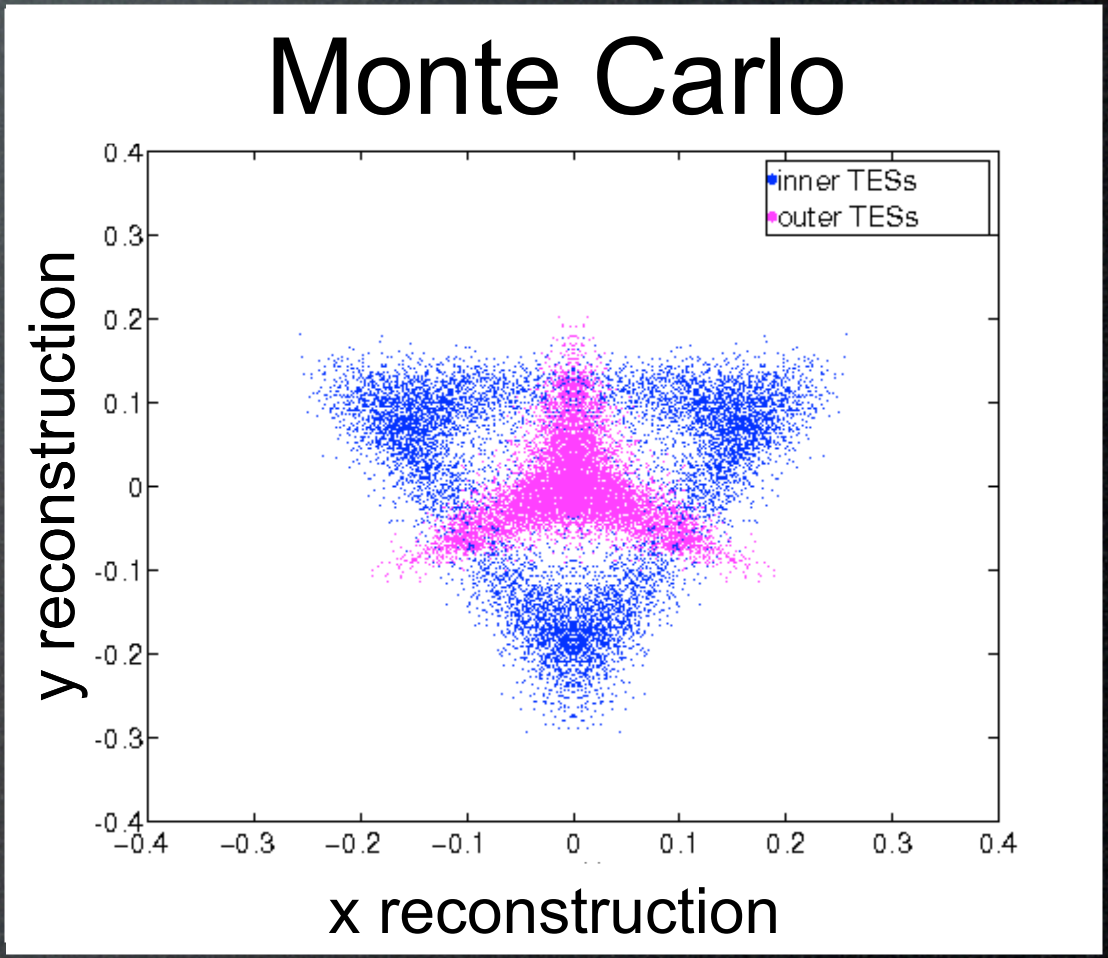

Energy Partitioning

- Phonon-aluminum interaction probability, QP-phonon downconversion

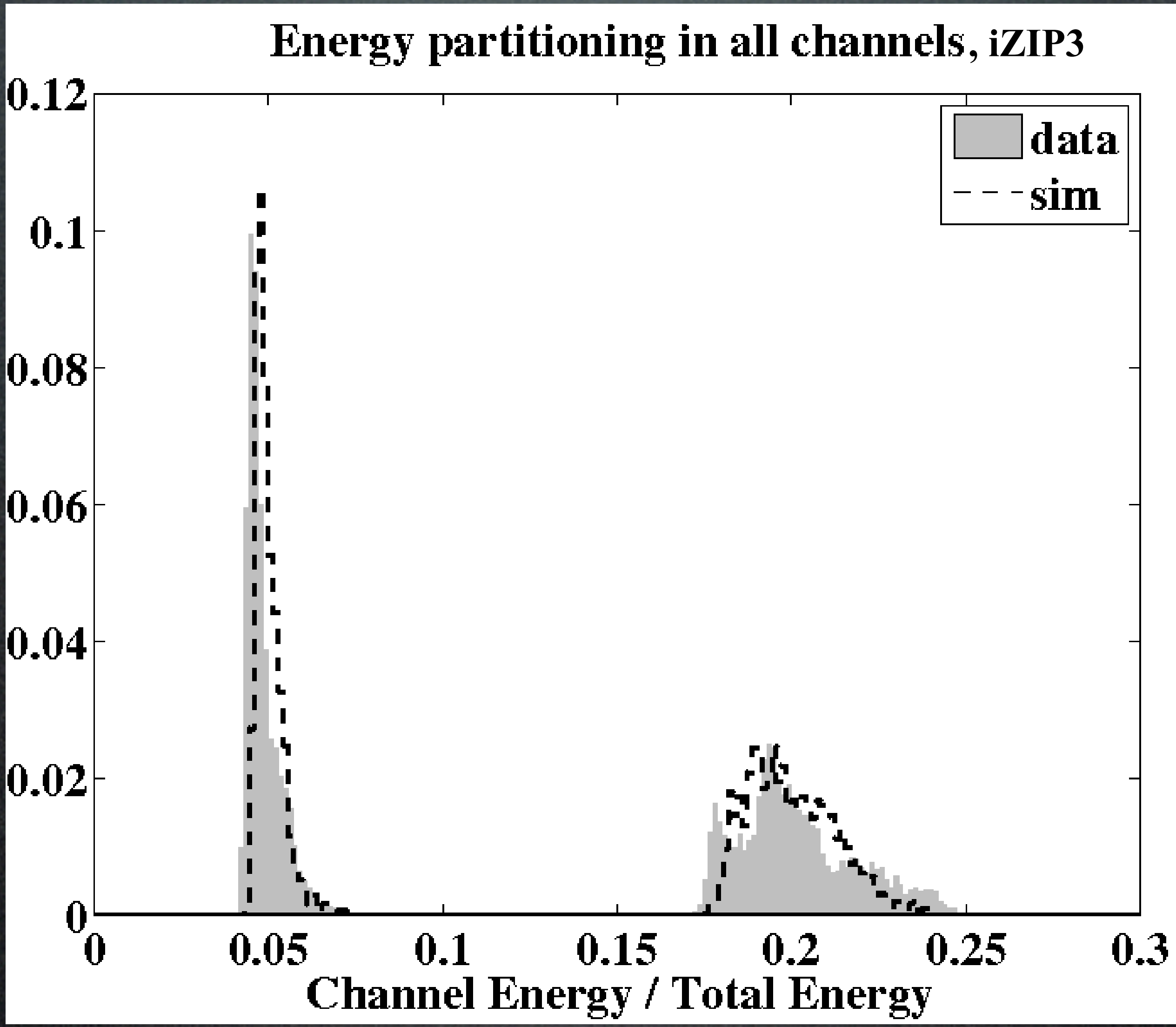

Decay Times

Phonon-aluminum interaction probability, QP-phonon downconversion

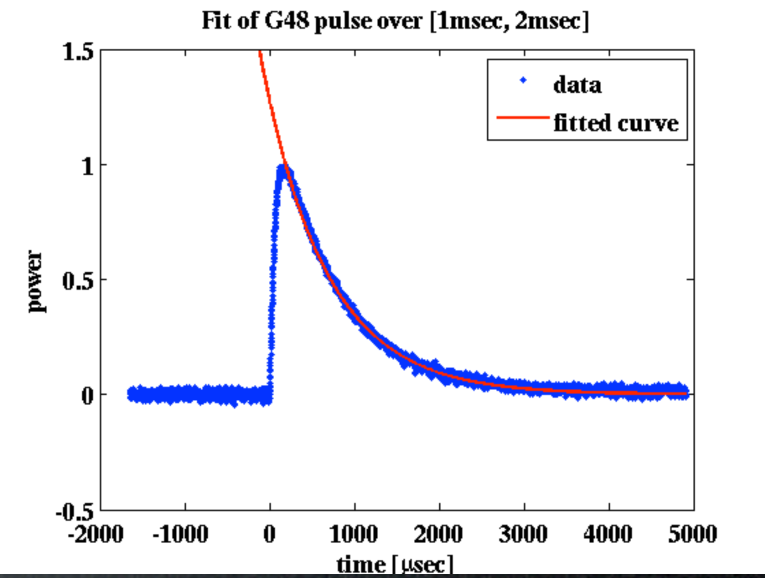

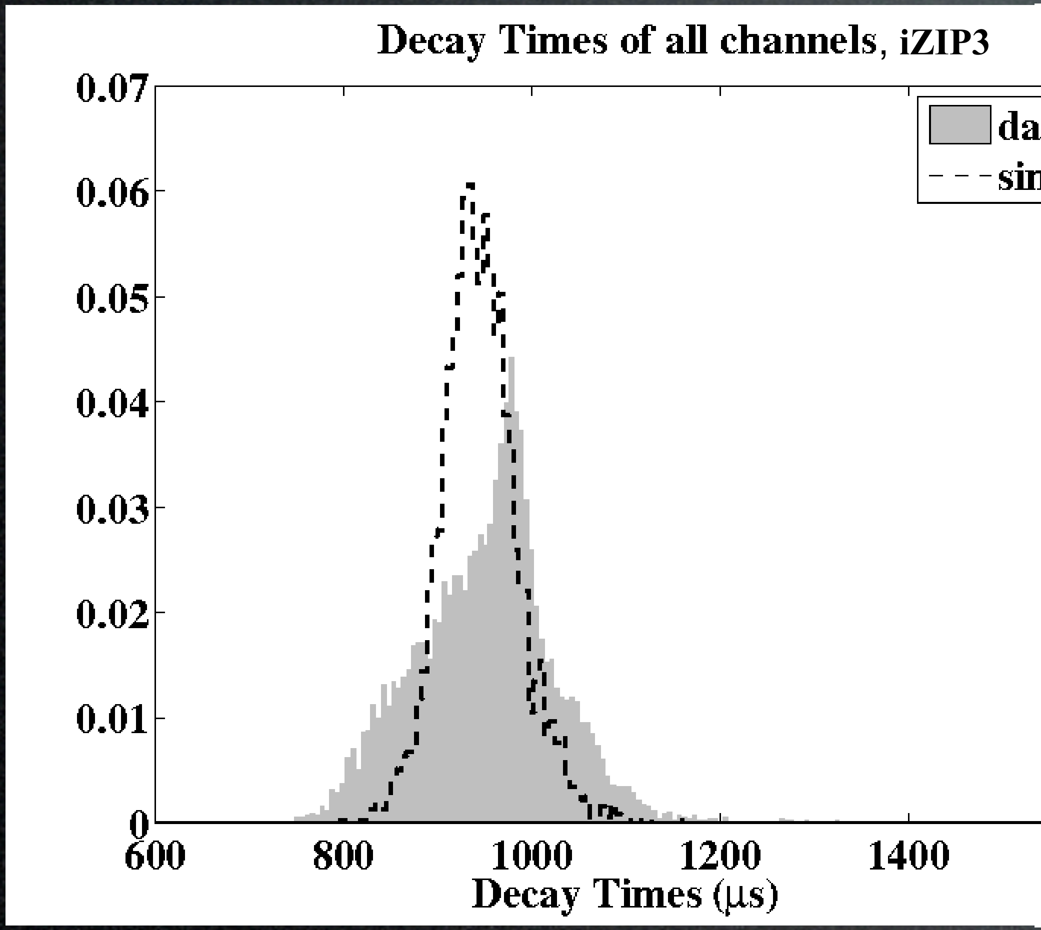

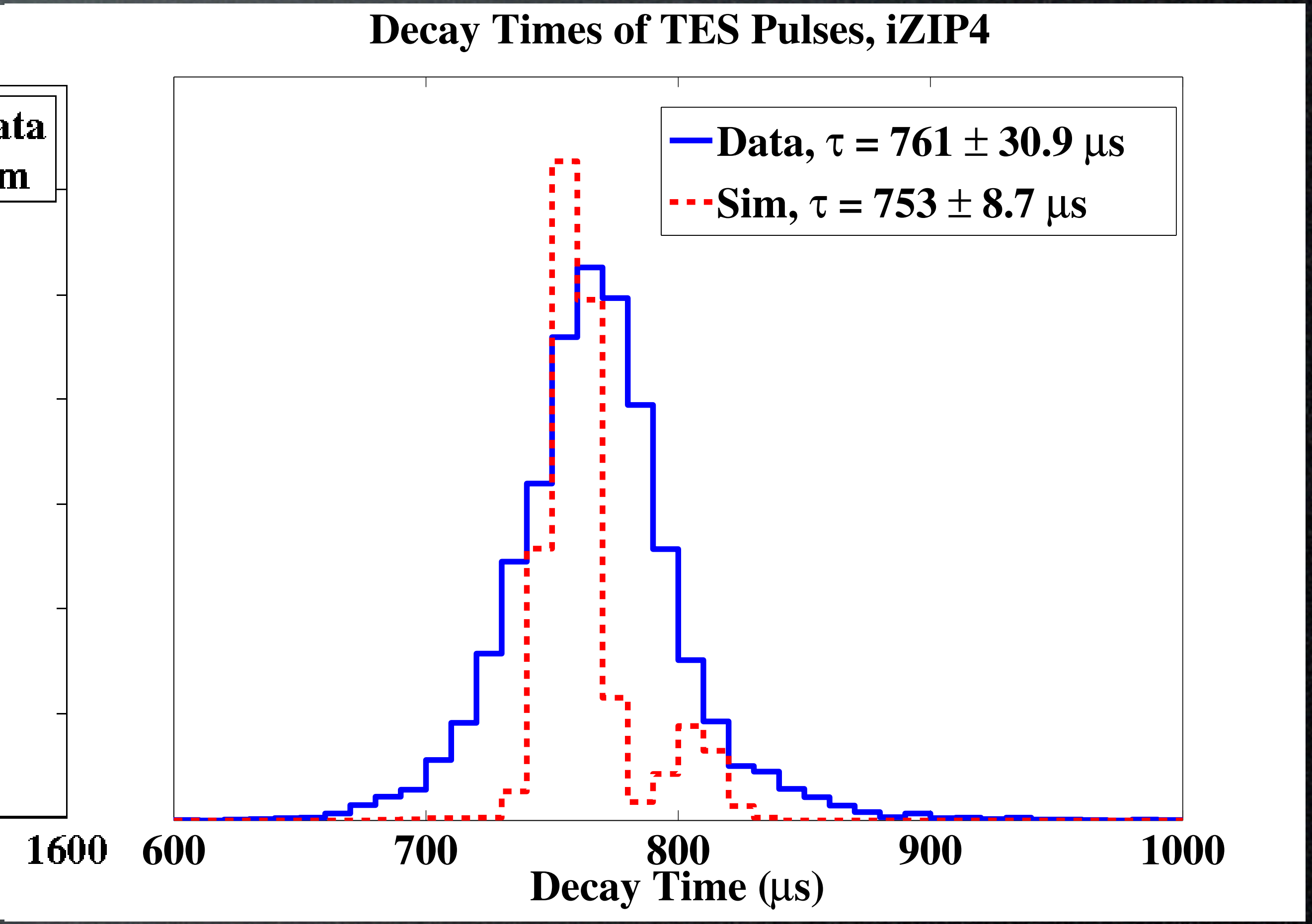

iZIP3 Rise Times - G3D

- Luke phonons, Phonon-aluminum interaction probability, QP-phonon downconversion and TES dynamics

Low Tc Side = 55 mK

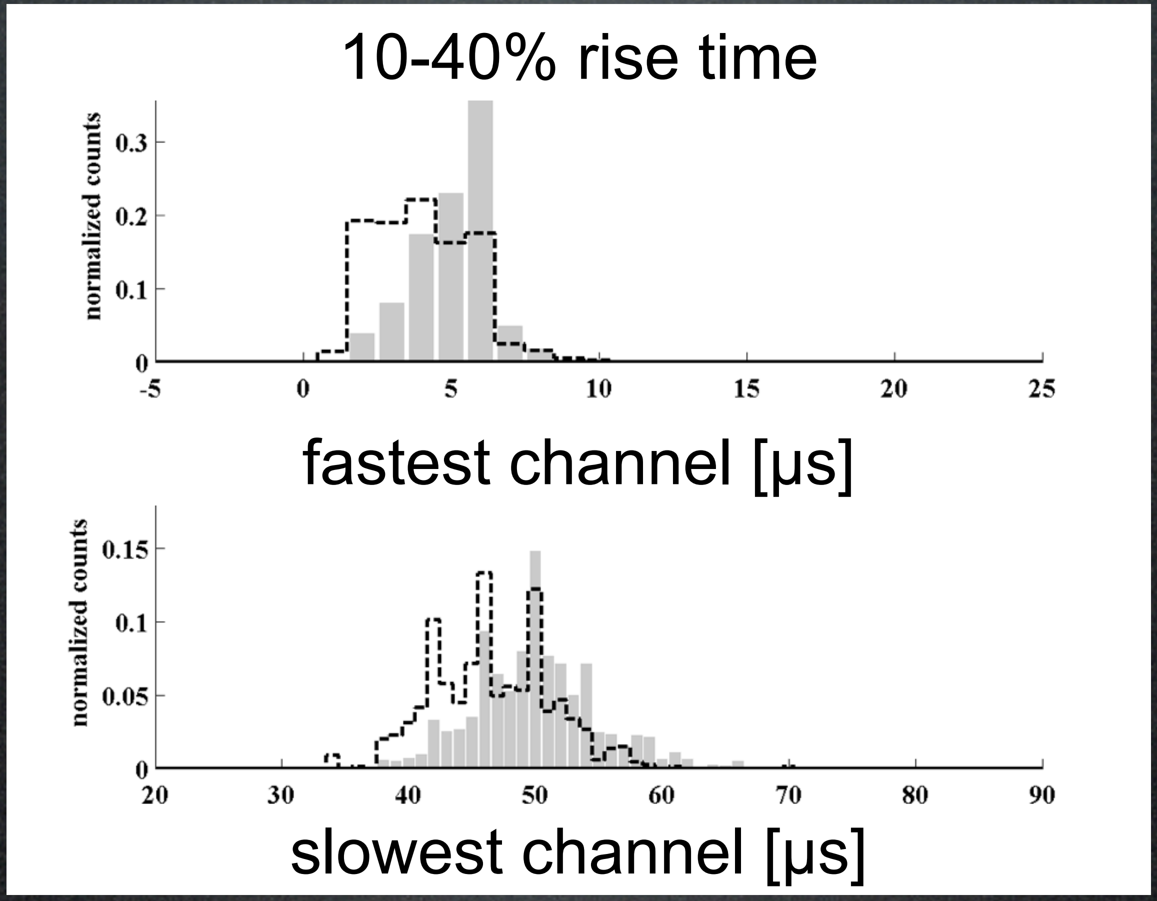

iZIP4 Rise Times - G48

- Luke phonons, Phonon-aluminum interaction probability, QP-phonon downconversion and TES dynamics
    - Need to improve detector physics or GEANT4 input?

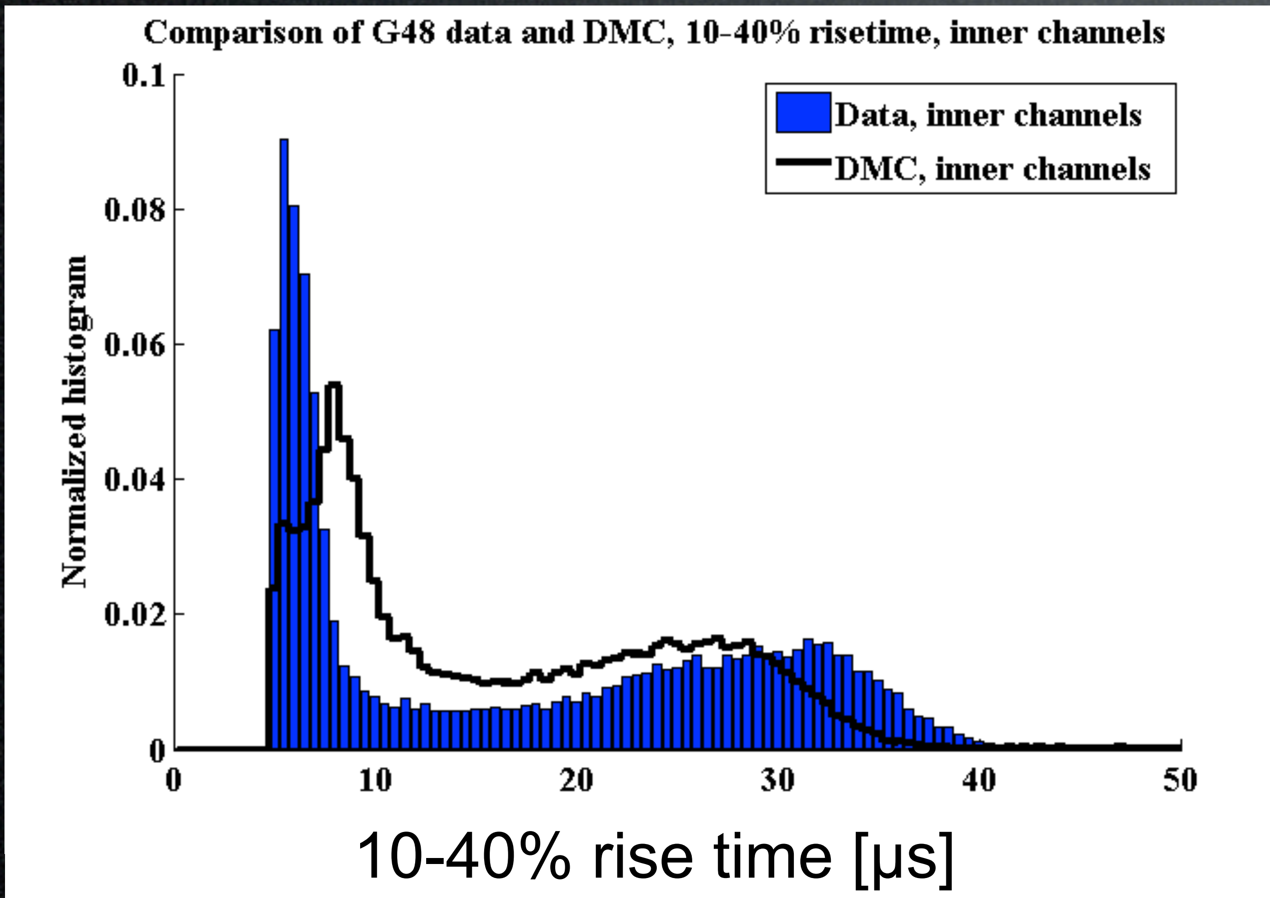

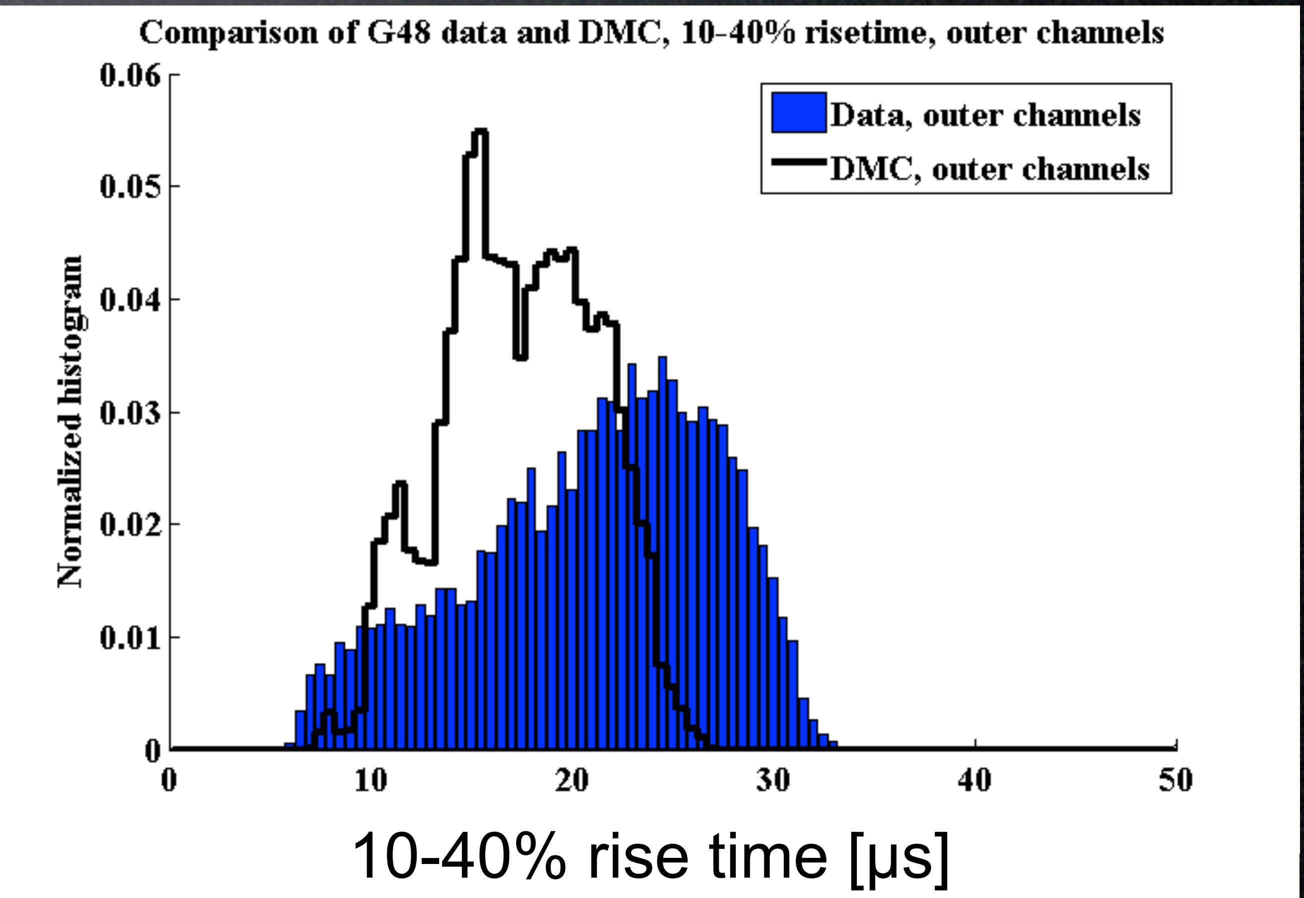

TES Pulse Matching

- Direct comparison of TES pulses from data and MC (2 mm raster scan).

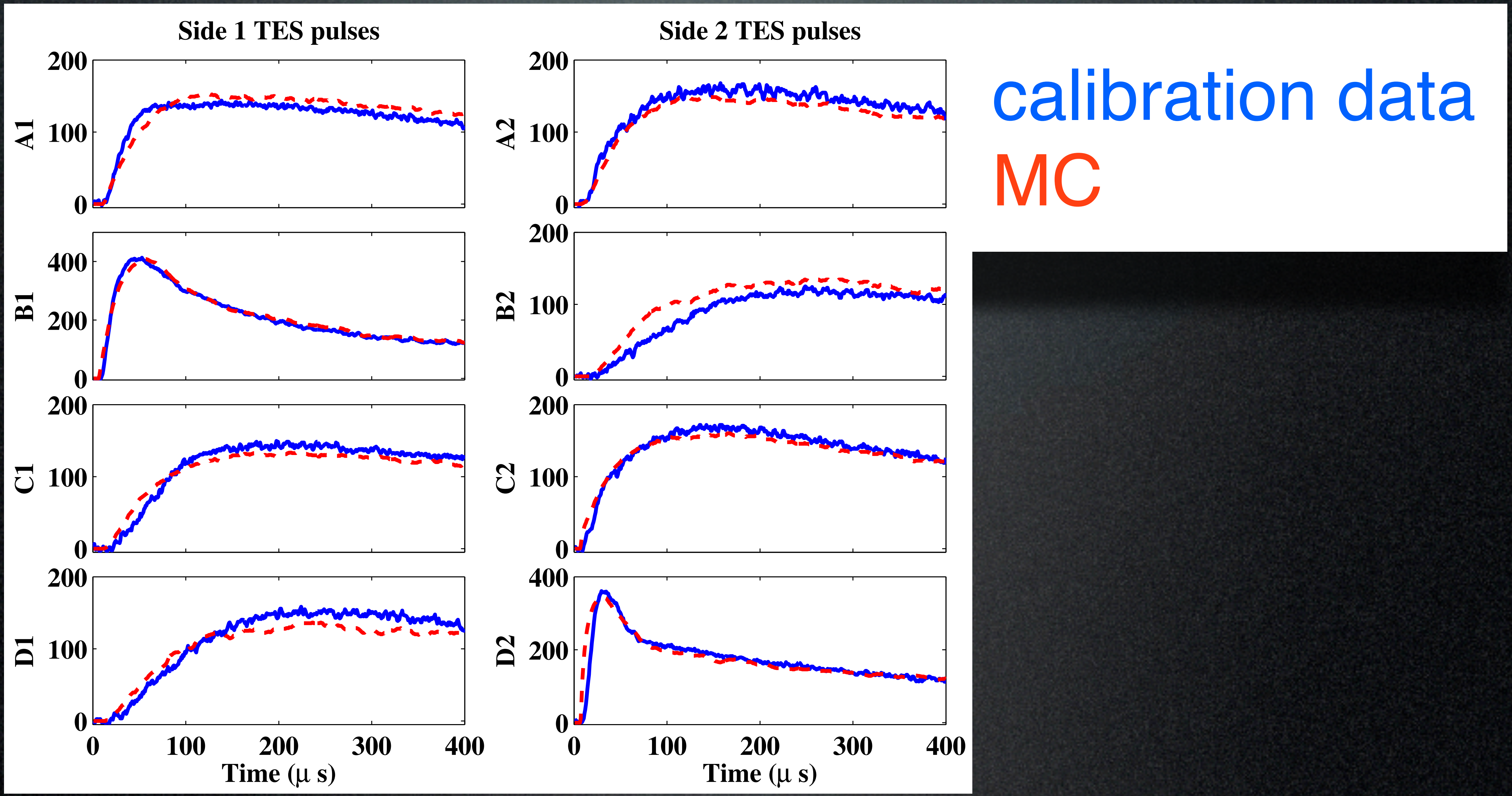

Surface Events

Reduced ionization

MC tuning with charge carrier momentum and surface interaction dynamics

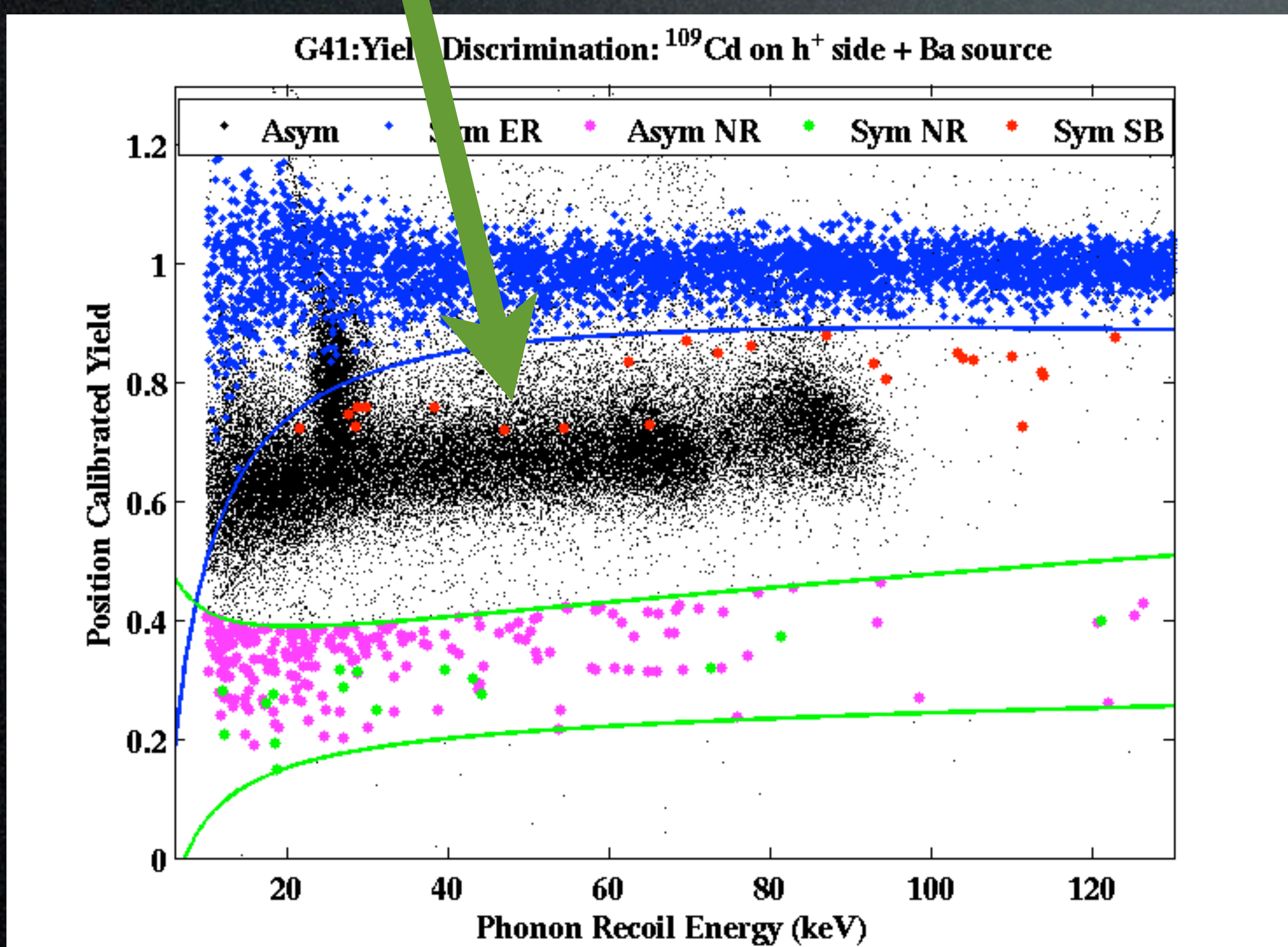

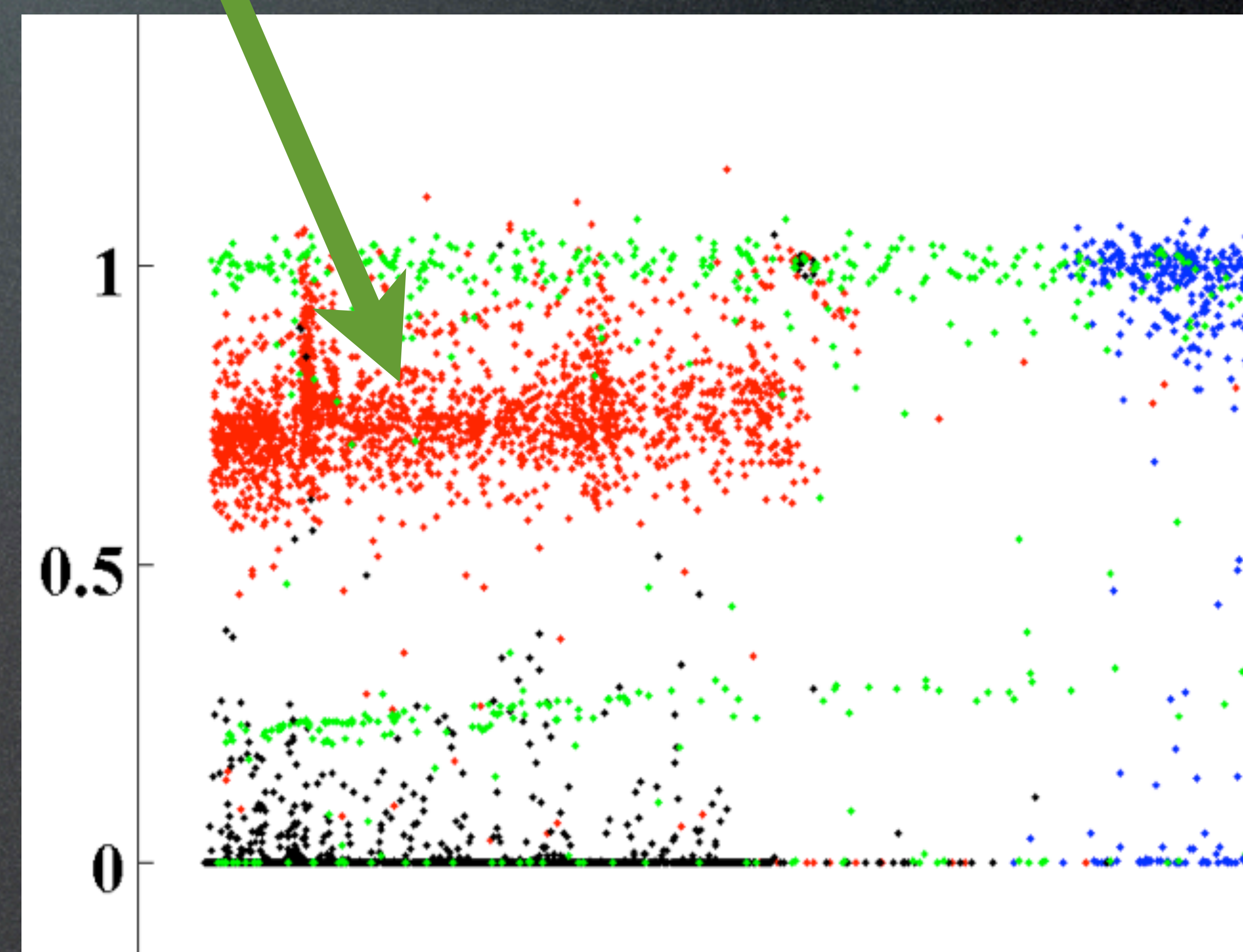

Implications for Design, Operation and Data Analysis

Optimize TES Length

Analytical, 1st order Fourier expansion of TES Joule power and thermal diffusion overestimates PS length

$$l_{\rm PS} = \sqrt{\frac{\pi^2 L}{\alpha \Sigma T_c^3 \rho_n}}$$ ~250 μm

Numerical models more accurate

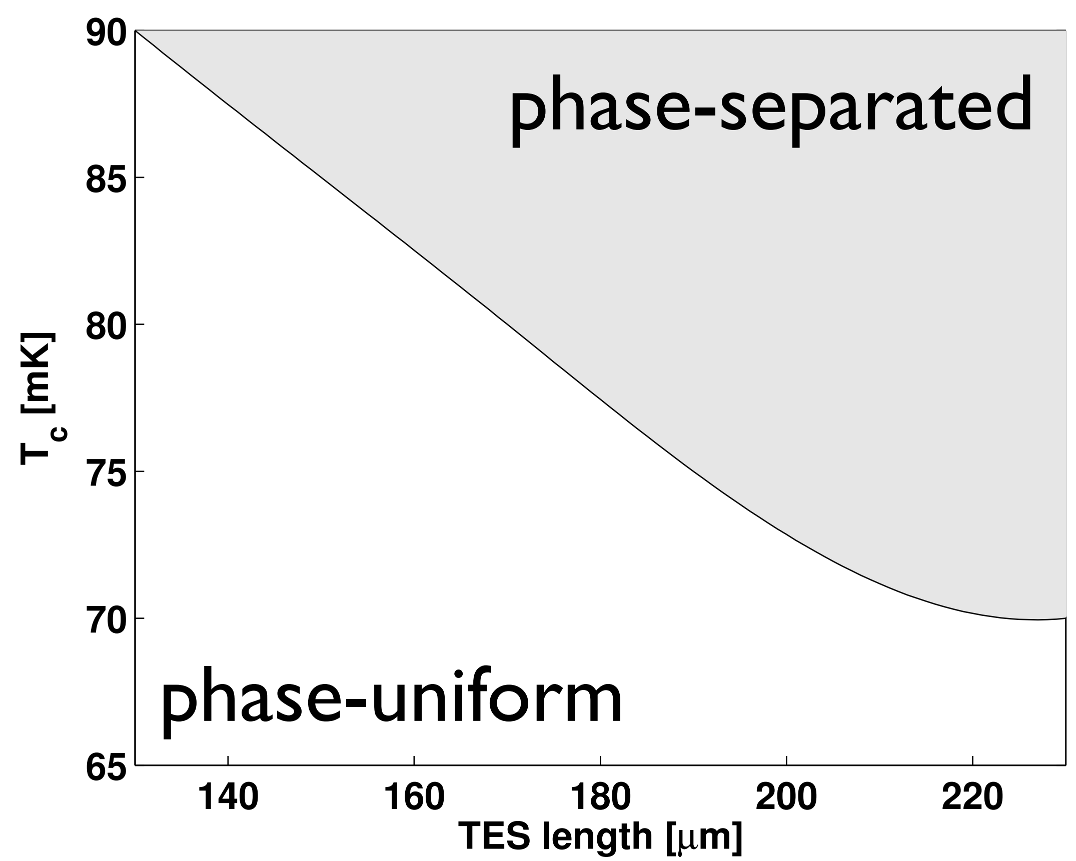

(simulation)

Multiple Surface Events

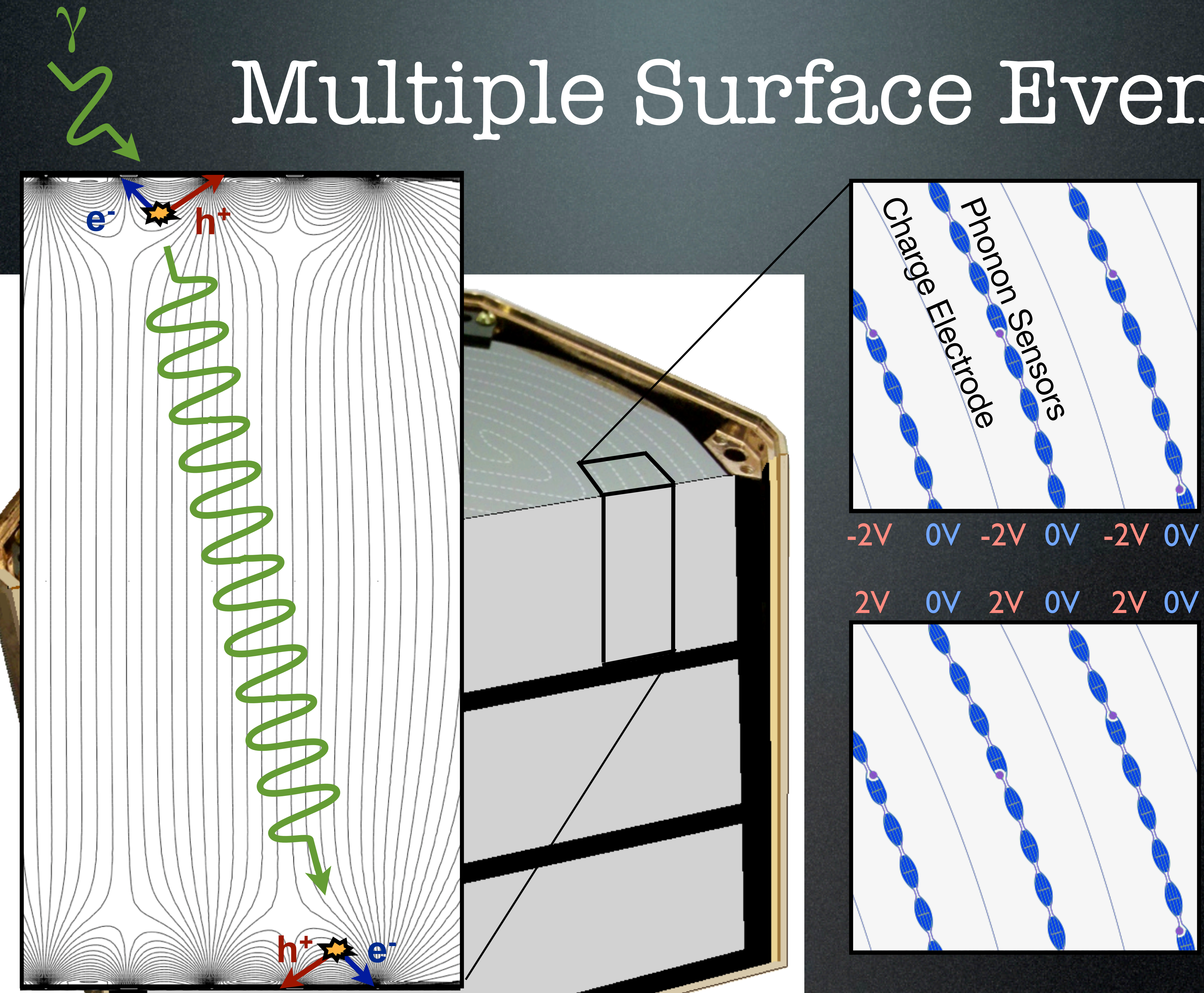

Multiple Surface Events

- GEANT4 + MC indicate 6.8-13.6 Multiple Surface events ton^{-1} year^{-1}

- Phonon pulse shape
  - rapid rise time for surface events

- Outer channel signals
  - no signal for surface events!

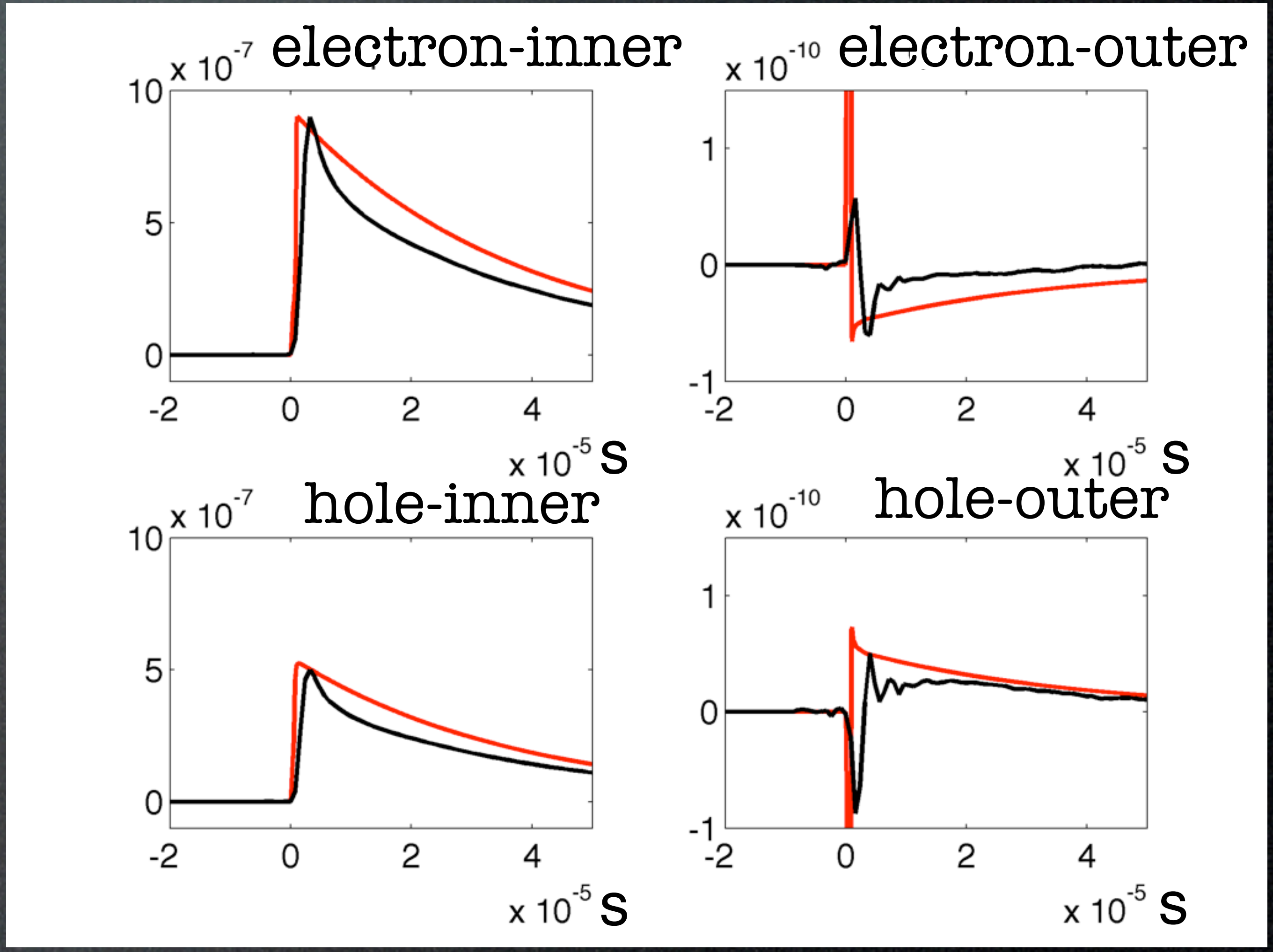

Reverse-MC Analysis

- Utilize all phonon pulse shape and charge information for
  - Event classification
    Bulk / surface
    Gamma / nuclear recoil
    Single / multiple
  - Energy estimation

Charge Fiducial Volume

diameter × thickness [mm]	orientation	Cu can diameter [mm]	Ge-Cu space [mm]	fiducial volume [g]	fiducial volume [%]
76.2 × 25.4	100	80.2	2	400	64
76.2 × 25.4	100	84.2	4	380	61
76.2 × 25.4	100	92.2	8	360	58
100 × 25.4	100	104	2	720	67
100 × 25.4	100	108	4	700	66
100 × 25.4	100	116	8	700	65
100 × 33.33	100	104	2	980	70
100 × 33.33	100	108	4	950	68
100 × 33.33	100	116	8	920	66
76.2 × 25.4	111	80.2	2	380	61
76.2 × 25.4	111	84.2	4	380	61
76.2 × 25.4	111	92.2	8	370	59
100 × 25.4	111	104	2	700	66
100 × 25.4	111	108	4	700	66
100 × 25.4	111	116	8	700	65
100 × 33.33	111	104	2	950	68
100 × 33.33	111	108	4	950	68
100 × 33.33	111	116	8	940	67

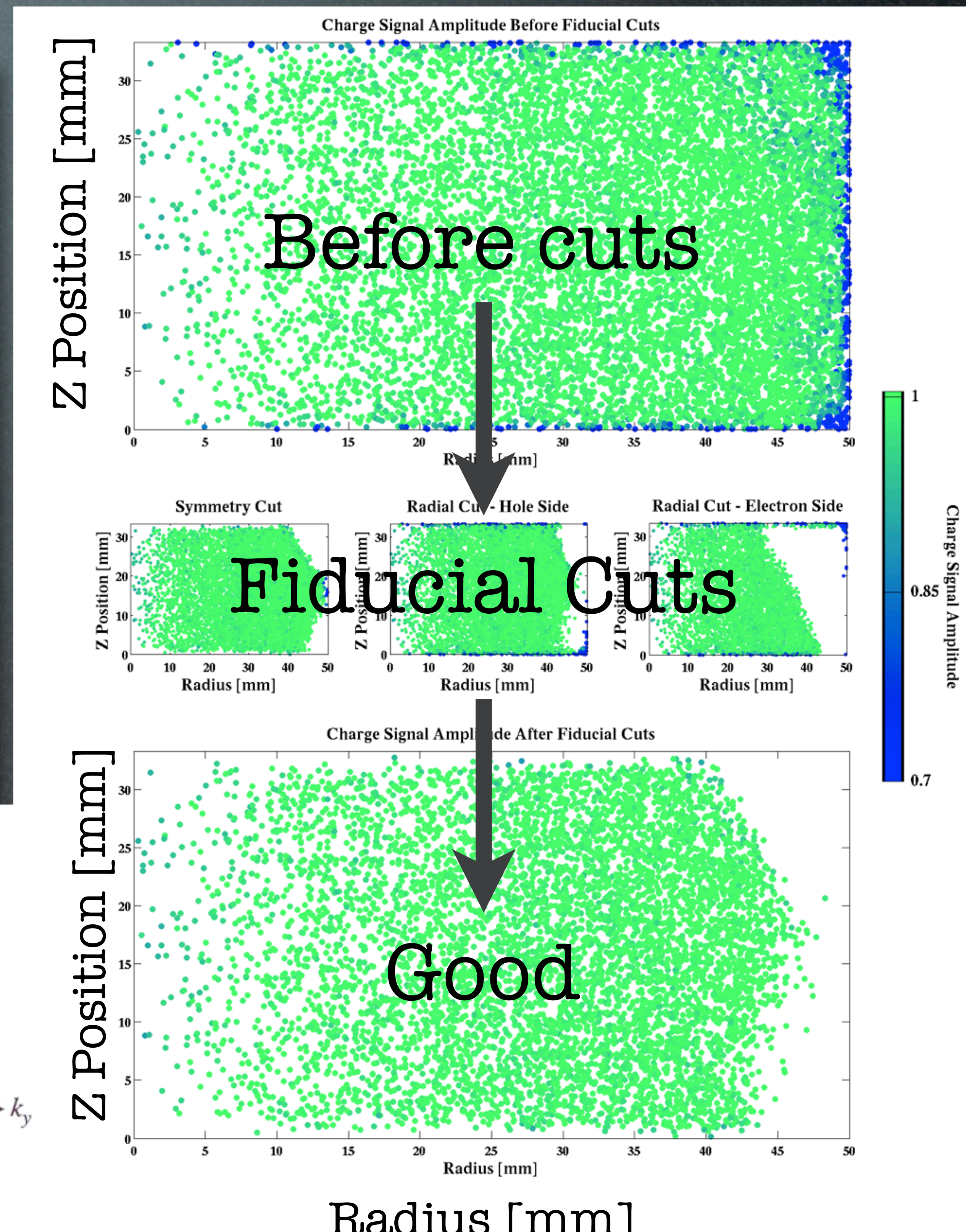

Design work on electrode structure and tower design ongoing

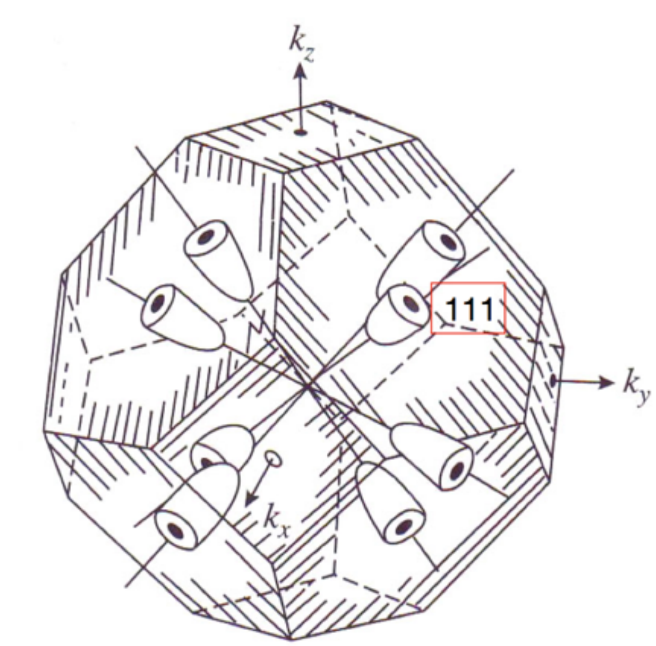

L valleys of Ge

Advanced detector MC of cryogenic, phonon and ionization detectors

Charge

- E-field models
- Electron mass tensor
- Electron inter-valley scattering
- Neganov-Luke phonons
- Ramo-Shockley potential signal

Phonon

- Phonon focusing
- Isotope scattering
- Anharmonic decay
- Quasiparticle / phonon downconversion

Transition Edge Sensor

- Phase separation
- Internal fluctuation noise

Validation

- Electron inter-valley scattering
- Phonon pulse shape

Usage

- Phonon channel layout
- Charge channel layout
- Crystal orientation
- TES phase separation length
- TES noise
- Background rejection
- Reverse-MC data analysis

Backup Slides

100-110 Crystal Orientation

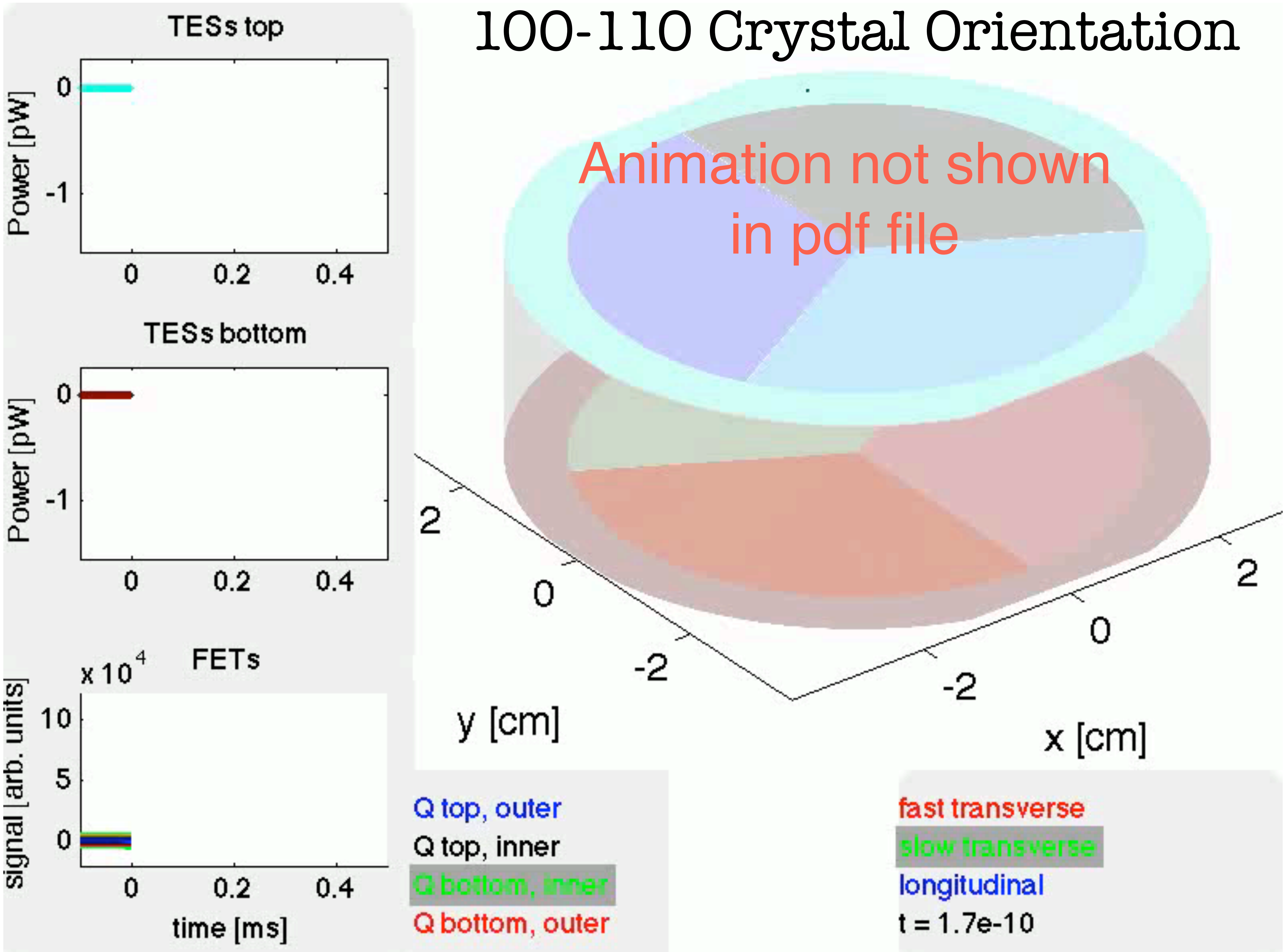

111-122 Crystal Orientation

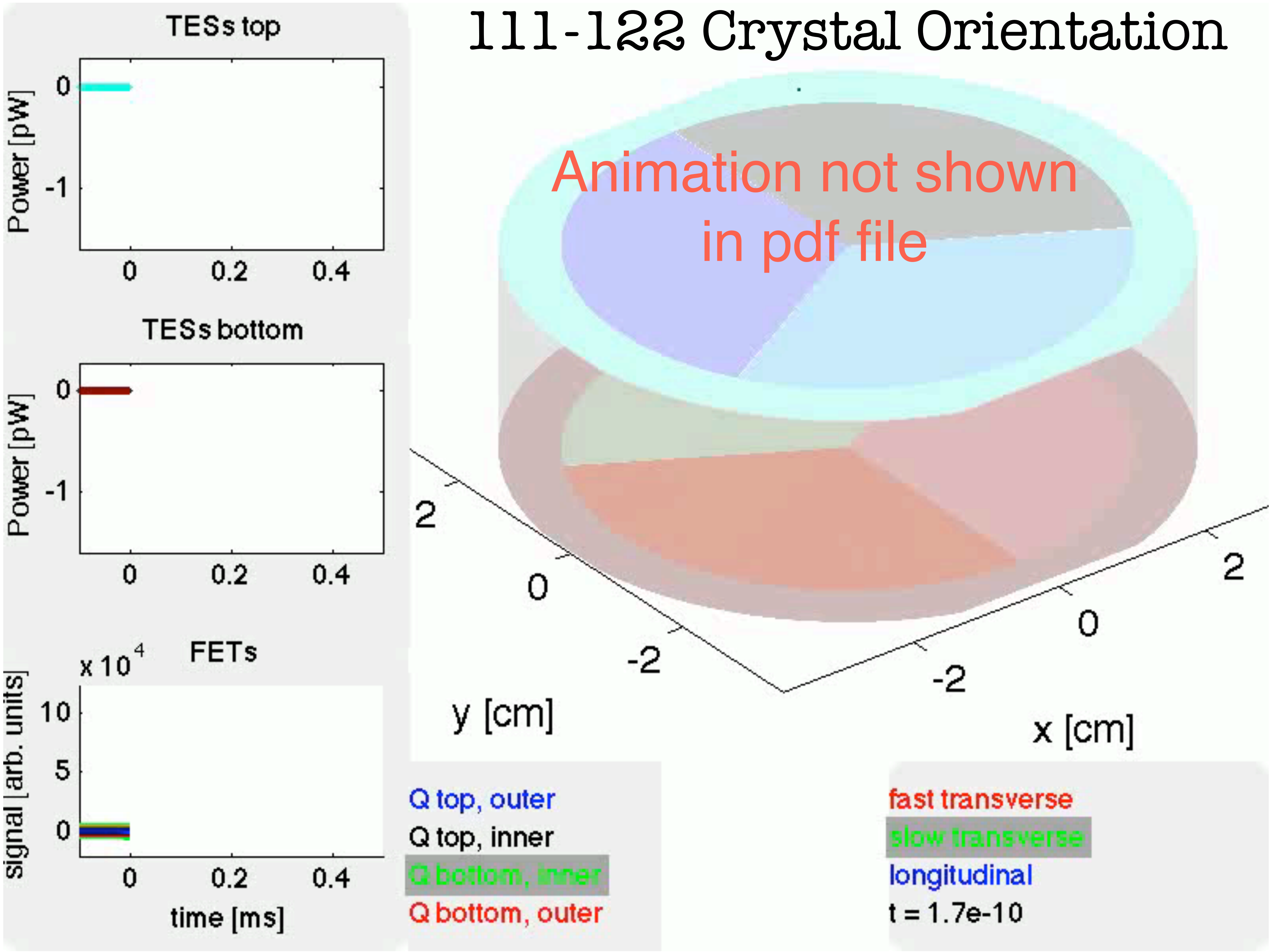

Charge Degradation

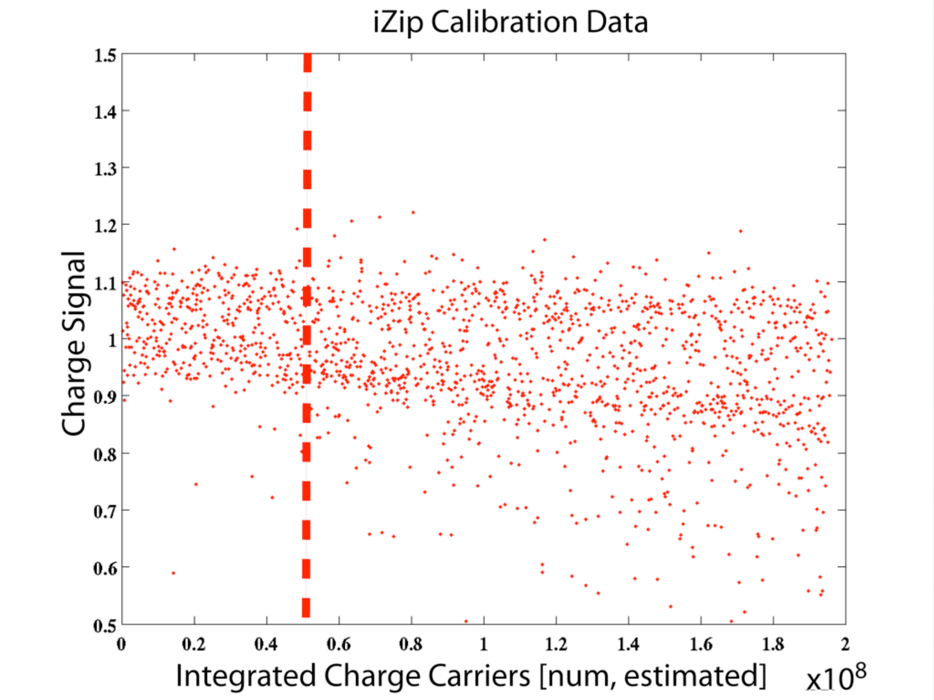

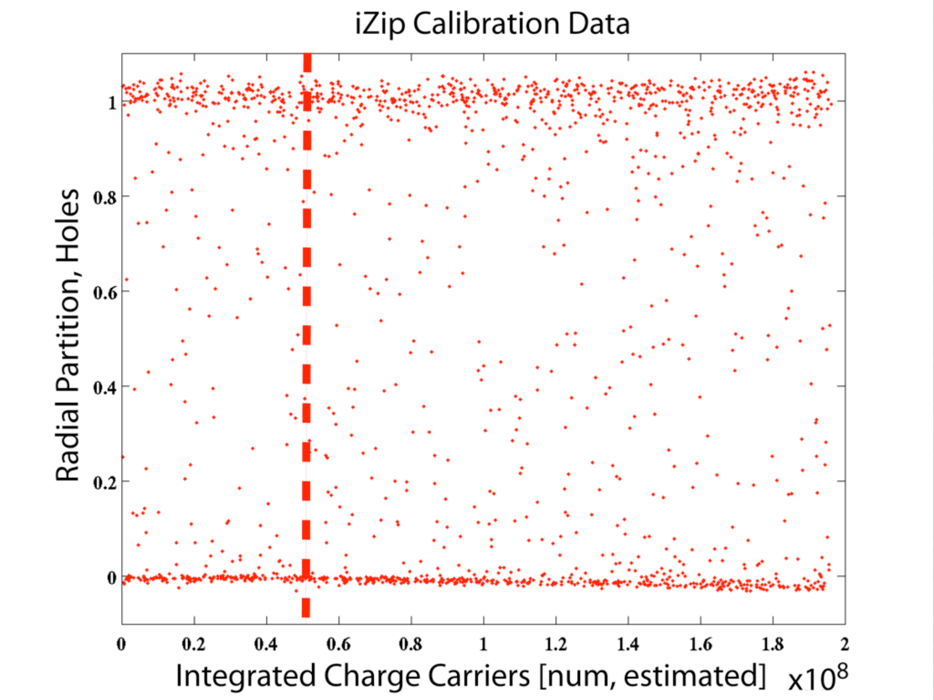

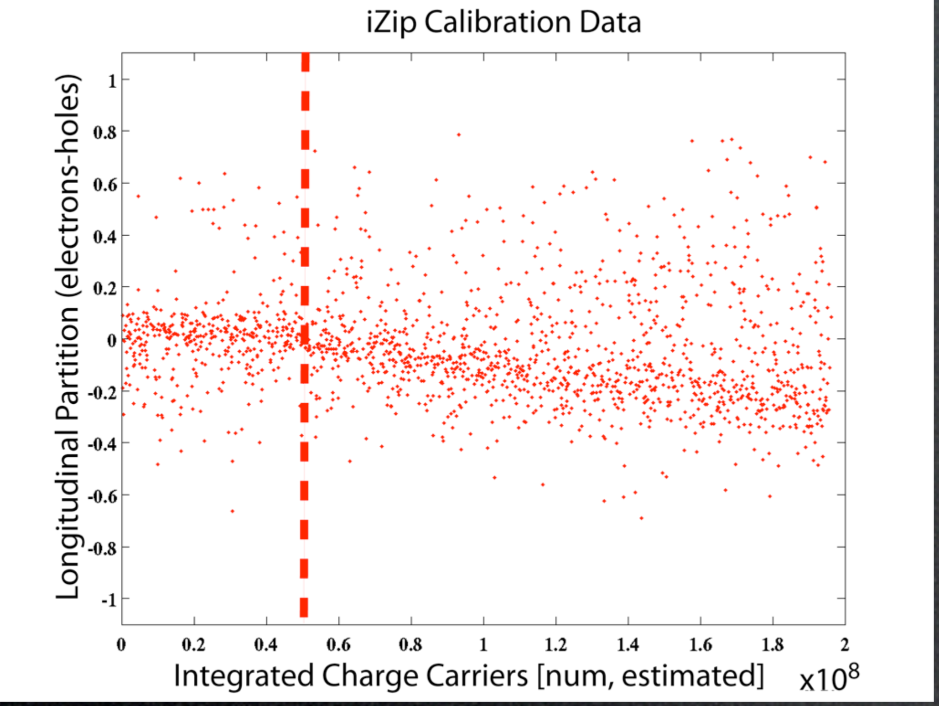

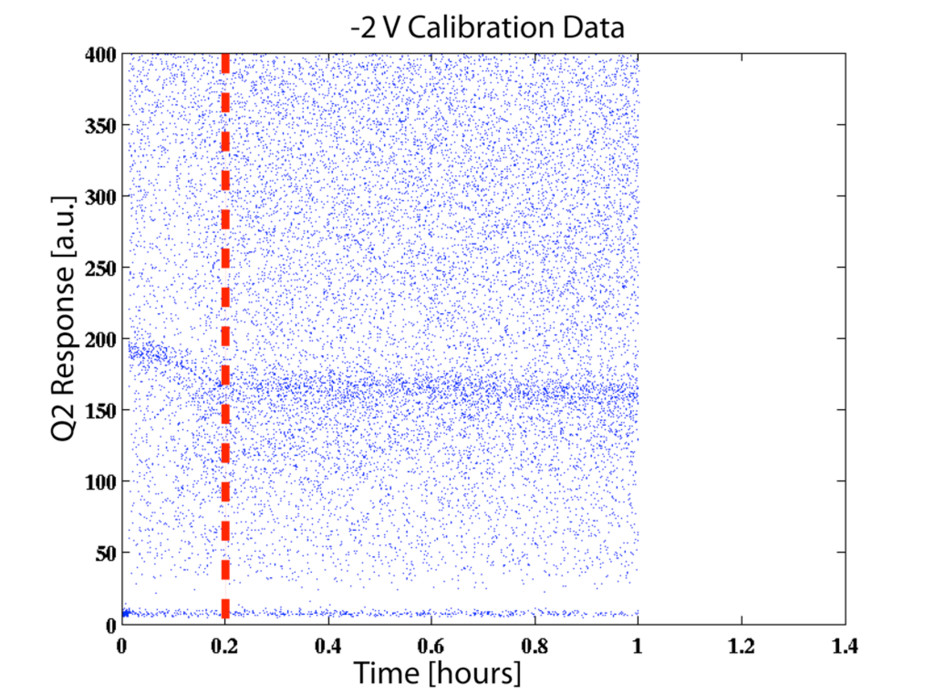

Event Induced Potential

Initial

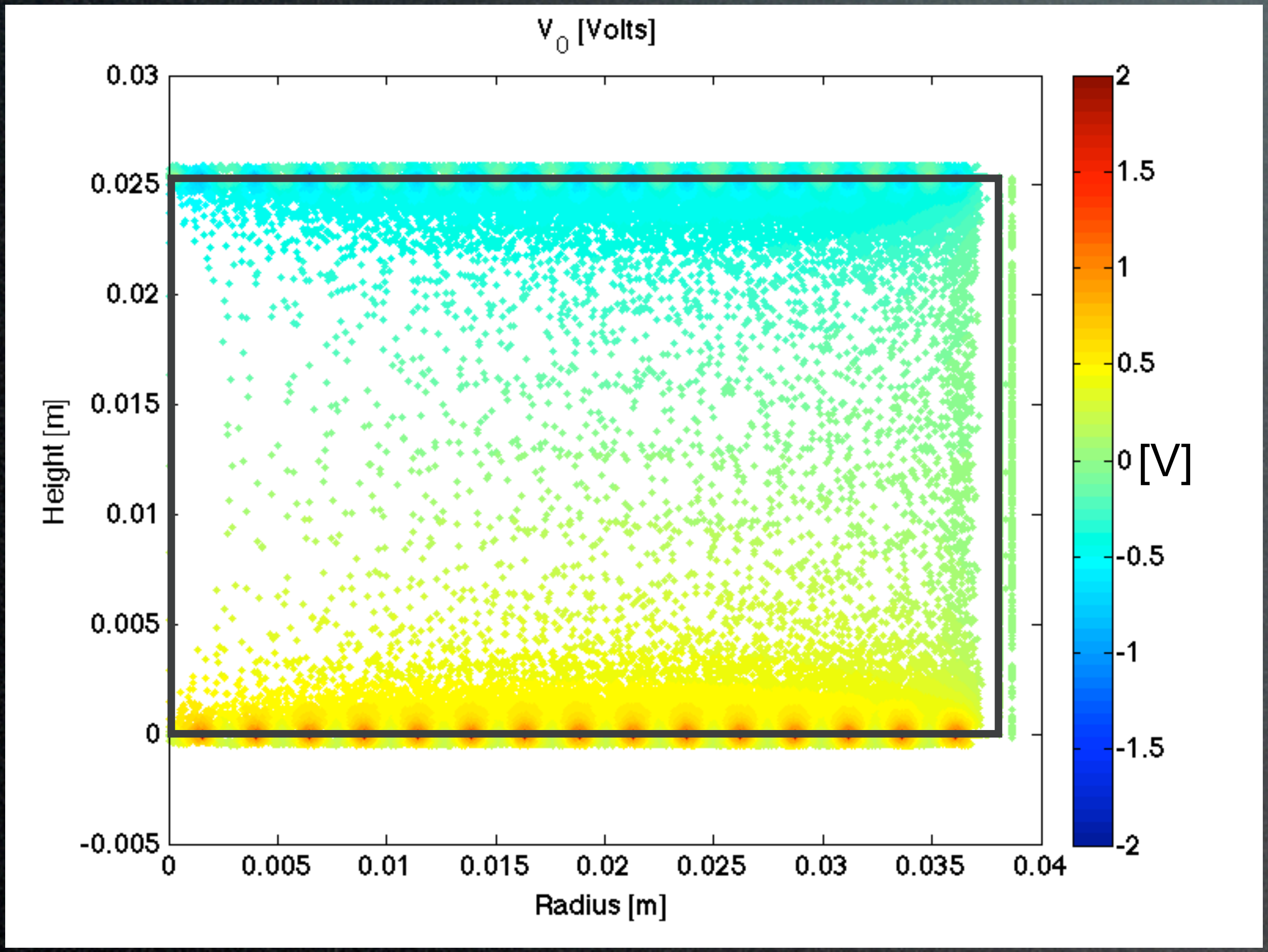

After gamma exposure

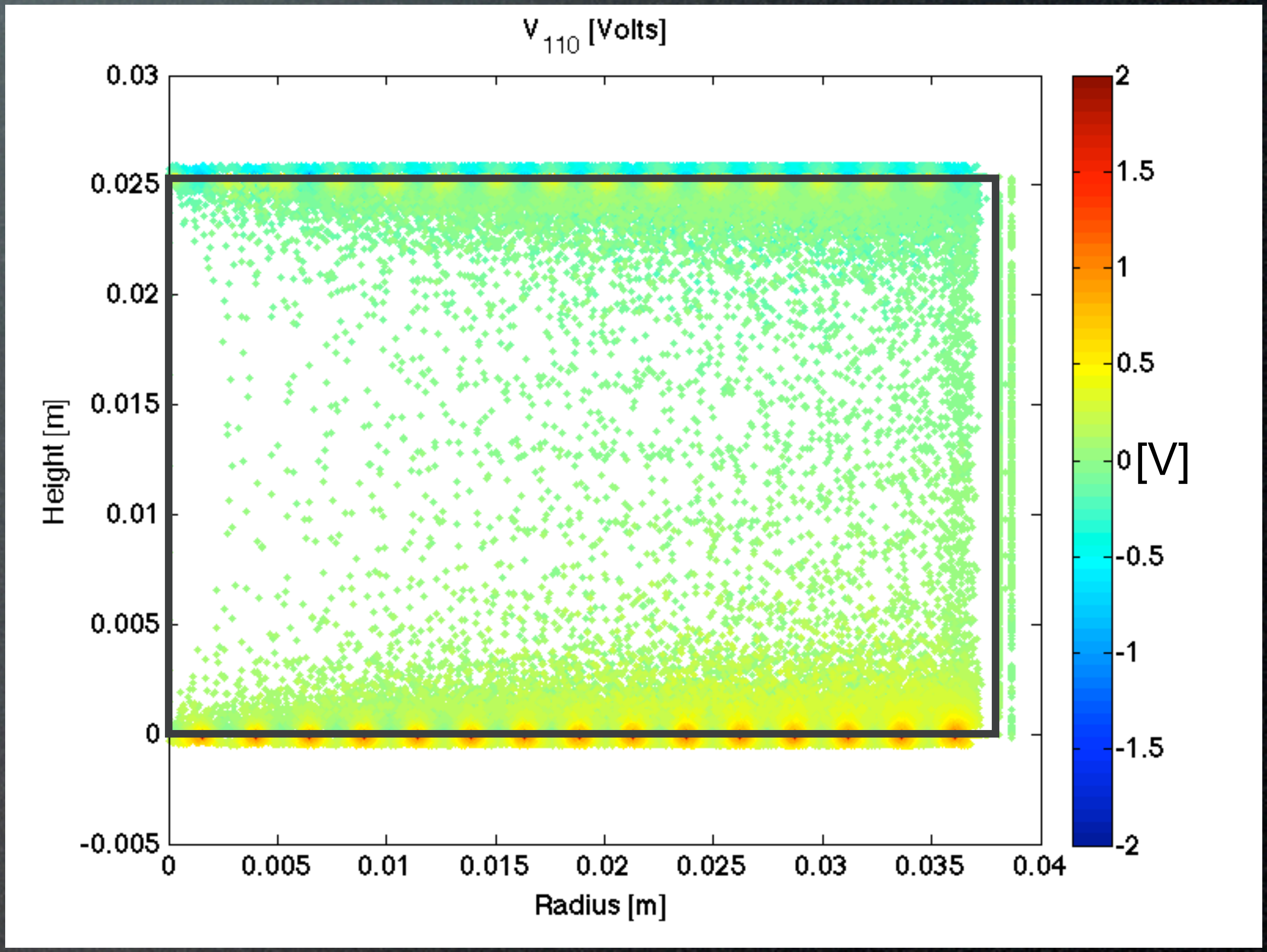

dots indicate mesh points

Data vs. MC

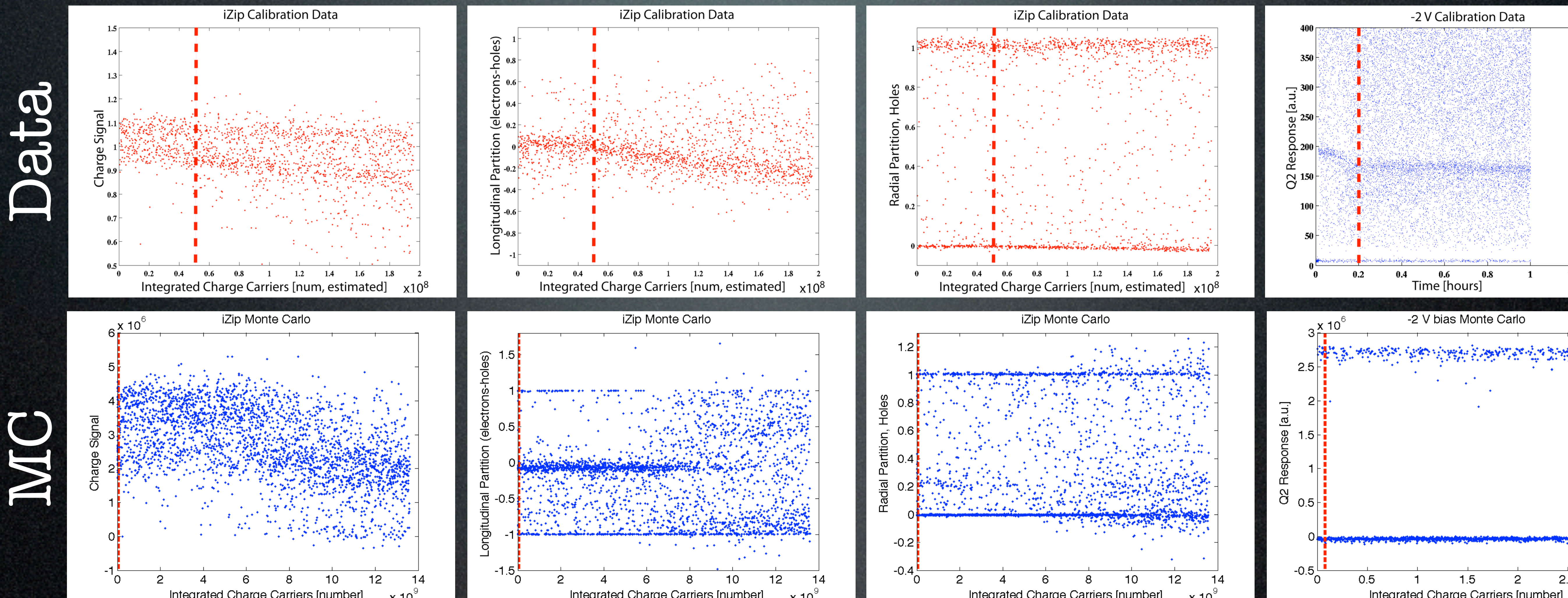

- - - - - - Period of comparable gamma exposure

- Not the right model! A red herring?

Polarization In CdTe

- Similar effect seen in CdTe
  - Independent of radiation rate
  - Depolarization faster than polarization
  - Consistent with negative space charge

CdTe Conclusion

- Ionization of deep acceptors
- Mitigation steps
  - Pulsing bias off
  - Different contact materials

Early Identification

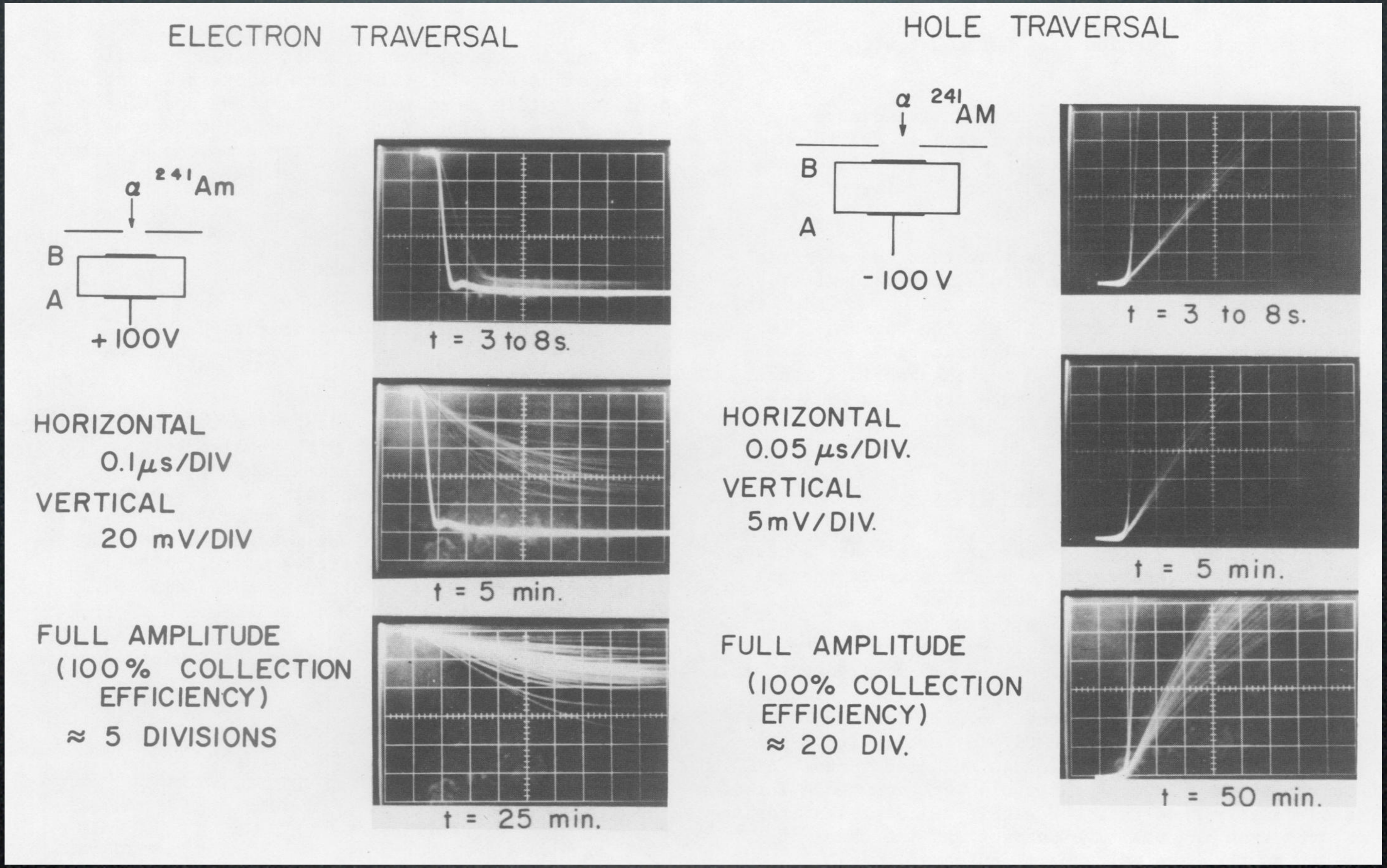

- Possibly can be identified by slowing of electron transport times

Temperature Dependence

$$\tau_I = \frac{1}{N_0 \sigma < v >} \exp(E/kT)$$

$$\tau_D = \frac{1}{N_v \sigma < v >}$$

- But temperature dependence not observed in iZIP
- Are we seeing polarization similar to CdTe? Or is this a red herring?

Infrared Radiation?

- 0.7 eV bandgap is > IR energy
- Ge is an indirect gap semiconductor, no phonons to mediate excitation at 50 mK

against IR model

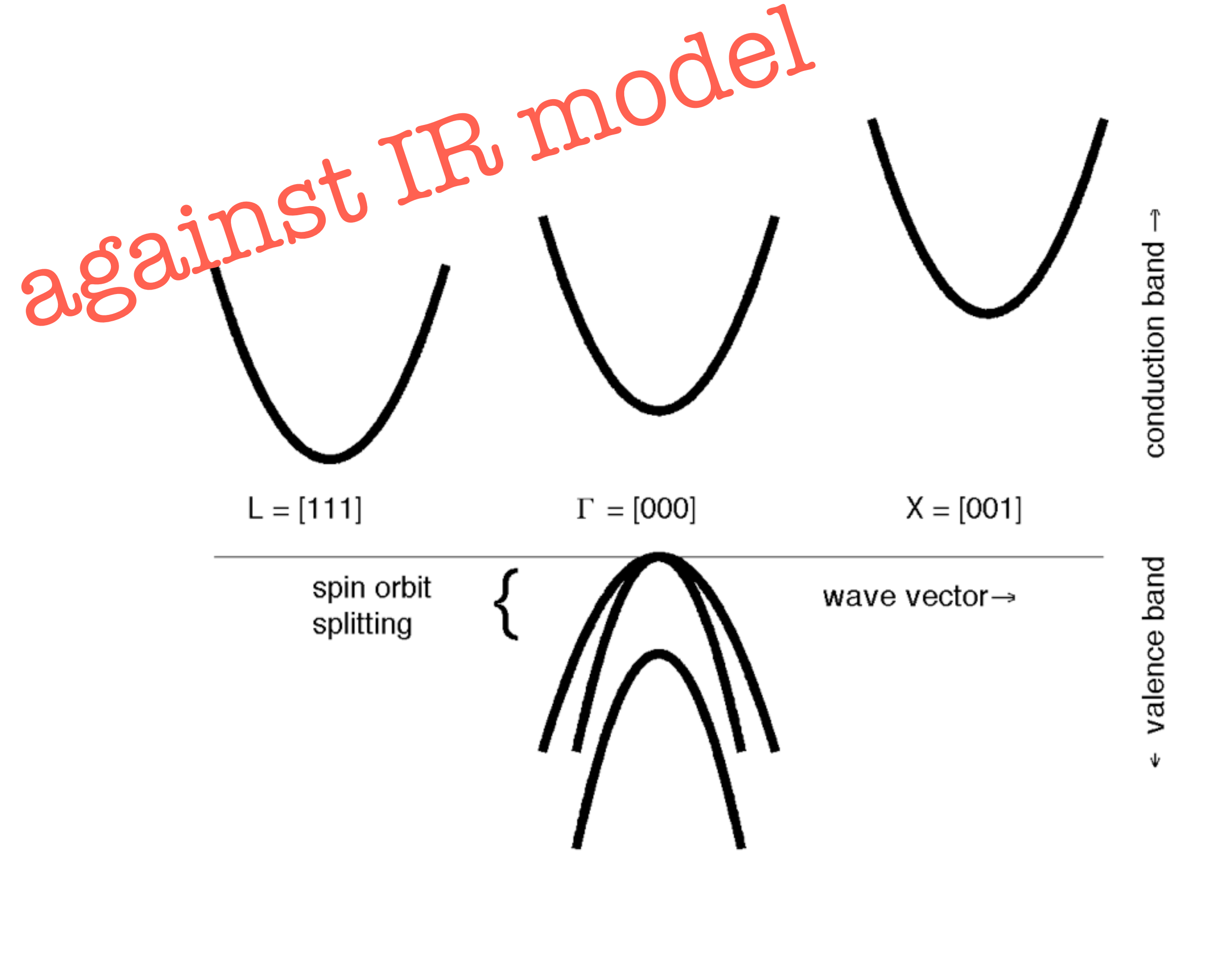

Infrared Radiation?

Optical efficiency of far-infrared photoconductors

J.-Q. Wang, P. L. Richards, J. W. Beeman, N. M. Haegel, and E. E. Haller

We report an experimental and theoretical study to optimize the geometry of far-IR photoconductive detectors with diffraction-limited throughput. Factors considered in this optimization include internal optical path relative to measured absorption length, photoconductive gain, uniformity of illumination, cosmic ray cross section, and compatibility of the design with the requirements of 1- and 2-D arrays. A rod-shaped detector geometry with square cross section, electrodes on the lateral faces, and a beveled backface to trap the radiation by total internal reflection was found to have nearly equal responsivity to the best detectors in integrating cavities.

- Doped germanium detectors are used for IR detection!!!
- Gap reduced at dopants
- Not indirect gap at dopants

Evidence for IR

- Difference seen in Berkeley vs Soudan could be due to different IR environment.
- However attempts to reduce / increase IR at Berkeley show no change in degradation.
- Performance in present run much improved!

Fano Fluctuations

- $E_{creation}$ = 3 eV to create charge carrier
- 0.75 eV bandgap
- Fluctuation in carriers

  $\sigma^2 = F * E_{gamma} / E_{creation}$

  $F_{Ge} = 0.1$

Phonon Group Velocity

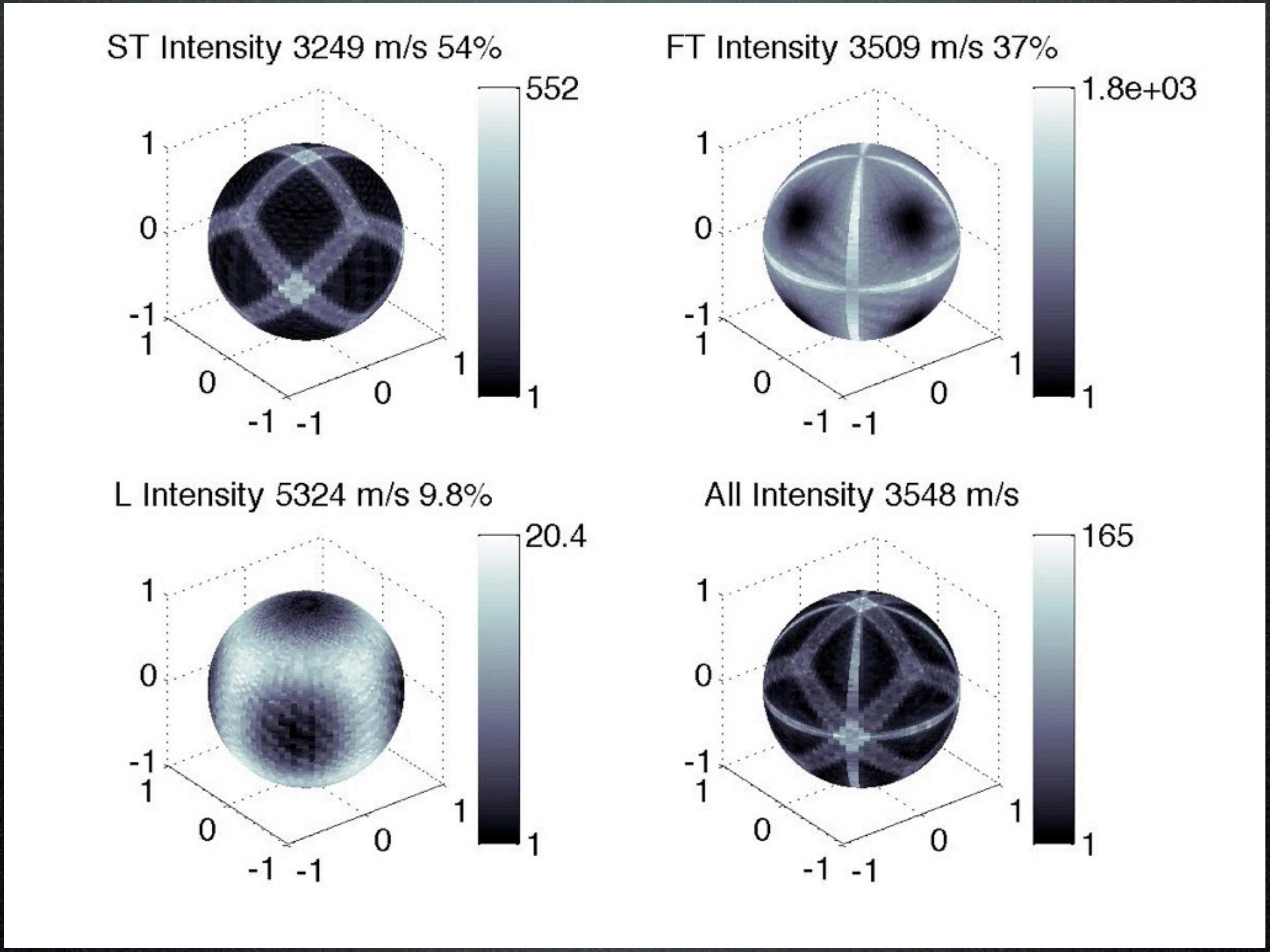

Phonon Focusing Images in [100] Si

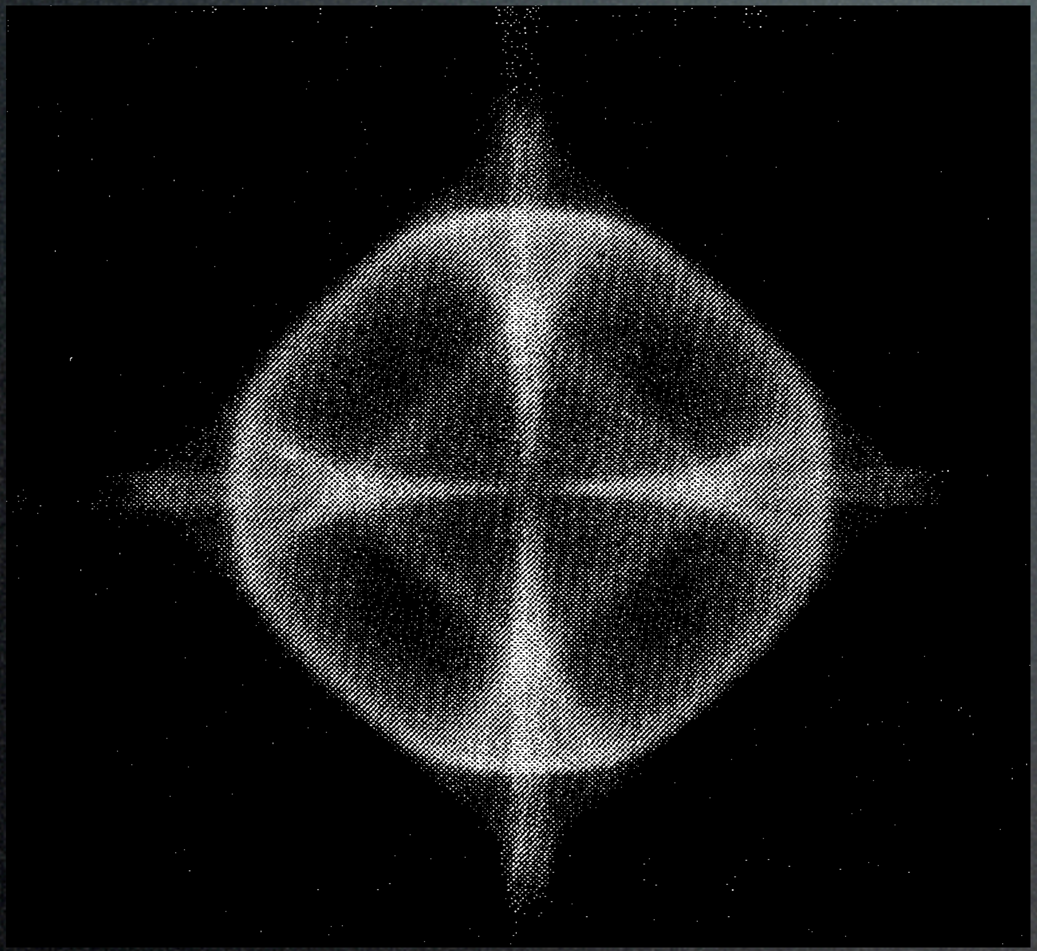

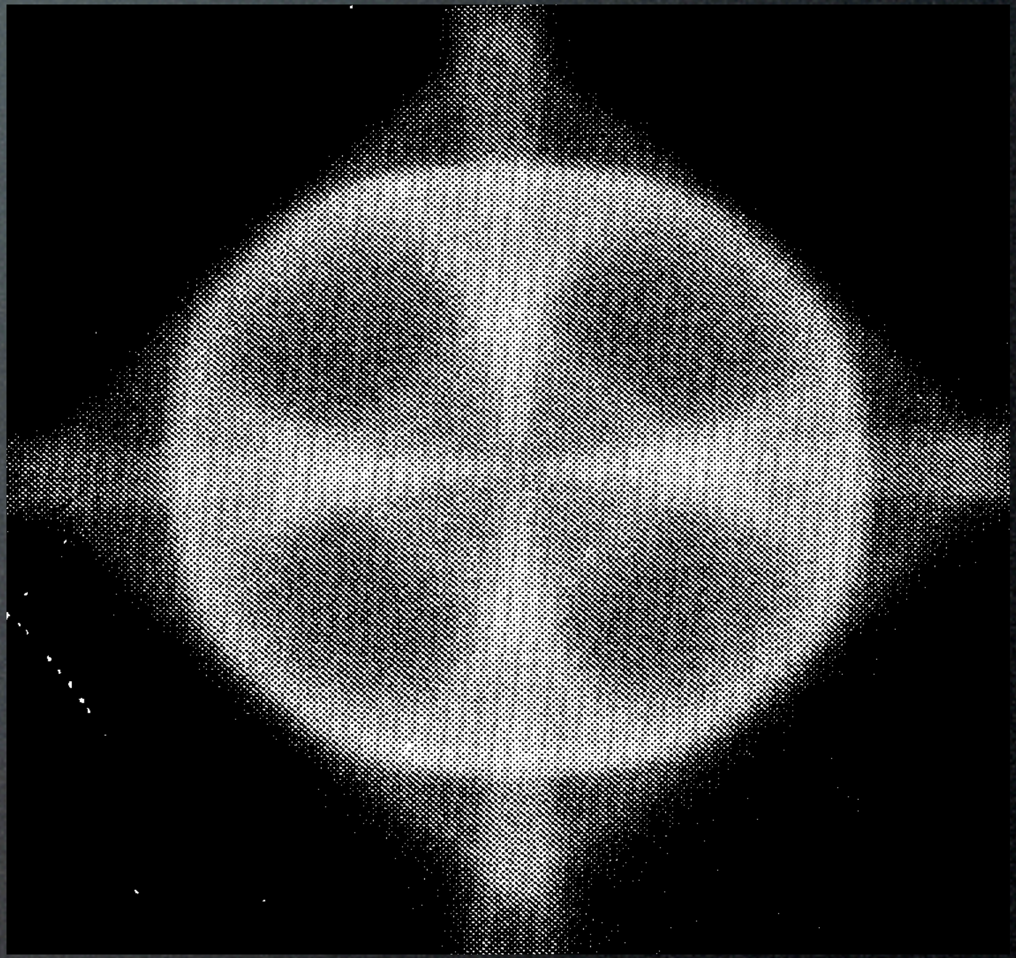

Quasiparticle / Phonon Downconversion

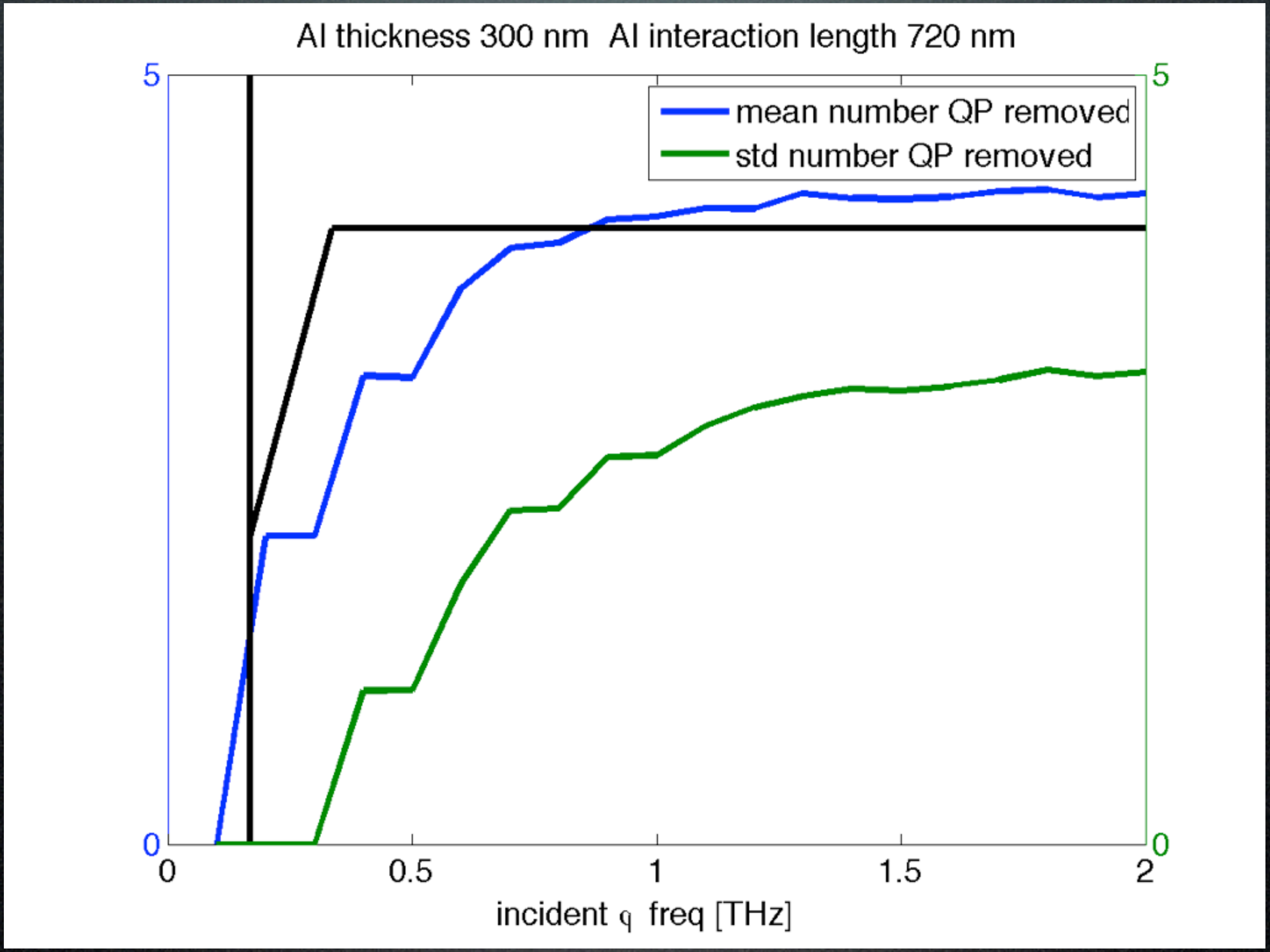

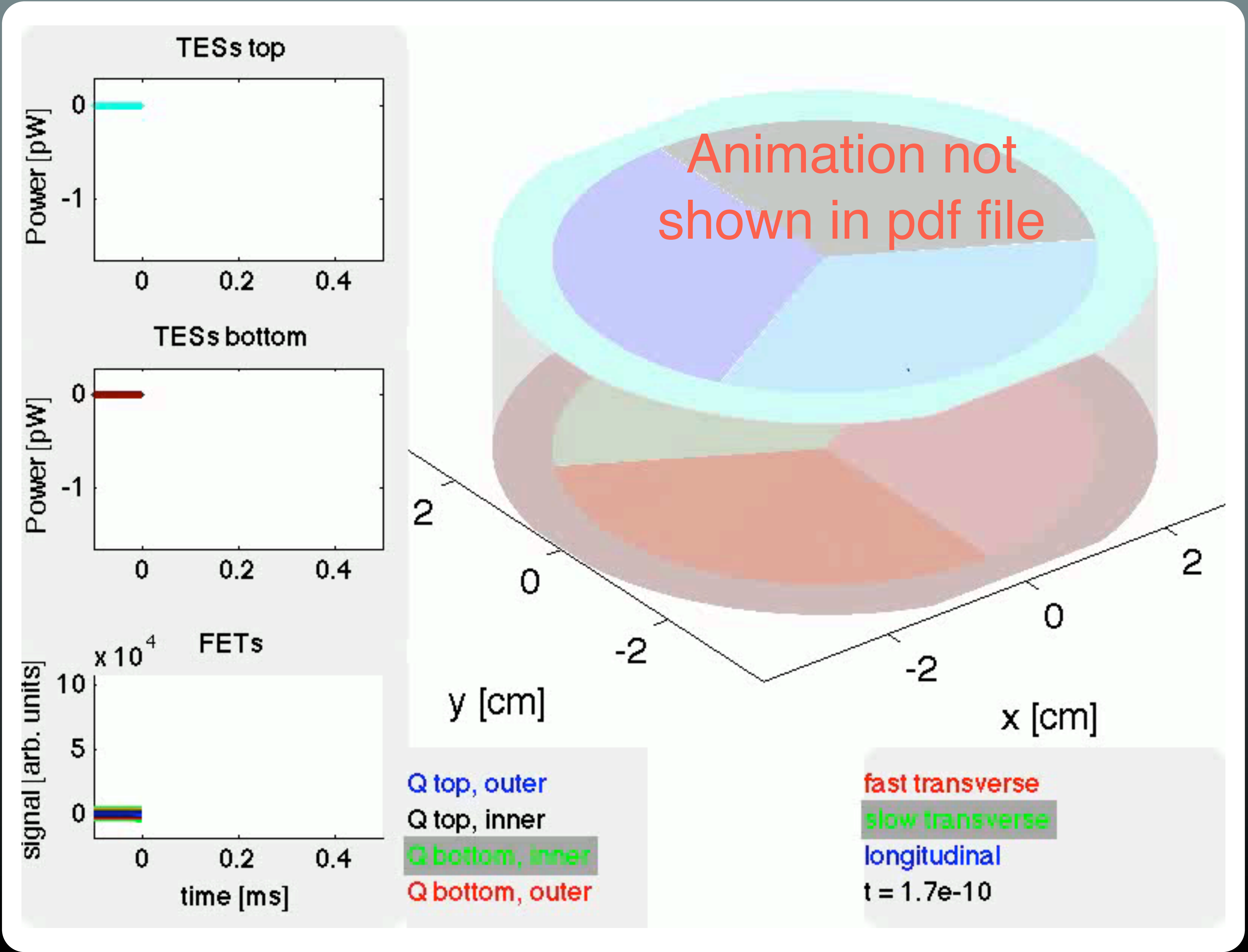

TESs top
Power [pW]
0
-1
0
0.2
0.4
TESs bottom
Power [pW]
0
-1
0
0.2
0.4
FETs
x 10^4
signal [arb. units]
10
5
0
0
0.2
0.4
time [ms]
Animation not shown in pdf file
2
0
-2
y [cm]
2
0
-2
x [cm]
Q top, outer
Q top, inner
Q bottom, inner
Q bottom, outer
fast transverse
slow transverse
longitudinal
t = 1.7e-10

Phonon Timing

Timing Cut, expected 0.5 surface event leakage into nuclear recoil band

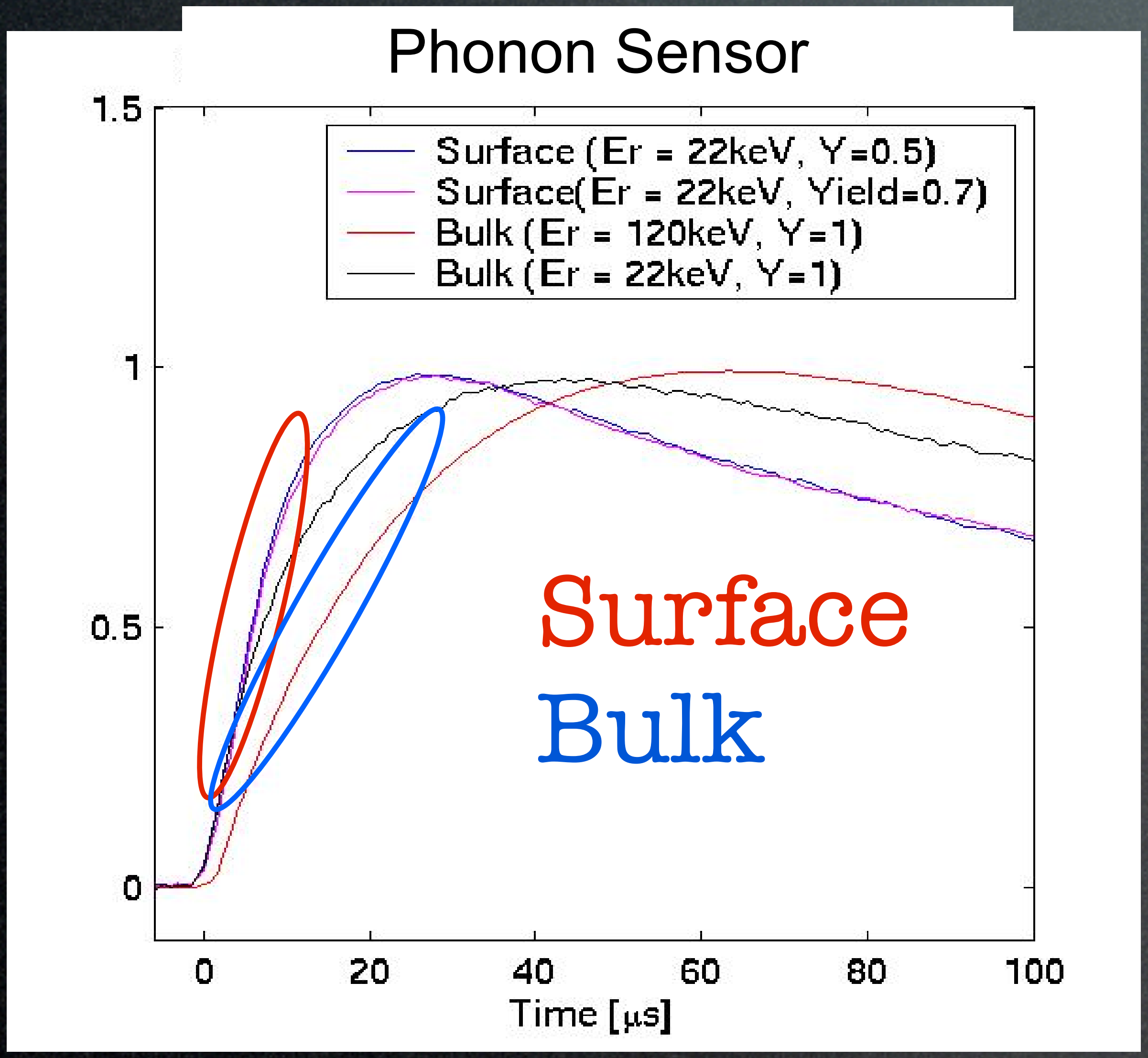

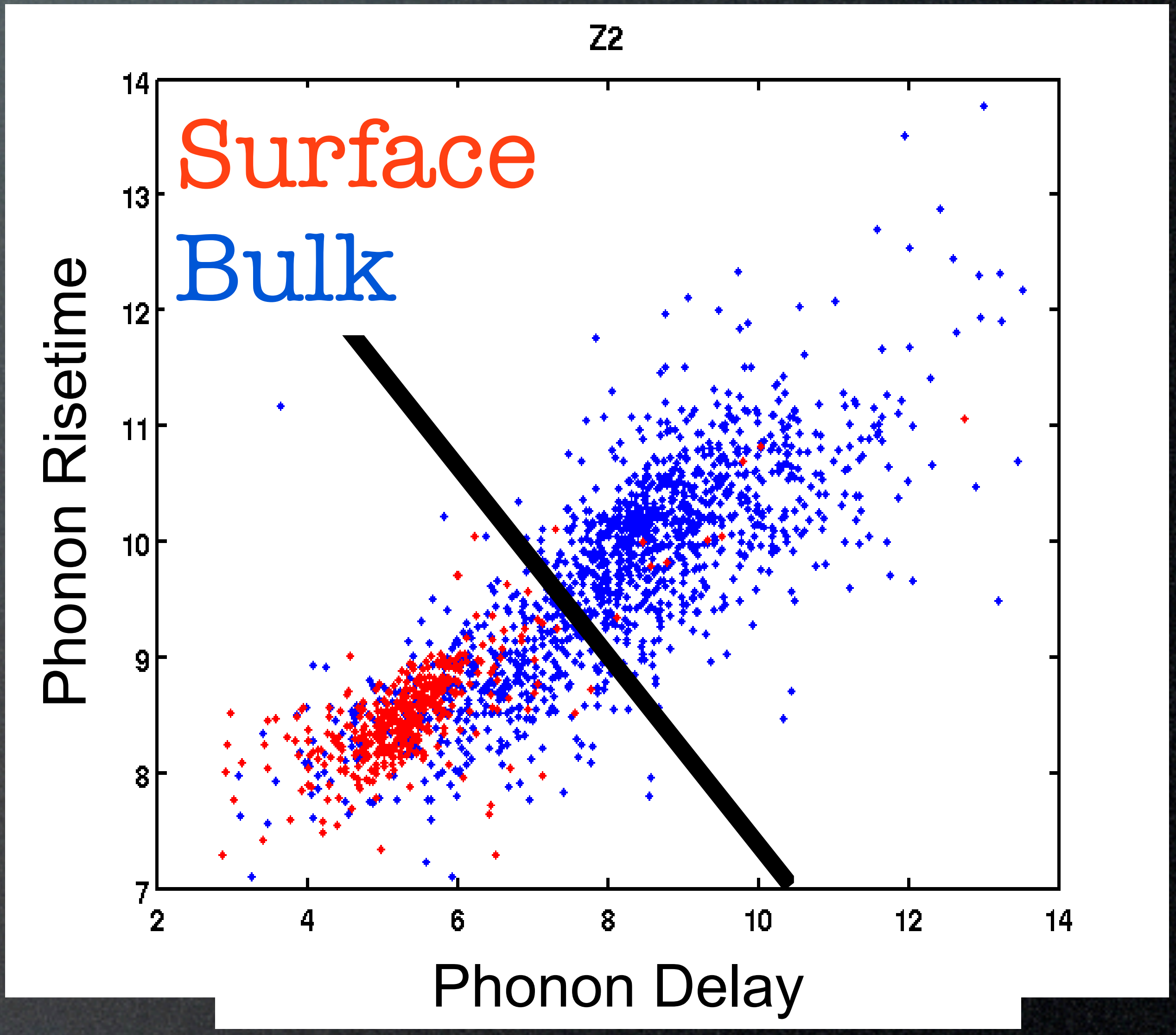

Z-Position in iZIP

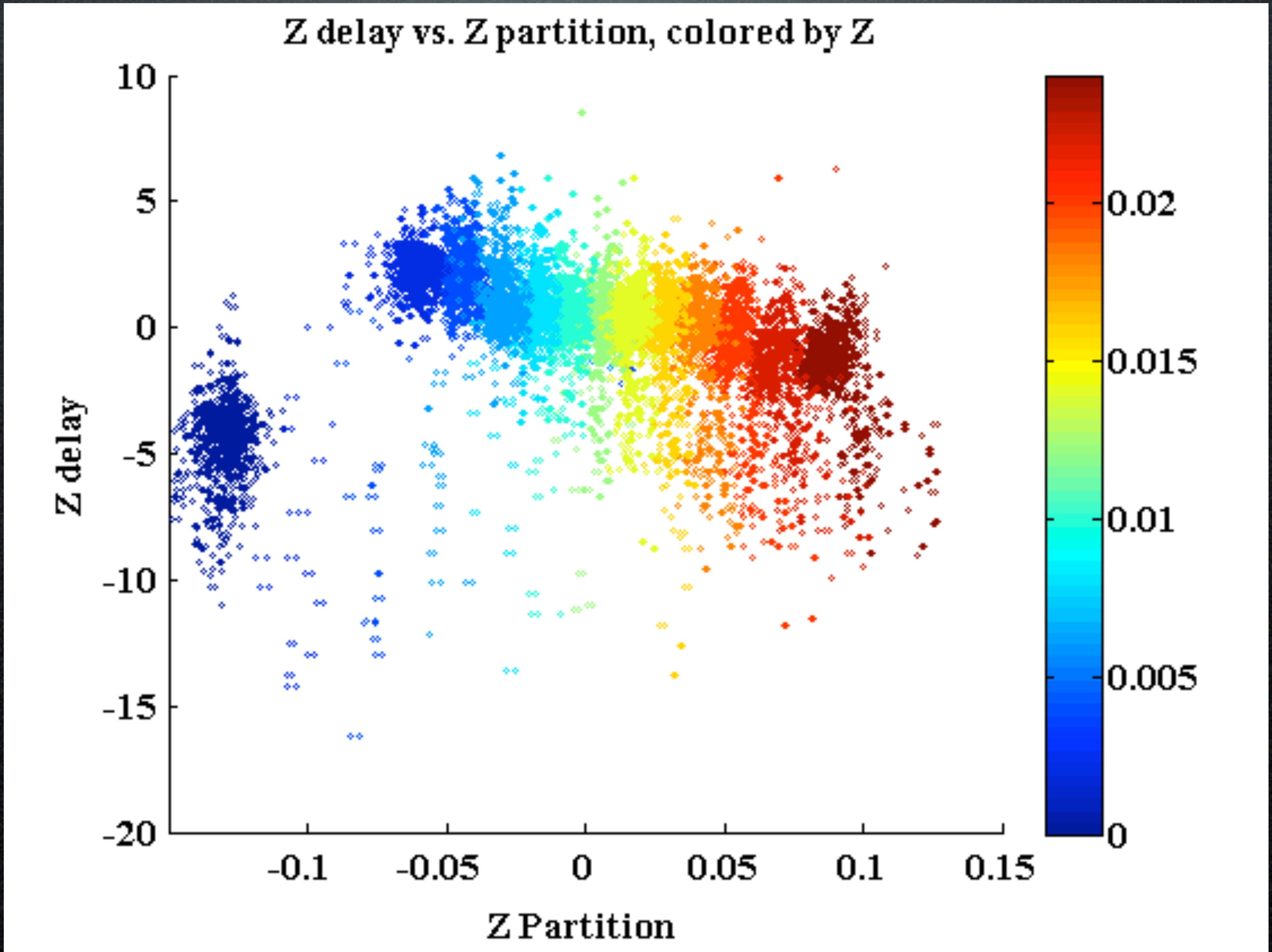

Phonon-only Discriminators

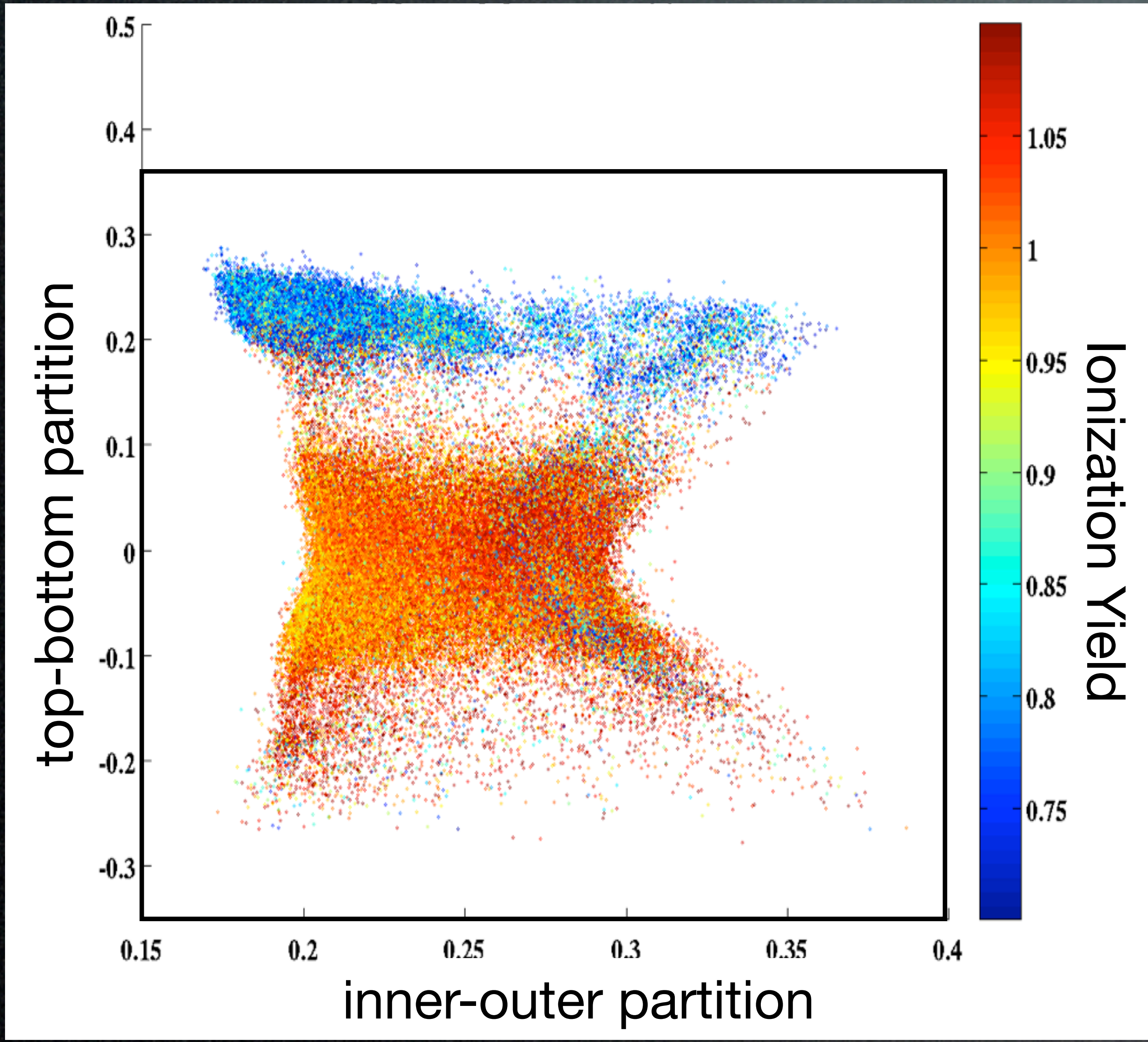

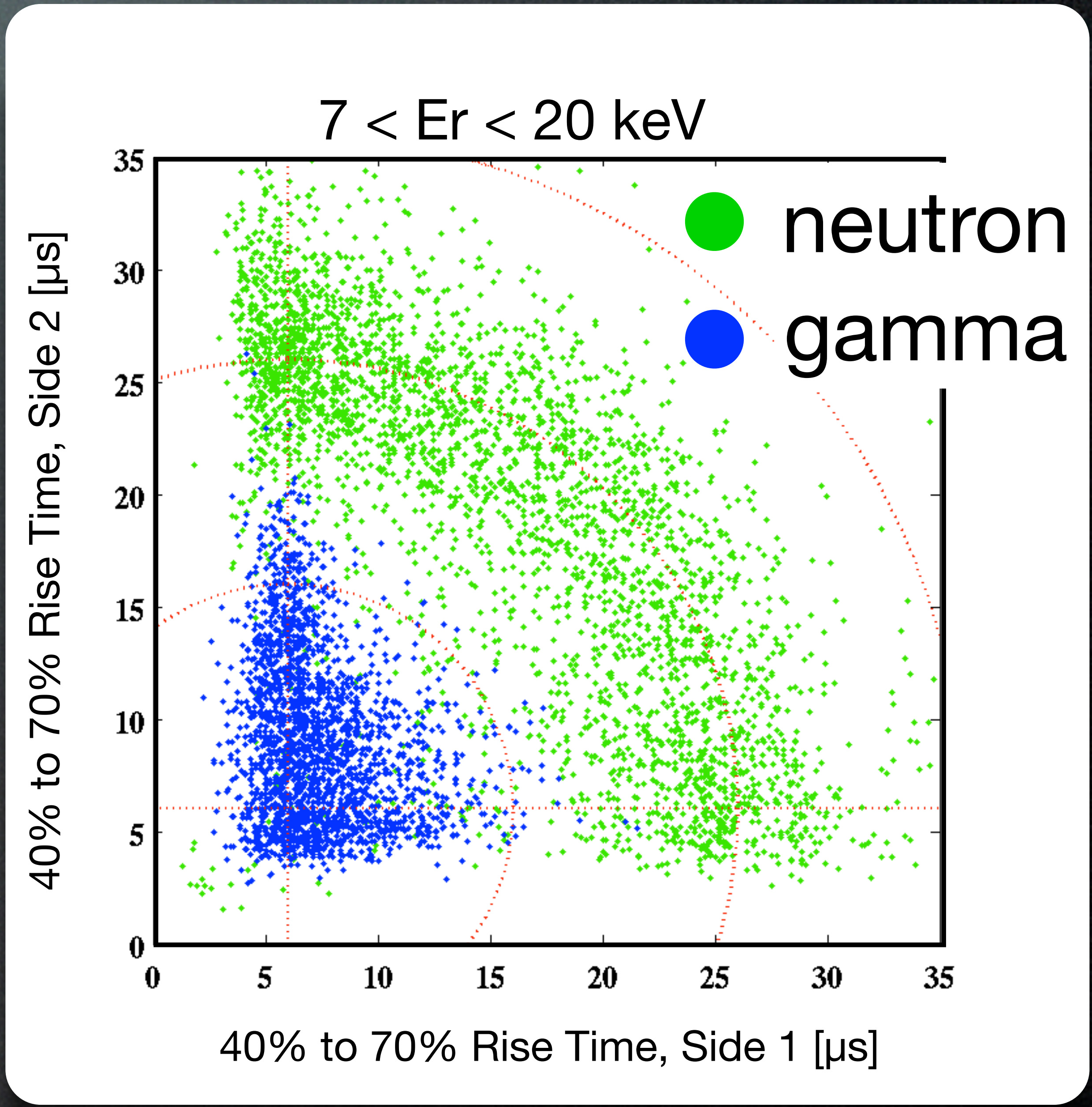

T3Z4-Candidate Timing

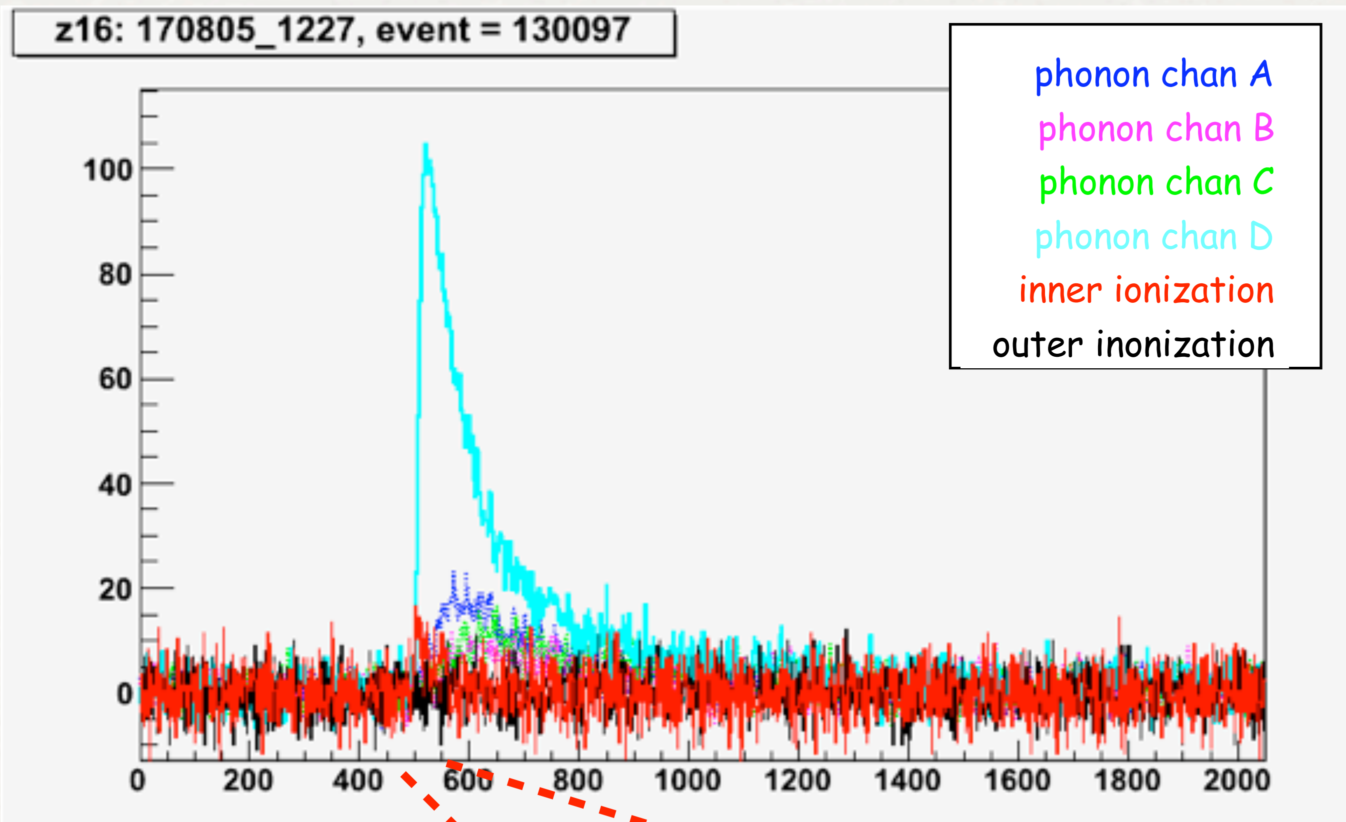

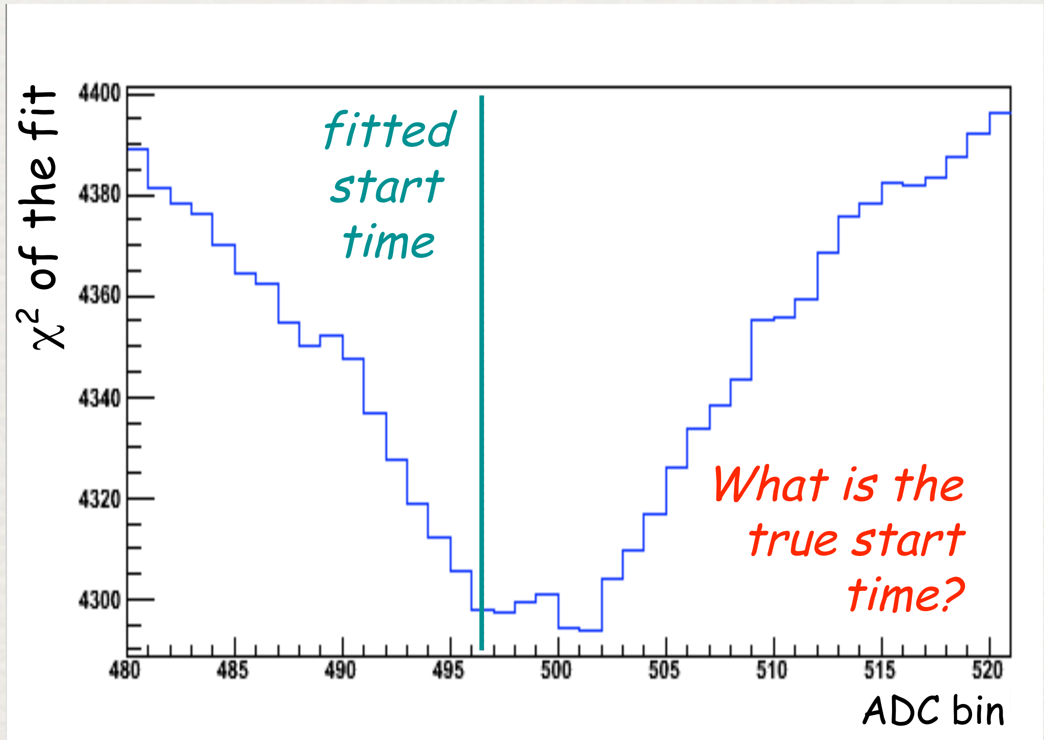

Unfiltered

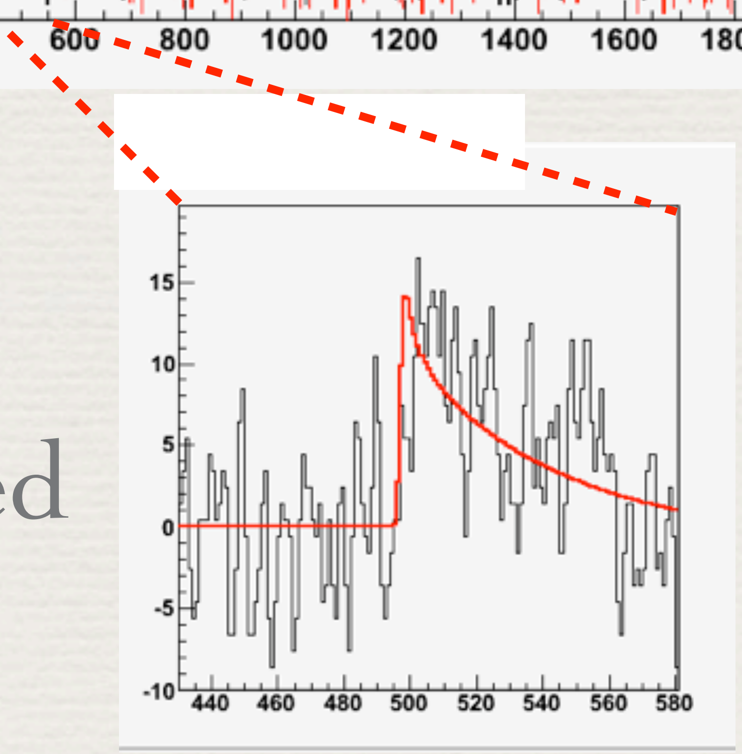

This effects some events with ionization energy < ~6 keV.

It does not effect candidate event on T1Z5.